Granular fluids, a short walkthrough

Andrea Puglisi

May 3, 2010

Preface

This is a collection of ten 2-hours lectures given to an audience of Ph. D. students (and not only) at the Physics Department of the Sapienza University, Rome, on March-April 2010. Parts of the first lectures are excerpts of my Ph. D. thesis, defended on February 2002. This is the reason of a net difference between the first and the last lectures, which - on the contrary - have been arranged following several papers and textbooks and not a unitary source. I expect to write, in the next months, a more refined version where such a discontinuity is smoothed and the reader can follow a more homogeneous line of reasoning.

For these lectures, I have selected a few arguments with the aim of using granular fluids as "benchmarks" for more general ideas and concepts. Any classical description of fluids (for instance kinetic theory) needs a careful revision when equilibrium cannot be assumed. Equilibrium is a powerful symmetry which often offers *shortcuts* to conclusions without too much care for subtle details, microscopic mechanisms and so on. Without equilibrium, one is compelled to look at all the passages and the assumptions involved. This is a good occasion to learn these passages and assumptions, with an over-critic eye, underlining the issues which are in doubt in the granular case.

Some useful general references:

- *a divulgative useful introduction*: Barrat, Trizac and Ernst, J. Phys.: Condens. Matter **17**, S2429 (2005), http://arxiv.org/pdf/cond-mat/0411435

- *on the Boltzmann equation for elastic gases*: The Mathematical Theory of Dilute Gases, C. Cercignani et al., Springer-Verlag (1994)

- *on the Boltzmann equation for granular gases*: van Noije and Ernst, Gran. Matt. **1**, 57 (1998), http://arxiv.org/pdf/cond-mat/9803042

- *a good handbook for granular kinetic theory (focused to cooling only)*: Kinetic Theory of Granular Gases, Pöschel and Brilliantov, Oxford Univ. Press (2003)

- *a review of models of driven granular fluid*: A. Puglisi, F. Cecconi and A. Vulpiani, J. Phys.: Condens. Matter **17**, S2715 (2005), http://arxiv.org/pdf/cond-mat/0411165

Other useful references:

- H. M. Jaeger, S. R. Nagel and R. P. Behringer, *Granular solids, liquids, and gases*, Rev. Mod. Phys. **68**, 1259 (1996)

- J. W. Dufty - Granular Fluids - http://arxiv.org/abs/0709.0479

- I. Goldhirsch, *Scales and kinetics of granular flows*, Chaos, Vol. **9**, 659, (1999).

- L. P. Kadanoff, *Built upon sand: Theoretical ideas inspired by granular flows*, Rev. Mod. Phys. **71**, 435 (1999)

- U. M. B. Marconi, A. Puglisi, L. Rondoni and A. Vulpiani, *Fluctuation-Dissipation: Response Theory in Statistical Physics*, Phys. Rep. **461**, 111 (2008)

Contents

Lecture 1

Introduction to granular "states"

Inspired to a long history of problems in engineer and industrial application, with roots in the 19th century, a large and heterogeneous family of experiments has demonstrated the richness of granular phenomenology. Moreover, the fundamental properties of granular media (inelasticity of collisions and entropic constraints) have motivated the study of a zoo of minimal models displaying an intriguing behavior in spite of their simplicity. "Granular gas" models are an important category in this realm. As for spin glasses, some "granular gas" models are observed only in the silicon cage of a computer simulation, but their importance for a substantial criticism of the basic assumptions (and limits) of Kinetic Theory, Hydrodynamics and general non-equilibrium Statistical Mechanics, is widely recognized.

What are granular materials?
A granular material is a substance made of grains, i.e. macroscopic particles with a spatial extension (average diameter) that ranges from tenths of microns to millimiters. In line of principle the size of grains is not limited as far as their behavior can be described by classical mechanics. For example, the physics of planetary rings (made of objects with a diameter far larger than centimeters) is sometimes studied with models of granular media. More often the term "granular" applies to industrial powders: in chemical or pharmaceutical industries the problem of mixing or separating different kinds of powders is well known; the problem of the transport of pills, seeds, concretes, etc. is also widely studied by engineers; the prevention of avalanches or the study of formation and motion of desert dunes are the subject of important studies all around the world, often involving granular theories; silos containing granular products from agriculture sometimes undergo to dramatic breakages, or more often their content become irreversibly stuck in the inside, because of huge internal force chains; the problem of diffusion of fluids through densely packed granular materials (earths) is vital for the industry of natural combustibles; the study of ripples formations in the sand under shallow sea waters can solve important emergencies on many coasts of the world. Rough estimates of the losses suffered in the world economy due to "granular ignorance" amount to billions of dollars a year.

The physicists usually have reduced the complexity of real situations, performing experiments to probe the fundamental behavior of granular media. The models proposed by theoretical physicists are even more idealized, in order to catch the essential ingredients of single phenomena. In an experiment the grains are often all smooth spheres with the same size, same restitution coefficient, perfectly dry, in the void, and so on. In a numerical simulation the grains can become rods moving on a segment or disks without rotational freedom. However some ingredients are common in all the approaches to granular systems and, in some sense, can be considered the very definition (from the point of view of Physics) of the granular state of matter.

What are the basic properties of granular materials?
In the study of granular physics the properties usually shared by different models are the following:

- the grains are **macroscopic**: they are described by rules of classical mechanics and, moreover, the volume occupied by a grain is excluded by the volume available for the motion of all the other grains; when total occupied volume is a relevant fraction of the available volume this

property has important consequences: mainly geometrical frustration, strong spatial correlations, relevance of collisional transport versus streaming transport, enhancement of re-collisions in the kinetic equations (breakdown of molecular chaos);

- as a consequence of macroscopicity, the grains interact (with each other as well as with the boundaries) by means of **dissipative interactions**: this means that friction is always at work and that collisions are inelastic; the energy lost is transferred to internal degrees of freedom, i.e. heat, and then dispersed to the environment;

- the environmental thermal temperature plays a negligible role in the dynamics of the grains, i.e. they are almost always considered at $T = 0$; this is due again to the macroscopic nature of grains and in particular to their masses, which are usually of the order of 10^{20} molecular masses: the kinetic or potential energy of a grain is therefore many orders of magnitude larger than the thermal energy conserved in the internal degrees of freedom; in the kinetic theory of granular gases the role of "microscopic degrees" is played by the grains themselves, so that a **granular temperature** can be introduced in terms of the random motion of grains.

What are the open problems in the physics of granular materials?

It is useful to stress here the existence of a main division between two different "states" in which the granular materials can be, depending upon the external conditions (available volume, intensity of the driving, degree of inelasticity of the collisions, presence of fluids, and so on):

- Stable or metastable granular systems: this family of problems comprehends the study of the distribution and the analysis of correlations in the internal forces in a pile or silo of grains, the characterization of the propagation of mechanical perturbations (sound) inside densely packed arrays of grains, the very slow compaction dynamics observed when a box full of grains is vibrated (the grains can rest in a metastable state, in the absence of vibration, which is far from the minimum packing fraction attainable), the study of time and size distributions of avalanches in a pile which has reached its critical slope.

- Flowing granular systems: this set of problems is instead composed of all the situations where an uninterrupted flow is present. Typically granular flows are divided in slow dense flows and rapid dilute flows. When the stationary velocity of the flow increases (due to an increase of external driving forces) the shear work induced by internal friction generates granular temperature and granular pressure, which in exchange produces a decrease of volume fraction occupied by grains [34]. This ensures that, almost always, a rapid flow is also dilute and that theoretical methods belonging to kinetic theory, as well as a hydrodynamic description, can be tried and are sometimes successful. Every kind of typical fluid experiment has been performed on granular systems: from Couette cells to inclined channels to rotating drums, finding non-linear constitutive relations. High amplitude vibrations can generate interesting convection phenomena in a box containing grains, always associated to size and density segregation (apparently violating entropic principles). Patterns (two dimensional standing waves) can form on the free surface of a vibrated granular layer. The study of simulated models have arisen new questions on the constitutive behavior in rapid flows, and recently new experiments have focused on this subject, measuring the velocity probability distribution functions and finding that in a wide set of situations this distribution is not Gaussian. The study of internal stress fluctuations and of velocity structure factors has given further elements to the investigation of kinetics of granular flows. A strong debate is still alive, on the limits of application of hydrodynamic formalism (and on the possibility of its derivation through kinetic theory).

1.1   Janssen effect and the distribution of internal stresses

In 1895 H. A. Janssen [83] discovered that in a vertical cylinder the pressure measured at the bottom does not depend upon the height of the filling, i.e. it does not follow the Stevin law which is valid for Newtonian fluids at rest [101]:

$$p_v(h) = \rho g h \tag{1.1}$$

where p_v is the vertical pressure, ρ the density of the fluid, g the gravity acceleration and h the height of the column of fluid above the level of measurement. The pressure in the granular material follows instead a different law, which accounts for saturation:

$$p_v(h) = \Lambda \rho g - (\Lambda \rho g - p_v(0)) \exp(-h/\Lambda) \tag{1.2}$$

where Λ is of the order of the radius R of the cylinder. This guarantees the flow rate in a hourglass to be constant. Moreover, this law is very important in the framework of silos building, as the difference between ordinary hydrostatic and granular hydrostatic is mainly due to the presence of anomalous side pressure, i.e. force exerted against the walls of the cylinder. It happens that the use of a fluid-like estimate of the horizontal and vertical pressure leads to an underestimating of the side pressure and, consequently, to unexpected (and dramatic) explosions of silos.

The first interpretation of the law has been given by Janssen in his paper, in terms of a simplified model with the following assumptions:

1. The vertical pressure p_v is constant in the horizontal plane.

2. The horizontal pressure p_h is proportional to the vertical pressure p_v where $K = p_h/p_v$ is constant in space.

3. The wall friction $f = \mu p_h$ (where μ is the static friction coefficient) sustains the vertical load at contact with the wall.

4. The density ρ of the material is constant over all depths.

In particular the first assumption is not true (the pressure depends also upon the distance from the central axis of the cylinder) but is not essential in this model (as it is formulated as a one-dimensional problem), while the second assumption should be obtained by means of constitutive relations, i.e. it requires a microscopic justification.

Imposing the mechanical equilibrium of a disk of granular material of height dh and radius R (the radius of the container) the following equation is obtained:

$$\pi R^2 \frac{dp_v}{dh} dh + 2\pi R \mu K p_v dh = \pi R^2 \rho g dh \tag{1.3}$$

which becomes:

$$\frac{dp_v}{dh} + \frac{p_v}{\Lambda} = \rho g \tag{1.4}$$

where $\Lambda = \frac{R}{2\mu K}$. This equation is exactly solved by the function (1.2).

The particular behavior of the vertical pressure in granular materials is mainly due to the anomalies in the *stress propagation*. The configuration of the grains in the container is random and the weight can be sustained in many different ways: every grain discharges its load to other grains underlying it or at its sides, creating big arches and therefore propagating the stress in unexpected directions. Moreover, arching is not only a source of randomness, but also of strong fluctuations, i.e. disorder: in a granular assembly some force chains can be very long and span the size of the entire system, posing doubts on the validity of (local) mean field modeling.

Further interesting phenomena have been experimentally observed in the statics of granular materials:

- the fluctuations of the pressure at the bottom of a silo are large, they can change of more than 20% in repeated pouring of grains in the same container [31], and in a single pouring the distribution of stresses, measured deep inside or at the bottom of the silo, show an exponential tail [108, 130, 30].
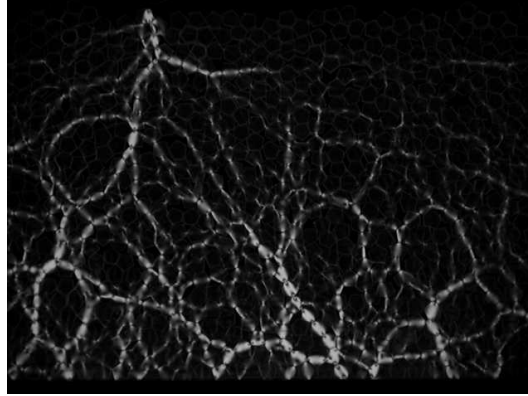
Figure 1.1: Force chains generated after a localized (on top) perturbation

- the vertical pressure below conical sandpiles does not follow the height of the material, but rather has a *minimum* underneath the apex of the pile [168]

Different models have been proposed and debated in the last years, in order to understand the problem of the distribution of forces in a silo or in a granular heap.

The *q-model* has been introduced in 1995 (remarkably a century after the work of Janssen) by Liu et al. [108, 42] in order to reproduce the stress probability distribution observed in experiments. The model consists of a regular lattice of sites each with a particle of mass unity. Each site i in layer D is connected to exactly N sites j in layer $D+1$. Only the vertical components of the forces $w = \sigma_{zz}$ are considered explicitly: a random fraction $q_{ij}(D)$ of the total weight supported by particle i in layer D is transmitted to particle j in layer $D+1$. Thus the weight supported by the particle in layer D at the i-th site, $w(D, i)$, satisfies a stochastic equation:

$$w(D + 1, j) = 1 + \sum_i q_{ij}(D)w(D, i) \tag{1.5}$$

The random variables $q_{ij}(D)$ are taken independent except for the constraint

$$\sum_j q_{ij} = 1 \tag{1.6}$$

which enforces the condition of force balance on each particle. Given a distribution of q's, it can be obtained the probability distribution $Q_D(w)$ of finding a site that bears a weight w on layer D. By means of mean field calculations, exact calculations and numerical solutions, the authors conclude that (apart of some limiting cases) a generic continuous distributions of q's lead to a distribution of weights that, normalized to the mean, is independent of depth at large D and which decays exponentially at large weights. They find also a good agreement with molecular dynamics simulations of the packing of hard spheres. The q-model has many limits:

- it is a scalar model, i.e. it takes into account only one component of the internal stress (this was solved by P. G. de Gennes [48] who introduced a vectorial version of the q-model, obtaining a more realistic propagation of forces)

- it does not reproduce the minimum (the "dip") of the pressure measured under central axis at the bottom of a sand heap

- it does not reproduce the Janssen law [119]; this problem appears as a consequence of the diffusive nature of the q-model solution: the saturation depth D_s where the stress distribution becomes independent of depth scales with the silo width R as $D_s \sim R^2$, at odds with the Janssen observation that predicts $D_s \equiv \Lambda \sim R$.

A more refined version of the Janssen model has been introduced by Bouchaud et al. [20]: the authors have considered a local version of the Janssen assumption on the proportionality between horizontal and vertical stresses:

$$\sigma_{xx} = k\sigma_{zz} \tag{1.7a}$$

$$\sigma_{yy} = k\sigma_{zz} \tag{1.7b}$$

$$\sigma_{xy} = 0 \tag{1.7c}$$

which lead to the linear equation:

$$\frac{\partial^2 \sigma_{zz}}{\partial z^2} - k \left(\frac{\partial^2}{\partial x^2} + \frac{\partial^2}{\partial y^2} \right) \sigma_z z = 0 \tag{1.8}$$

This equation for the vertical stress is hyperbolic and therefore differs from the equivalent equation for an elastic medium, which is elliptic [100], and from the q-model equation that is parabolic (as a diffusion equation): it is equivalent to the equation for the wave propagation with z as the "time" variable and k as the inverse of the propagation velocity. This model well reproduces the dip in the measure of the pressure under the bottom of the conical heap [168]. A cellular automaton was introduced by Hemmingsson [76] which was capable of reproduce the dip under the heap as well as the correct Janssen law (with the linear scaling).
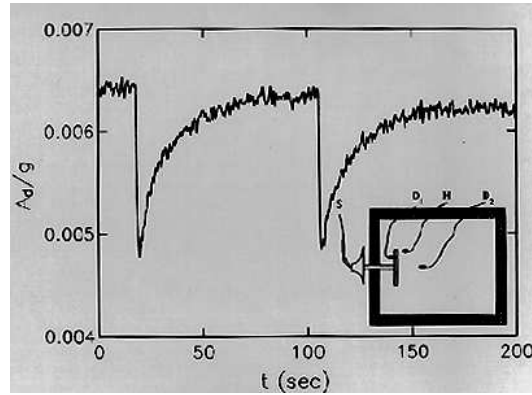
Figure 1.2: Propagation of sound

In the framework of the study of force networks in the bulk of a static arrangement of grains a key role was played by the experiments on the **propagation of sound**. The inhomogeneities present inside a granular medium can drastically change the propagation of mechanical perturbations. Liu and Nagel [106, 107, 105] have addressed this issue in several experiments. They have discovered [106] that the in the bulk of a granular medium perturbed by a harmonic force (4 Hz) the fluctuations could be very large, measuring power-law spectra of the kind $1/f^\alpha$ with $\alpha = 2.2 \pm 0.05$. Then they have seen [107] that the sound group velocity can reach 5 times the phase velocity and that a change in the amplitude of vibration can result in a hysteretic behavior (due to a rearrangement of force chains). They have also measured [105] a 25% variation of the sound transmission as a consequence of a very small (compared to the size of the grains) thermal expansion of a little carbon resistor substituted to a grain of the granular medium. This sensitivity to perturbation is another signature of the strong disorder (arching and chain forces) in the bulk of the medium.

1.2   Vibration induced compaction and glassy granular systems

Another frontier of the experimental granular physics is the problem of *vibration induced compaction*: the granular material poured in a container (for example a simple box) quickly reaches the equilibrium, i.e. the balance of all internal and external forces. At that point one can measure the volume fraction, or packing fraction, i.e. the ratio:

$$\phi = \frac{\sum_i V_i}{V_{box}} \tag{1.9}$$

where the V_i are the volumes of the grains and V_{box} is the volume of the container measured up to the maximum (or average) height reached by the material. The packing fraction measured at the end of the filling, for spheres, has been estimated to be bounded by the limiting values $\phi_{min} = 0.55$ and $\phi_{max} = 0.64$. After the initial filling, some external force, i.e. a vibration, can change the arrangement of grains and therefore its volume fraction, usually increasing it. S. F. Edwards and A. Mehta [125] have proposed a new formalism that resembles thermodynamics and that describes the evolution of a granular system subject to slow vibration: in this formalism the energy is the occupied volume V and the Hamiltonian is a functional W that gives the occupied volume if applied to a certain configuration (spatial positions) of the grains. The granular system is assumed to evolve through states of equilibrium (in this new thermodynamics). The entropy S is defined as the logarithm of the number of possible configurations with the same occupied volume V, while the temperature is substituted by the "compactivity" X which is defined as

$$X = \frac{\partial V}{\partial S} \tag{1.10}$$

With this formalism, Barker and Mehta [11] have shown that the relaxation of the volume fraction in response to a continuous sequence of vibrations is fast exponential with two relaxation times associated with collective and individual modes. Another mechanism has been proposed to describe the vibration-induced compaction: in this theory the motion of the voids filling the space between the particles is effectively diffusive and as a result a power-law relaxation is predicted [38].

The careful experiment of Knight et al. [90] demonstrated that the vibration-induced compaction (in a tube subject to tapping followed by long pauses) is governed by a logarithmically slow relaxation (see Fig. 1.3 on the facing page):

$$\phi(t) = \phi_f - \frac{\Delta\phi_\infty}{1 + B\ln(1 + t/\tau)} \tag{1.11}$$

where the parameters ϕ_f, $\Delta\phi_\infty$, B and τ depend only on the acceleration parameter Γ that is the ratio between the peak acceleration of a tap and the gravity acceleration g. The discover of this inverse logarithmic behavior (very slow with respect to previous predictions) has motivated the introduction of new models and has also attracted the interest of specialists of other fields: in particular the slow relaxation is a typical phenomenon observed in glassy states of matter, e.g. the aging in amorphous solids like glasses.

E. Ben-Naim et al. [15] have explained the slow relaxation law (1.11) in terms of a simple stochastic adsorption-desorption process: the desorption process is unrestricted and happens with a well defined rate, while the adsorption process is restricted by the occupied volume, i.e. new particles cannot be adsorbed on top of previously adsorbed particles. This model has been also called *car parking model*, as it reproduces the increasing difficulty of parking a car in a parking lot as the number of parked cars get larger and larger. The inverse logarithmic law has been recovered solving this model.

Another way, perhaps more realistic, of recovering the inverse logarithmic relaxation, is described by Caglioti et al. [33] by means of a "Tetris-like" model (displayed in Fig. 1.4 on the next page). In this model the grains are represented by objects disposed on a regular lattice: the different shapes of the objects induce geometrical frustration, i.e. some kinds of grains cannot stay near some other kinds of grains and therefore the equilibrium configuration of a filled box is disordered and present a
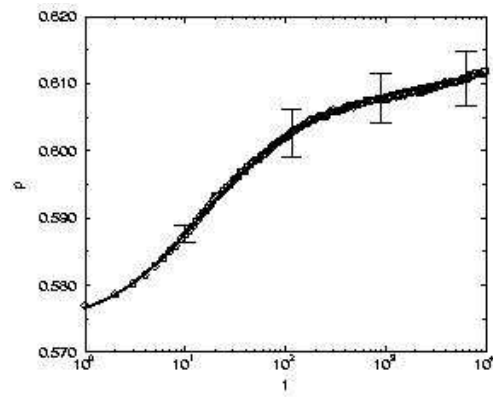
Figure 1.3: Slow Compaction: the packing fraction vs. time (in units of taps)
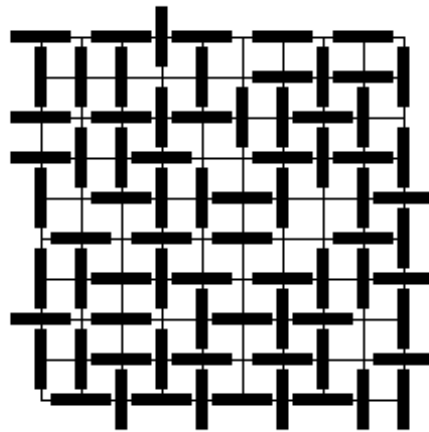
Figure 1.4: An example configuration of the Tetris-model

random packing fraction: a computer simulation of the vibration dynamics (short periods of tapping followed by long periods of undriven rearrangement until the new equilibrium is reached) shows that this model reproduces the inverse logarithmic relaxation. The study of this model has shed light on many features of the dynamics of dense granular media, such as vibration-induced segregation, bubbling and avalanches. Moreover, the possibility of mapping the dynamics of the Tetris model onto that of a Ising-like spin system with vacancies has introduced a new bridge between the physics of granular media and that of disordered systems (like spin glasses and structural glasses) [132]. In particular the interest of researchers has focused on the following remarkable fact: spin glass models [21] (such as the Sherrington- Kirkpatrick model or the Edwards-Anderson model) always contain a quenched (frozen) disorder, usually given by the set of J's that weight the interactions among spins. A dense granular media evolve without any frozen disorder, nevertheless its dynamics presents many "glassy" features (such as history dependence of the dynamics, hysteresis, frustration, metastable equilibria and so on). This consideration is at the base of all the recent studies on spin lattice models *without* quenched disorder. It must be said that many of these models have little in common with the real granular materials and are often more useful tools in the study of the behavior of spin or structural glasses.

1.3   Sandpiles

When sand is added on the top of a sand heap (also known as sandpile problem) two phenomena are observed:

- the slope of the pile grows (with little flowing of sand on it) until a critical angle is reached; after that (if sand is still poured on the top) the slope stays almost constant and the sand flows along it;

- at the critical angle the flowing of sand is made of "avalanches" of different sizes and durations;
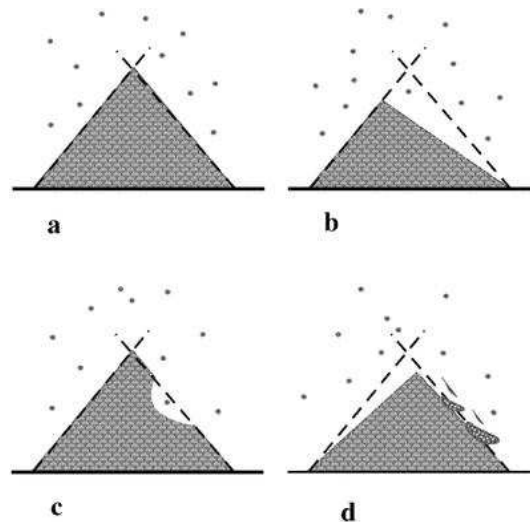
Figure 1.5: Possible configurations of a sandpile

Starting from this qualitative observation, P. Bak et al. [8, 9] have introduced a cellular automaton model (see Fig. 1.5) where each site (for example in two dimensions (i,j)) of the lattice has associated a slope $z(i,j)$. If the slope exceeds a critical value z_c a rearrangement of the neighboring sites is performed, e.g. 4 is subtracted to the exceeded value and 1 is added to its 4 neighboring sites. The automaton may be executed in two different ways:

1. the field at time 0 has an average slope greater than z_c, and the system evolves freely;

2. the field at time 0 is everywhere equal to zero and at every step a randomly chosen site is incremented;

In both cases the systems reaches a stable configuration corresponding to the critical slope: every successive perturbation (i.e. increasing the field on some site) generates an avalanche that involves the rearrangement of a certain number of sites of the lattice. The authors show that the distribution of the extension of the avalanche follows a power law:

$$D(s) \sim s^{-\tau} \tag{1.12}$$

with $\tau \simeq 0.98$ for three or four logarithmic decades. In another work [159] the same authors define and study a set of critical exponents similar to those used in statistical mechanics of phase transitions.

The novelty of the work of Bak and coworkers is represented by the fact that a model was found that showed a critical behavior (i.e. power law relaxations, correlations at all sizes) without any fine tuning of the external parameter, whereas usual critical phase transitions need a precise tuning of the temperature to the critical temperature T_c. This self-organized critical behavior was intriguing as it seemed to be a key concept to understand the ubiquity of power laws in nature (e.g. $1/f$ noise, self-similar structures like fractals, turbulence and so on). The sandpile model is still studied, with all its variants, but it has been recognized to be not a good paradigm for the self-organized criticality: it was seen in fact [166] that the driving rate (i.e. the rate of falling of grains on the top of the pile) acts exactly as a control parameter that has to be fine tuned to zero in order to observe criticality. However many important issues are still open: the interplay between the self-organization into a stationary state and the dynamical developing of correlations, the (numerical) measure of critical exponents, universality classes, upper critical dimensions and so on.
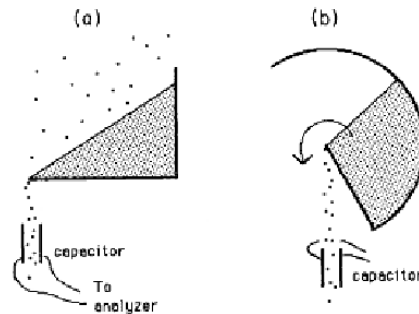
Figure 1.6: The experiment of Nagel and coworkers to measure avalanches in sandpiles

More remarkably, it has been pointed out that the sandpile model has little to do with sand (and granular matter) in general. In 1992 Nagel has published [131] the results of a series of experiments on sand in order to verify the predictions of Bak and coworkers. He has initially shown the difficulty of performing an exactly constant rate in the pouring of grains from above the top of a pile. Therefore he has introduced a different kind of experiment (see Fig. 1.6), where the sand fills partially a rotating drum: the constant angular velocity of the drum guarantees the constant driving needed to reach the critical slope and the avalanche regime. The statistical analysis of the avalanches has clearly demonstrated that sand does not reproduce the critical behavior expected in self-organized criticality. The sandpile has *two* critical slopes: Θ_r is the rest angle (when the slope is less than Θ_r the pile is stable), Θ_m is maximum angle (when the slope is larger than Θ_m avalanches form and reduce the slope to an angle less than Θ_r). If the slope is comprised in between Θ_r and Θ_m there is *bistability*, i.e. the sand can rest or can produce avalanches, based on its previous history. The avalanches have a typical duration and the hysteretic cycle between the two angles has a well defined average frequency. No power laws have been observed.

1.4 *Slow* vs. *rapid* granular flows

If the motion of granular material occurs slowly, particles will stay in contact and interact frictionally with their neighbors over long periods of time. This is the "quasi-static" regime of granular flow and has been classically studied using modified plasticity models [14, 13, 19] based on a Coulomb friction criterion [44, 45].

At the other extreme is the rapid-flow regime which corresponds to high-speed flows [154, 35]. Instead of moving in many-particle blocks, each particle moves freely and "independently". In the rapid-flow regime, the velocity of each particle may be decomposed into a sum of the mean velocity of the bulk material and an apparently random component to describe the motion of the particle relative to the mean. The analogy between the random motion of the granular particles and the thermal motion of molecules in the kinetic-theory picture of gases is so strong that the mean-square value of the random velocities is commonly referred to as the "granular temperature" - a term first used by Ogawa [133]. As pointed out in the introduction, however, granular temperature has nothing to do with environmental thermal temperature, which usually plays no role in the dynamics of granular flows. Nevertheless, using this kinetic analogy, granular temperature generates pressure and governs the internal transport rates of mass, momentum and energy. Thus, while the term temperature sometimes leads to some semantical confusion for the uninitiated, the physical analogy between the two temperatures is so apt that its use has become standard throughout the field.

1.4.1 Couette cylinders

The first tentatives of studying granular media under the point of view of rheology, i.e. transport properties (discussed in more detail in Lecture 5) have been performed using typical shear experiments used to probe ordinary fluids. In particular the Couette geometry has been largely used and is still now an important tool of investigation.
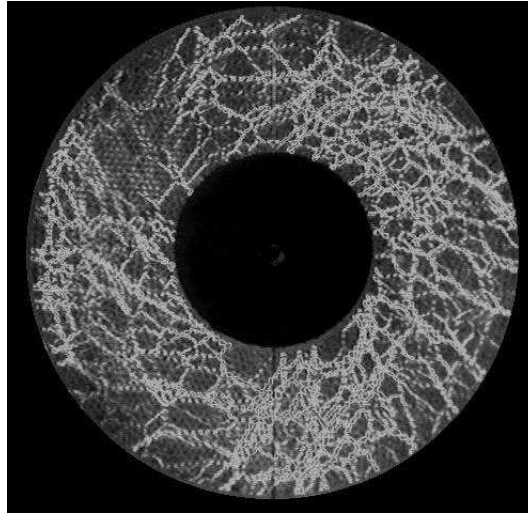
Figure 1.7: The experiment of Mueth and coworkers on a Couette cylinder: the paths of the internal forces are evidenced by means of non-invasive X-ray imaging

Even if there were earlier important experimental studies on the flow properties of granular materials (mainly initiated by Hagen [74] and Reynolds [146]), the modern pioneering work on the constitutive behavior of rapid granular flows was Bagnold's experimental study [6] of wax spheres, suspended in a glycerin-water-alcohol mixture and sheared in a coaxial cylinder rheometer (Couette experiment). His main finding was a constitutive relation between internal stresses and shear rate:

$$\mathcal{T}_{ij} = \rho_p \sigma^2 \gamma^2 \mathcal{G}_{ij}(n) \tag{1.13}$$

with ρ_p the particle density, σ the particle radius, γ the shear rate and $\mathcal{G}_{ij}$ a tensor-valued function of the solid fraction ϕ. This relation has been confirmed in shear-cell experiments with both wet or dry mixtures by Craig et al. [46], Hanes et al. [75], Savage et al. [156], and in many computer simulations [36, 37, 171].

Bagnold measured not only shear stresses (i.e. transversal components, say $i \neq j$ in $\mathcal{T}_{ij}$), but also normal stress ($i = j$), that is the analogous of pressure in gas kinetics: he referred to them as "dispersive stresses" as they tend to cause dilation of the material.

Many experiments have focused on different phenomena observed in the Couette rheometer:

- **Fluctuations of stresses:** already in the experiments of Savage and Sayed [156] large fluctuations of internal (normal) stresses were observed; Howell and Behringer [80] have seen that in a 2D Couette experiment the mean internal stress follows a continuous transition when the packing fraction of the granular material changes and passes through a critical value $\phi_c = 0.776$: when the packing fraction is above the critical threshold the material shows strong fluctuations of internal stress, while under the threshold the stresses are averagely zero and the system is highly compressible.

- **3d experiments:** Mueth et al. [129] have studied the formation of microstructures in the dense shearing regime in a 3D Couette rheometer, using non-invasive imaging by X-Ray microtomography (see Fig. 1.7 on the facing page); they have found that the velocity parallel to the shear direction decays more rapidly than linear (from exponential to Gaussian-like decay, depending upon the regularity of the grains). A similar strong decay of the flow with the distance from the moving wall was observed in many experiments, for example by Losert et al. [110]

- **Diluted (air-fluidized) shear:** Losert et al. [169] have performed a Couette experiment with a flow of air coming from the bottom of the cylinder, in order to fluidize the material and obtaining smoother profiles. They have put in relation the RMS fluctuations of velocity and the shear forces, observing that $T^{1/2}(y) \sim \gamma(y)^{\alpha}$ with $\alpha = \simeq 0.4$, and suggesting a phenomenological model that explains the shear velocity profiles.

- **Size segregation:** Khosropour et al. [87] have observed convection patterns and size segregation in a Couette flow with spherical glass beads; they also checked the effect of interstitial fluids finding it irrelevant.

- **Planetary rings:** planetary rings (those of Saturn for example) have been sometime studied in the framework of granular rheology, whereas the "geometry" of the planetary experiment is similar to a Couette cell (grains are circularly sheared because the angular velocity depends upon the distance from the planet). A review of these study can be found in the work of Brahic [22].

1.4.2 Flow under gravity acceleration

Another way to probe hydrodynamic descriptions of rapid granular dynamics is the study of flows along inclined channels. In this kind of experiments the whole material is accelerated by gravity, but the friction with the plane induce shearing, so that measurements similar to the ones performed in Couette cells can be performed. The first experiments in this configuration were performed by Ridgway and Rupp [147], and reviews can be found in the works of Savage [153] and Drake [51]. Interest has focused on constitutive relations, as before, but also on the profiles of the hydrodynamic fields, mainly flow velocity and solid fraction: computer simulations (see for example Campbell and Brennen [36] and for an exhaustive review the classical work of Campbell [35]) have allowed the measurement of the temperature field: this has confirmed the picture of a fluid-like behavior, explaining the reduction of density (solid fraction) near the bottom by means of an increase of granular temperature, due to the shear work. In this framework the scheme representing the "mechanical energy path" sketched by Campbell in his review on rapid granular flow [35] is enlightening. The external driving force (i.e. gravity) induces mean motion (kinetic energy) which consequently generates friction with boundaries, that is shear work (granular temperature). The randomization represented by the granular temperature induces collisions

among the grains, which are dissipative and therefore produce heat. Moreover, granular temperature generates internal (transversal as well as normal) stresses.
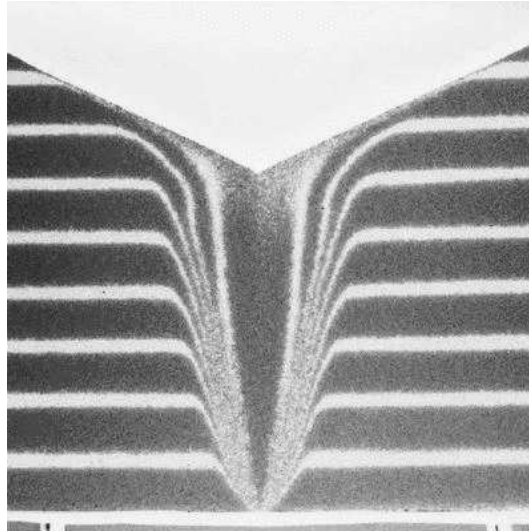
Figure 1.8: The draining from the bottom of a silo: it is clear the separation between a region where grain move downward and a region where grain do not move at all

Another configuration of granular flow under the force of gravity is the simple hopper geometry (a hopper is a funnel-shaped container in which materials, such as grain or coal, are stored in readiness for dispensation). The bottom of hopper is opened and the grains start to pour out. As already discussed the pressure (and therefore the flow rate) does not depend upon the height of the column of material. However the flux of grains leaving the container produces complex flow regions inside the container. Four regions of density and velocity can be identified, most notably a tongue of dense motion just above the aperture and an area of no grain motion below a cone extending upwards from the opening (a similar can be observed in a silo, see Fig. 1.8). Baxter et al. [12] have showed that for large opening angles, density waves propagate upward from above the aperture against the direction of particle flow, but downwards for small angles. The flow can even stop due to "clogging", i.e. the grains can form big arches above the aperture and sustain the entire weight of the column.

More recent experiments have been performed on granular flows along inclined planes or chutes, evidencing other interesting phenomena:

- **Validations of kinetic theory** Azanza et al. [53] have repeated the experiment of grain flow along an inclined channel, studying the stationary profiles of velocity, solid fraction and granular temperature. They have verified that there is a limited range of inclinations of the channel that allow for a stationary flow. Moreover they have probed the validity of the kinetic theories developed in the previous years [155, 85, 118, 84, 116], based on the assumption of slight perturbation to the Maxwellian equilibrium. The profiles of hydrodynamic fields show two different regions: a collisional region (higher density) where the transport is mainly due to collisions, and a ballistic region (on the upper free surface) where the grains fly almost ballistically.

- **Size segregation in silo filling or emptying:** Samadani et al. [152] have studied the phenomena of size segregation in a quasi-two dimensional silo emptying out of an orifice. They [151] have also studied the effects of interstitial fluids.

- **Size segregation in rotating drums:** another typical experiment, inspired to many industrial situations, is the tumbling mixer, or rotating drum, i.e. a container with some shape that rotate around a fixed axis, usually used to mix different kind of granular materials (typically powders, in the pharmaceutical, chemical, ceramic, metallurgical and construction industry). Depending on

the geometry of the mixer, the shapes of the grains, the parameters of the dynamics and so on, the grains can mix as well as separate. A very large literature exists on this phenomena (see the review by Ottino and Khakhar [137]). Usually segregation is strictly tied to convection: there is a shallow flowing layer on the surface of the material inside the rotating drum, the grains at the end of it are transported into the bulk and follow a convective path so that they emerge again in another point of the surface. Segregation happens in many different ways: segregated bands appear and slowly enlarge (like in a coarsening model), segregation can emerge in different directions, e.g. parallel to the rotation axis as well as transversal to it.

- **Granular jets** several experiments have been conducted on the phenomenon of granular jets (see Fig. 1.9), where a heavy object falls on a fine granular bed determining an eruption followed by a very high expelled granular column, which (during the successive falldown) breaks into small clusters [160, 109].
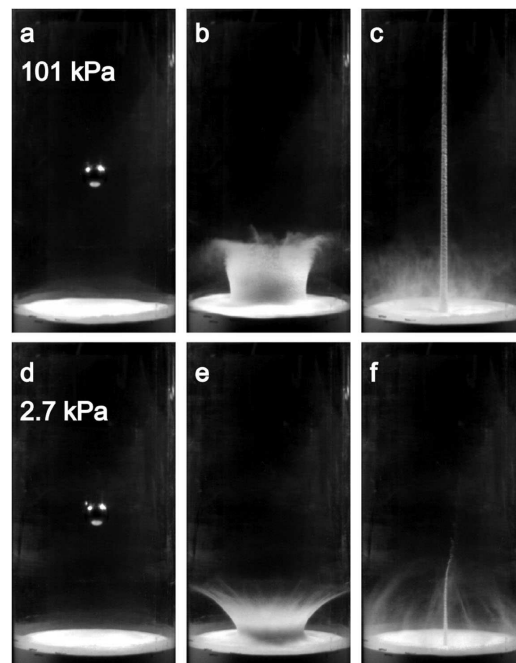
Figure 1.9: Formation of a granular "jet"

1.4.3 Vibrated grains

Many interesting observations can be done when the granular medium is subject to periodic vibration. As already discussed (see paragraph 1.2) the effect of slow vibration under of the bottom of a container filled of grains induces a very slow compaction of the material. When the amplitude of vibration is strong enough, i.e. when

$$\Gamma = \frac{a_{max}}{g} > 1 \tag{1.14}$$

(where a_{max} is the maximum acceleration of the vibrating plate, e.g. $a_{max} = A\omega^2$ if the plate is harmonically vibrating with A amplitude and ω frequency), then the granular shows several new phenomena.

- **Convection and segregation**: A large literature [62] exists on the convection and segregation phenomena observed in granular media contained in a box shaken from the bottom (or from the

sides). Faraday [63] was perhaps the first to observe such a phenomenon. The geometry of
the container can change dramatically the quality of the convection (e.g. in a cylinder may
happen that the grains near the walls move downwards and the ones in the bulk move upwards,
while inside an inverted cone the convection occurs in the opposite direction). Usually the larger
grains (independent of their density) tend to move upwards (see Fig. 1.10), so that the material
segregate (see for example [91, 54, 98, 89, 88]).
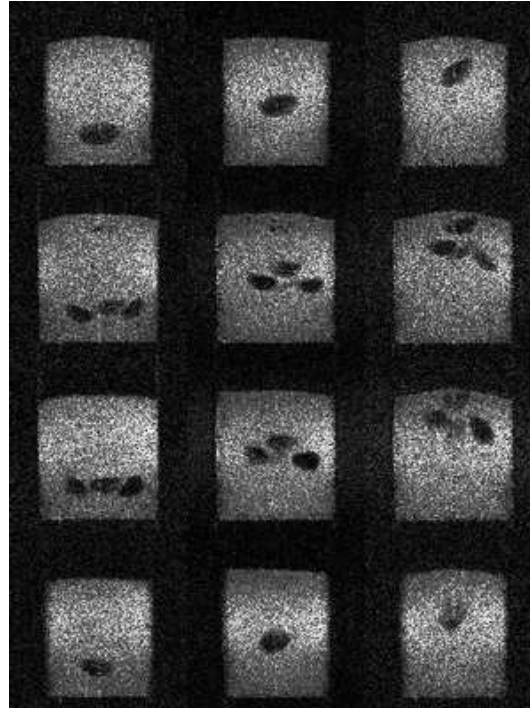
Figure 1.10: Segregation and convection in a vibrated mixture of grains of different sizes

- **Pattern formation in surface waves**: another problem that has been extensively studied in
  recent years is the formation of patterns on the surface of vibrated layers of grains. Depending
  on the whole set of parameters (amplitude and frequency of the vibration, shapes and sizes of the
  grains, size of the container, depth of the bed and so on) different qualities of standing waves can
  be observed, leading to unexpected and fascinating textures [126, 127, 161, 128] (see Fig. 1.11
  and Fig. 1.12 on the next page).
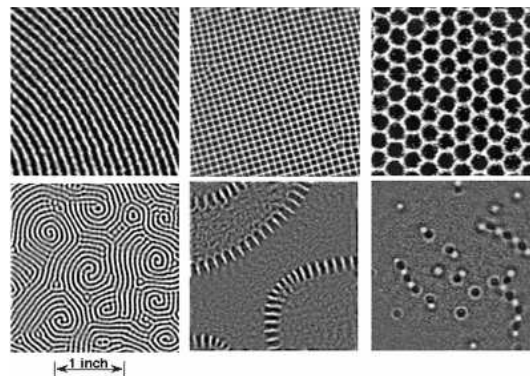
Figure 1.11: Different surface patterns obtained by vertical vibration of granular layers

Figure 1.12: The oscillon: a two-dimensional solitary standing wave on the surface of a granular monolayer

- **Clustering:** Kudrolli and Gollub [94, 96] have studied the formation of clusters measuring the density distribution in an experiment consisting of steel balls rolling on a smooth surface which could or could not be inclined with a vibrating side. The experiment takes into account a monolayer (not completely covered) of grains, in order to study a true $2d$ setup. In both cases (inclined or horizontal), at high enough global densities, the distribution of density (going from Poissonian to exponential) indicates strong clustering. The formation of high density clusters has also been studied in a vibrated cylindrical piston [59, 61, 60]. A transition has been observed with the increasing number of particles in the cylinder, from a gas-like behavior to a collective solid-like behavior. Such a transition has been also observed in the framework of fluidized beds [134], i.e. vertically shaken granular monolayers: the authors have observed a transition (with reducing the vibration amplitude) from a gas-like motion to a coexistence between a crystallized state (a pack of particles arranged in an ordered way) surrounded by gas.

- **Non-Gaussian velocity distributions:** After the recent progresses in the numerical study of granular rapid dynamics, the question of the true form of the velocity distributions has arisen and has induced many new experiments in order to give a realistic answer to it. Kudrolli and Henry [95] have studied the distributions of velocities in the same setup cite above, with varying angles of inclination, obtaining non-Gaussian statistics with enhanced high energy tails; moreover they have seen that increasing the angle of inclination the distributions tends toward the Maxwellian (see Fig. 1.13 on the following page).

  The experiment of Olafsen and Urbach [134, 135] with a horizontal granular monolayer subject to a vertical vibration (and measuring horizontal velocities) has proven that, in the presence of clustering, the distributions are non-Gaussian, showing nearly exponential tails. The experiment of Losert et al. [112] on a similar monolayer with vertical vibration verify that both the predictions of van Noije and Ernst [162] on the high energy tails for cooling and driven granular gases are correct, measuring exponential tails for the former and $\exp(-v^{3/2})$ for the latter. Very recently Rouyer and Menon [150] have again measured the velocity fluctuations in a vertically vibrated vertical monolayer of grains, obtaining again a velocity distribution with $\exp(-v^{3/2})$ tails.

- **Velocity correlations:** An experiment by Blair and Kudrolli [17] with the same experimental
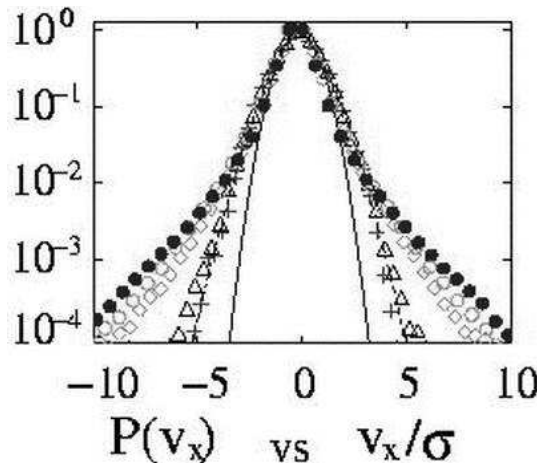
Figure 1.13: The experiment of Kudrolli and Henry [95]: distributions of horizontal velocities of grains rolling on an inclined plane, with the inferior wall vibrating.

setup of the previous ones has revealed strong correlations between velocity particles.

- **Validations of kinetic theory**: a part of the experimental effort [114, 174, 173, 172] has also devoted to the study of hydrodynamic and kinetics fields (i.e. packing fraction profiles, granular temperature profiles, self-diffusion, velocity statistics) in vertically vibrated boxes (or vertical slices, that is 2d setups). The interest has also focused on the difficulties of imposing boundary conditions to the existing kinetics model, due to the existence of non-hydrodynamic boundary layers. This has also led to the formulation of hypothesis of scaling for the granular temperature as a function of the amplitude of vibration [97, 158]. For more recent experiments see [175].

- **Non-equilibrium behavior**: a few experiments have been devoted to the study of non-equilibrium granular properties. In particular Feitosa and Menon have led two important experiments to verify the breakdown of energy equipartition [64] and to measure the fluctuations of internal energy flow [65]: in the last experiment they have claimed a verification of the Gallavotti-Cohen Fluctuation theorem [66], but successive theoretical work has proven that it was not the case [144].

Lecture 2

Inelastic collisions

2.1 Kinematics of the elastic collision

Let us consider two point-like particles with masses m_1 and m_2, coordinates $\mathbf{r}_1$ and $\mathbf{r}_2$ and velocities $\mathbf{v}_1$ and $\mathbf{v}_2$. One can introduce the center of mass vector $\mathbf{r}_c$:

$$\mathbf{r}_c = \frac{m_1\mathbf{r}_1 + m_2\mathbf{r}_2}{m_1 + m_2} \tag{2.1}$$

and the relative position vector:

$$\mathbf{r} = \mathbf{r}_1 - \mathbf{r}_2. \tag{2.2}$$

Their time derivatives are: the velocity of the center of mass:

$$\mathbf{v}_c = \frac{m_1\mathbf{v}_1 + m_2\mathbf{v}_2}{m_1 + m_2} \tag{2.3}$$

and the relative velocity:

$$\mathbf{V}_{12} = \mathbf{v}_1 - \mathbf{v}_2. \tag{2.4}$$

The forces between these two particles depends only on their relative position and are of equal magnitude and pointing in opposite directions:

$$\mathbf{F}_{12}(\mathbf{r}) = -\mathbf{F}_{21}(\mathbf{r}). \tag{2.5}$$

This is equivalent to say that the center of mass does not accelerate, i.e.:

$$\frac{d^2\mathbf{r}_c}{dt^2} = 0 \tag{2.6}$$

while the relative position obeys to the following equation of motion:

$$m^* \frac{d^2\mathbf{r}}{dt^2} = \mathbf{F}_{12}(\mathbf{r}) \tag{2.7}$$

where

$$m^* = \left(\frac{1}{m_1} + \frac{1}{m_2} \right)^{-1} \tag{2.8}$$

is the reduced mass of the system of two particles. If the collision is elastic an interaction potential can be introduced so that:

$$\mathbf{F}_{12} = -\frac{dU(r)}{dr}\hat{\mathbf{r}} \tag{2.9}$$

where $\hat{\mathbf{r}}$ is the unit vector along the direction of the relative position of the two particles. The force vector lies in the same plane where the relative position vector and relative velocity vector lie. The evolution of the relative position r is the evolution of the position of a particle of mass m^* in a central potential $U(r)$. The angular momentum of the relative motion $\mathbf{L} = \mathbf{r} \times m^*\mathbf{V}_{12}$ is conserved. This means that the particle trajectory, during the collision, will be confined to this plane. In Fig. 2.1 is sketched the typical binary scattering event when the interacting force is repulsive (monotonically decreasing potential), in the center of mass frame.
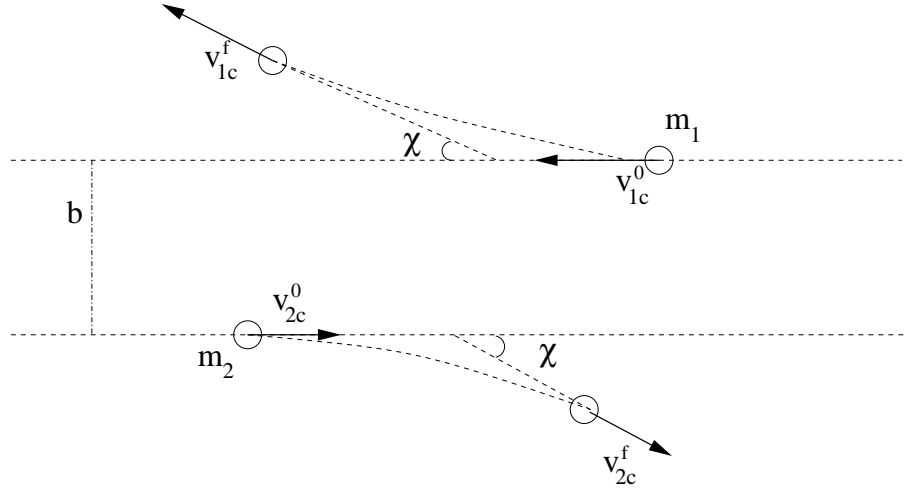
Figure 2.1: The binary elastic scattering event in the center of mass frame, with a repulsive potential of interaction

In the center of mass frame the elastic scattering has a very simple picture: the velocities of the particles are $\mathbf{v}_{1c} = \mathbf{V}_{12}m^*/m_1$ and $\mathbf{v}_{2c} = -\mathbf{V}_{12}m^*/m_2$. The elastic collision conserves the modulus of the relative velocity V_{12} and therefore also the moduli of the velocities of the particles in the center of mass frame. If one consider the collision event as a black box and observes the velocities of the particles "before" and "after" the interaction (i.e. asymptotically, when the interaction is negligible), then the velocity vectors are simply rotated of an angle χ called *angle of deflection*, which also represents the angle between asymptotic initial and final directions of the relative velocity. During the collision the total momentum is conserved (this happens also for inelastic collisions) but is redistributed between the two particles, i.e. the variation of the momentum of the particle 1 is $\delta(m_1\mathbf{v}_1) = m^*(\mathbf{V}'_{12} - \mathbf{V}_{12})$ where the prime indicates the post-collisional relative velocity. Obviously $\delta(m_1\mathbf{v}_1) = -\delta(m_2\mathbf{v}_2)$. Finally, one can calculate the components of the momentum transfer parallel and perpendicular to the relative velocity:

$$\delta(m_1 v_1)_{\parallel} = -m^* V_{12}(1 - \cos\chi) \qquad (2.10\text{a})$$

$$\delta(m_1 v_1)_{\perp} = m^* V_{12}\sin\chi. \qquad (2.10\text{b})$$

To calculate the angle of deflection χ one needs the exact form of the interaction potential, the asymptotic initial relative velocity V_{12}^0 (i.e. at a distance such that the interaction is negligible) and the *impact parameter* b that is the minimal distance between the trajectories of the particles if there were no interaction between them:

$$\chi = \pi - 2\int_{r_m}^{\infty} dr \frac{b}{r}\left[r^2 - b^2 - \frac{2r^2 U(r)}{m^*(V_{12}^0)^2}\right]^{-1/2} \qquad (2.11)$$

where r_m is the closest distance effectively reached by the two particles. From Eq. (2.11) it is evident that the angle of deflection decreases as the initial relative velocity increases.

2.2 Hard spheres

Hard spheres are one of the simplest models of molecular fluids and have represented for many years the testing ground for the predictions of the kinetic theory, thanks to the pioneering efforts of physicists who have developed hard spheres simulations on the old computers which were huge in encumbrance and very small in power (the work of Alder and Wainwright is considered the foundation of this subject [2, 3, 1, 4, 5]). Nowadays liquids and gases are almost always simulated with different tools and models (e.g. Lenard-Jones potentials or others), i.e. typically *soft spheres* models. Nevertheless the study of granular materials has again awakened the interest in hard spheres molecular dynamics, as the geometric character of the grain-grain interaction seems to be better modeled by an hard core interaction. Here we define the hard core potential and give expressions for the quantities calculated in the previous paragraphs.

Two hard spheres in 3D (hard disks in 2D, hard rods in 1D) of diameters σ_1 and σ_2 interact by means of a discontinuous potential $U(r)$ of the form:

$$U(r) = 0 \quad (r > \sigma_{12}) \tag{2.12a}$$

$$U(r) = \infty \quad (r < \sigma_{12}) \tag{2.12b}$$

where $\sigma_{12} = (\sigma_1 + \sigma_2)/2 = r_m$ is the distance of the centers of the spheres at contact. The potential in Eq. (2.12) can be taken as a definition of hard spheres systems. In this case the deflection angle is given by:

$$\chi = 2 \arccos\left(\frac{b}{\sigma_{12}}\right) \tag{2.13}$$

and the dependence from the initial relative velocity disappears (only geometry determines the deflection angle).
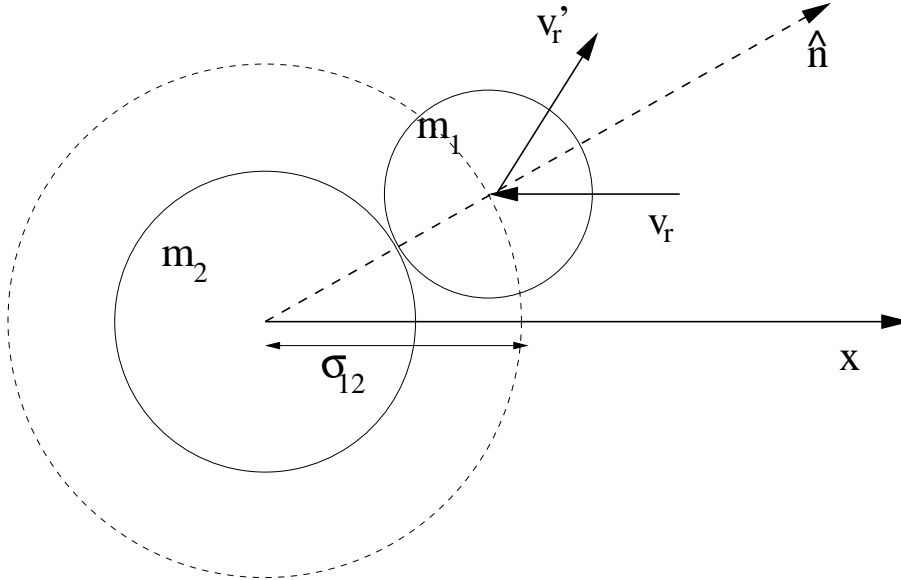
Figure 2.2: The collision between two elastic smooth hard spheres

Finally we give a definition of *smooth hard spheres* (we consider this model as a paradigm for granular gases): smoothness is the absence of irregularities on the surface of the spheres, i.e. the instantaneous collision does not change the rotational degrees of freedom of the spheres at contact. Therefore, in the study of smooth hard spheres systems, a complete description of the dynamics requires only the positions of the centers $\mathbf{r}$ and their velocities $\mathbf{v}$. In particular the collision is an instantaneous

transformation of the velocities of two particles i and j at contact which are "reflected" with the following rule (see Fig. 2.2 on the previous page):

$$\mathbf{v}'_i = \mathbf{v}_i - \frac{2m_2}{m_1 + m_2}\hat{\mathbf{n}}[\hat{\mathbf{n}} \cdot (\mathbf{v}_i - \mathbf{v}_j)] \tag{2.14}$$

$$\mathbf{v}'_j = \mathbf{v}_j + \frac{2m_1}{m_1 + m_2}\hat{\mathbf{n}}[\hat{\mathbf{n}} \cdot (\mathbf{v}_i - \mathbf{v}_j)] \tag{2.15}$$

$$\tag{2.16}$$

where $\hat{\mathbf{n}} = (\mathbf{r}_i - \mathbf{r}_j)/|\mathbf{r}_i - \mathbf{r}_j|$ and the primes denote the velocities after the collision. This collision rule conserves momentum and kinetic energy. It only changes the direction of the component of the relative velocity of the particles in the direction of $\hat{\mathbf{n}}$ (normal component), leaving unchanged the tangential component.

2.3   Statistics of hard spheres collisions

The concept of *mean free path* was introduced in 1858 by Rudolf Clausius [41] and paved the road to the development of the kinetic theory of gas. For the sake of simplicity (and coherently with the rest of this work, as well as with the literature on granular gases) we consider a single species gas composed of hard spheres, all having the same diameter σ and mass m (see [40]).

The *mean free time* is the average time between two successive collisions of a single particle. We define νdt the probability that a given particle suffers a collision between time t and $t + dt$ (ν is called collision frequency) and assume that ν is independent of the past collisional history of the particle. The probability $f_{time}dt$ of having a free time between two successive collisions larger than t and shorter than $t + dt$ is equal to the product of the probability that no collision occurs in the time interval $[0, t]$ and the probability that a collision occurs in the interval $[t, t + dt]$:

$$f_{time}(t)dt = P_{time}(t)\nu dt \tag{2.17}$$

where $P_{time}(t)$ is the survival probability, that is the probability that no collisions happen between 0 and t, and can be calculated observing that $P_{time}(t + dt) = P_{time}(t)P_{time}(dt) = P_{time}(t)(1 - \nu dt)$ so that $dP_{time}/dt = -\nu P_{time}$, i.e. $P_{time}(t) = e^{-\nu t}$.

Finally one can calculate the average of the free time using the probability density $f_{time}(t)$:

$$\tau = \int_0^\infty dt\, t\, f_{time}(t) = \int_0^\infty dt\, t\nu e^{-\nu t} = \frac{1}{\nu}. \tag{2.18}$$

With the same sort of calculations an expression for the mean free path, that is the average distance traveled by a particle between two successive collisions, can be calculated. One again assumes that there is a well defined quantity (independent of the collisional history of the particle) αdl which is the probability of a collision during the travel between distances l and $l + dl$. The survival probability in terms of space traveled is $P_{path}(l) = e^{-\alpha l}$ and the probability density of having a free distance l is $f_{path}(l) = e^{-\alpha l}\alpha$ so that the mean free path is given by:

$$\lambda = \frac{1}{\alpha} \tag{2.19}$$

The other important statistical quantity in the study of binary collisions is the so-called *differential scattering cross section* s which is defined in this way: in a unit time a particle suffers a number of collisions which can be seen as the incidence of fluxes of particles coming with different approaching velocities $\mathbf{V}_{12}$ and scattered to new different departure velocities $\mathbf{V}'_{12}$. Given a certain approaching velocity $\mathbf{V}_{12}$ the incident particles arrive with slightly different impact parameters (due to the extension of the particles), and therefore are scattered in a solid angle $d\Omega'$. If I_0 denotes the intensity of the beam of particles that come with an average approaching speed $\mathbf{V}_{12}$, which is the number of particles

intersecting in unit time a unit area perpendicular to the beam ($I_0 = nV_{12}$ with n the number density of the particles), then the rate of scattering dR into the small solid angle element $d\Omega'$ is given by

$$\frac{dR}{d\Omega'} = I_0 s(\mathbf{V}_{12}, \mathbf{V}'_{12}) \tag{2.20}$$

where s is a factor of proportionality with the dimensions of an area (in $3D$) which is called differential cross section and depends on the relative velocity vectors before and after the collisions. The total rate of particles scattered in all directions, R is the integral of the last equation:

$$R = I_0 \int \int_{4\pi} d\Omega' s(\mathbf{V}_{12}, \mathbf{V}'_{12}) = SI_0 \tag{2.21}$$

and defines the total scattering cross section S.

In the case of a spherically symmetric central field of force the differential cross section is a function only of the modulus of the initial relative velocity V_{12}, the angle of deflection χ, and the impact parameter b which in turn, once fixed the potential $U(r)$, is a function only of χ and V_{12}, that is $s = s(V_{12}, \chi)$. In particular it can be easily demonstrated that

$$s(V_{12}, \chi) = -\frac{b(V_{12}, \chi)}{\sin \chi} \frac{db}{d\chi}. \tag{2.22}$$

The differential scattering cross section for hard spheres is calculated from Eq. (2.22) obtaining a very simple formula: $s(V_{12}, \chi) = \sigma^2/4$ which can be integrated over the entire solid angle space giving an expression for the total cross section $S = \pi\sigma^2$. This result is consistent with the physical intuition of the cross section: it is the average of the areas of influence of the scatterer in the planes perpendicular to the approaching velocities of the incident particles.

In addition to the differential and total scattering cross sections, in non-equilibrium transport theory several other cross sections are defined:

$$S_k(V_{12}) = \int_0^{2\pi} d\epsilon \int_0^{\pi} d\chi \sin \chi (1 - cos^k \chi) s(V_{12}, \chi) \tag{2.23}$$

where k is a positive integer (n=1,2,....). For instance, the transfer of the parallel component of the particle momentum is proportional to $1 - \cos \chi$ (see Eq. (2.10)) and therefore S_1 is related to the transport of momentum and plays an important role in the study of diffusion. Moreover, viscosity and heat conductivity depend on S_2.

For hard spheres these quantities are easily calculated. The first two are given here:

$$S_1 = \pi\sigma^2 \tag{2.24a}$$

$$S_2 = \frac{2}{3}\pi\sigma^2 \tag{2.24b}$$

To conclude this paragraph we recall that the collision frequency defined at the beginning is strictly tied to the total scattering cross section by the relation

$$\nu = nS\overline{V_{12}} \tag{2.25}$$

where n is the average density of the gas and $\overline{V_{12}}$ is an average of the relative velocities. Generally speaking (in the framework of a non-equilibrium discussion) n and $\overline{V_{12}}$ are averages taken in space-time regions in which equilibrium can be assumed. Assuming that in this region the distribution of velocities of the particle is the Maxwell-Boltzmann distribution:

$$f(\mathbf{v}) = \frac{m^{3/2}}{(2\pi k_B T)^{3/2}} e^{-\frac{mv^2}{2k_B T}} \tag{2.26}$$

the collision frequency can be calculated obtaining the formula:

$$\nu = \sqrt{2}nS\overline{v} \tag{2.27}$$

where $\overline{v}$ is the average of the modulus of the velocities and, in this case, is given by:

$$\overline{v} = \sqrt{\frac{8k_BT}{\pi m}}. \tag{2.28}$$

In the same way the mean free path is given by

$$\lambda = \frac{1}{\sqrt{2}nS}. \tag{2.29}$$

2.4   The effects of inelasticity

Granular particles collide dissipating relative kinetic energy. This is due to the macroscopic nature of the grains which leads to the presence of internal degrees of freedom. During the interaction, irreversible processes happen inside the grain and energy is dissipated in form of heat. All these processes conserve momentum, so that the velocity of the center of mass of the two grains is not modified.

Many modelizations of the binary inelastic collision have been proposed (soft spheres [171, 170, 35, 77, 113] as well as hard spheres models [36, 79, 71, 124]): this is usually a difficult problem relatively to the information that can be gained from. Simplification often pays more, as very idealized models lead to interesting and physically meaningful results. The most used model in granular gas literature is also the most simple one, that is the inelastic smooth hard spheres gas with the *fixed restitution coefficient rule* given by the following prescriptions:

$$m_1\mathbf{v}'_1 + m_2\mathbf{v}'_2 = m_1\mathbf{v}_1 + m_2\mathbf{v}_2 \tag{2.30a}$$

$$(\mathbf{v}'_1 - \mathbf{v}'_2) \cdot \hat{\mathbf{n}} = -r(\mathbf{v}_1 - \mathbf{v}_2) \cdot \hat{\mathbf{n}} \tag{2.30b}$$

where, as usual, the primes denote the postcollisional velocities, $\hat{\mathbf{n}}$ is the unity vector in the direction joining the centers of the grains, and $0 \leq r \leq 1$. In this model the collisions happen at contact and are instantaneous. When $r = 1$ the gas is elastic and the rule coincides with the collision description for hard spheres given in the paragraph 2.2. When $r = 0$ the gas is perfectly inelastic, that is the particles exit from the collision with no relative velocity in the $\hat{\mathbf{n}}$ direction.

As a matter of fact, the transformation that gives the (primed) postcollisional velocities from the precollisional velocities of the two colliding particles is

$$\mathbf{v}'_1 = \mathbf{v}_1 - (1+r)\frac{m_2}{m_1 + m_2}((\mathbf{v}_1 - \mathbf{v}_2) \cdot \hat{\mathbf{n}})\hat{\mathbf{n}} \tag{2.31a}$$

$$\mathbf{v}'_2 = \mathbf{v}_2 + (1+r)\frac{m_1}{m_1 + m_2}((\mathbf{v}_1 - \mathbf{v}_2) \cdot \hat{\mathbf{n}})\hat{\mathbf{n}} \tag{2.31b}$$

Sometimes it may be useful to have the reverse transformation that give precollisional velocities from postcollisional ones, with the primes exchanged:

$$\mathbf{v}'_1 = \mathbf{v}_1 - \left(1 + \frac{1}{r}\right)\frac{m_2}{m_1 + m_2}((\mathbf{v}_1 - \mathbf{v}_2) \cdot \hat{\mathbf{n}})\hat{\mathbf{n}} \tag{2.32a}$$

$$\mathbf{v}'_2 = \mathbf{v}_2 + \left(1 + \frac{1}{r}\right)\frac{m_1}{m_1 + m_2}((\mathbf{v}_1 - \mathbf{v}_2) \cdot \hat{\mathbf{n}})\hat{\mathbf{n}} \tag{2.32b}$$

As it can be seen, the inverse transformation is equivalent to a change of the restitution coefficient $r \to 1/r$. Obviously in the case of a perfectly inelastic gas ($r = 0$) there is no inverse transformation. We also note that in 1D and when $m_1 = m_2$ Eqs. (2.31) become:

$$v_1' = \frac{1-r}{2}v_1 + \frac{1+r}{2}v_2 \tag{2.33a}$$

$$v_2' = \frac{1+r}{2}v_1 + \frac{1-r}{2}v_2 \tag{2.33b}$$

which coincide to an exact exchange of velocities in the elastic $(r = 1)$ case, and in a sticky collision in the perfectly inelastic $(r = 0)$ case. In dimensions higher than *one* the $r = 0$ case is very different from the so-called *sticky gas*, which is defined as a gas of hard spheres that in a collision become stuck together. In one dimension, instead, the $r = 0$ case may be considered equivalent to a sticky gas but a further prescription of "stickiness" must be given in order to consider collisions among more than two particles.

Variants of this models have been largely used in the literature. The importance of tangential frictional forces acting on the grains at contact may be studied taking into account the rotational degree of freedom of the particles, i.e. adding a variable ω_i to each grain. The most simplified model which takes into account the rotational degree of freedom of particles is the rough hard spheres gas ([84, 117, 116, 72, 122, 81, 115]). In this model the postcollisional translational and angular velocities are given by the following equations (where the bottom signs in $\pm$ are to be considered for particle 2):

$$\mathbf{v}_{1,2}' = \mathbf{v}_{1,2} \mp \frac{1+r}{2}\mathbf{v}_n \mp \frac{q(1+\beta)}{2q+2}(\mathbf{v}_t + \mathbf{v}_r) \tag{2.34a}$$

$$\sigma\boldsymbol{\omega}_{1,2}' = \sigma\boldsymbol{\omega}_{1,2} + \frac{1+\beta}{2q+2}[\hat{\mathbf{n}} \times (\mathbf{v}_t + \mathbf{v}_r)] \tag{2.34b}$$

where q is the dimensionless moment of inertia defined by $I = qm\sigma^2$ (with I the moment of inertia of the hard object), e.g. $q = 1/2$ for disks and $q = 2/5$ for spheres; $\mathbf{v}_n = ((\mathbf{v}_1 - \mathbf{v}_2) \cdot \hat{\mathbf{n}})\hat{\mathbf{n}}$ is the normal relative velocity component, $\mathbf{v}_t = \mathbf{v}_1 - \mathbf{v}_2 - \mathbf{v}_n$ is the tangential velocity component due to translational motion, while $\mathbf{v}_r = -\sigma(\boldsymbol{\omega}_1 - \boldsymbol{\omega}_2)$ is the tangential velocity component due to particle rotation. In Eqs. (2.34) the tangential restitution coefficient β appears: it may take any value between -1 and $+1$. When $\beta = -1$ tangential effects disappear, i.e. rotation is not affected by collision (rough spheres become smooth spheres). When $\beta = +1$ the particles are said to have perfectly rough surface. It can be easily seen that (when $r = 1$) energy is conserved for $\beta = \pm 1$.

Moreover, a new class of models for collisions has been recently introduced, justified by a deeper analysis of the collision process. In these models the restitution coefficient r (or the coefficients r and β in the more detailed description given above) depends on the relative velocity of the colliding particles. In particular it has been seen that the collision tends to become more and more elastic as the relative velocity tends to zero. This refined prescription, referred to as 'viscoelastic' model [78, 29], has relevance (usually quantitative rather than qualitative) in different issues of the statistical mechanics of granular gases. An important kinetic instability of the cooling (and sometimes driven) granular gases is the so-called *inelastic collapse* [123, 124], i.e. a divergence of the local collision rate due to the presence of a few particles trapped very close to each other: simulations of the gas with the viscoelastic model have shown that this instability is removed, suggesting that it is an artifact of the fixed restitution coefficient idealization.

Here we give an expression of the leading term for the velocity dependence of the normal restitution coefficient r in the viscoelastic model (the viscoelastic theory may be applied to give also a velocity dependent expressions for the tangential restitution coefficient):

$$r = 1 - C_1|(\mathbf{v}_1 - \mathbf{v}_2) \cdot \hat{\mathbf{n}}|^{1/5} + ... \tag{2.35a}$$

where C_1 depends on the physical properties of the spheres (mass, density, radius, Young modulus, viscosity).

2.5   A couple of examples of granular kinetic "problems"

2.5.1   The Kadanoff model

In 1995 Du, Li and Kadanoff [52] have published the results of the simulation of a minimal model of granular gas in one dimension. In this model N hard rods (i.e. hard particles in one dimension) move on a segment of length L interacting by instantaneous binary inelastic collisions with a restitution coefficient $r < 1$. To avoid the cooling down of the system (due to inelasticity) a thermal wall is placed at the one of the boundaries, i.e. when the leftmost particle bounces against the left extreme ($x = 0$) of the segment, it is reflected with a new velocity taken out from a Gaussian distribution with variance T. This particle carries the energy to the rest of the system. The main finding of the authors was that even at very small dissipation $1 - r << 1$ the profiles predicted by general hydrodynamic equations (they used constitutive relations of Haff [73] or Jenkins and Richman [84]) were not able to reproduce the essential features of the simulation. In particular the stationary state predicted by hydrodynamics is a flow of heat from the left wall to the right (it goes to zero at the right wall), with no macroscopic velocity flow ($u(x,t) = 0$), a temperature profile $T(x,t)$ which decreases from $x = 0$ to $x = L$, and a density profile inversely proportional to the temperature (as the pressure $p = nT$ is constant throughout the system). In Fig. 2.3 some snapshots of the system (i.e. the position of the grains at different instants) are shown. The system is in an "extraordinary" state with almost all the particle moving slowly and very near the right wall, while almost all the kinetic energy is concentrated in the leftmost particle. The system cannot be considered in a stationary state, even if its kinetic energy is statistically stationary (i.e. fluctuates around a well defined average which is time translational invariant). Moreover, reducing the dissipativity $1 - r$ at fixed N the cluster near the wall becomes smaller and smaller. If the heat bath is replaced by a sort of saw-tooth vibrating wall which reflects the leftmost particle always with the same velocity v_0, the evolution of the baricentrum changes in a stationary oscillation very near to the rightmost wall, so that this clustering instability does not disappear. The authors also point out the fact that the Boltzmann Equation can give a qualitative prediction of this clustering phenomena in the limit $N \to \infty$, $1 - r \to 0$ with $N(1 - r) \sim 1$. We have reproduced the results of Du et al. and have discovered the this model has no proper thermodynamic limit, i.e. when $N, L \to \infty$ with $N/L \sim 1$ the mean kinetic energy and the mean dissipated power reduce to zero. This is consistent with the scenario suggested by the authors: the equipartition of energy (i.e. local equilibration of the different degrees of freedom) is broken and the description of the system in terms of macroscopic (slowly varying) quantities no more holds. In this scenario, usual thermodynamic quantities such as mean kinetic energy or mean dissipated power, are not extensive quantities.
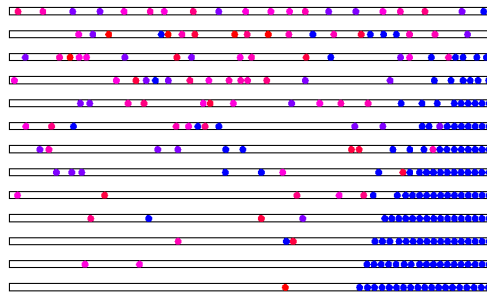
Figure 2.3: Some snapshots of the 1D system from the work of Du et al. [52]

L. P. Kadanoff has also addressed, in a recent review article [86], a set of experimental situations in which hydrodynamics seems useless. We have already discussed a well known experiment by Jaeger, Knight, Liu and Nagel [82] where a container full of sand is shaken from the bottom, when the shaking is very rapid. The observations indicate that there is a boundary layer of a thickness of few grains near

the bottom that is subject to a very rapid dynamics with sudden changes of motion of the particles. At the top of the container, instead, the particles move ballistically encountering very few collisions in their trajectory. Both the top and the bottom of the container cannot be described by hydrodynamics, as the assumption of slow variation of fields or that of scale separation between times (the mean free time must be orders of magnitude lower than the characteristic macroscopic times, as the vibration period) are not satisfied. On the other hand, the slow dynamics regime has been studied, when the vibration is reduced to a rare tapping, so that the system reaches mechanical equilibrium (stop of motion) between successive tappings [90]. The equilibrium is reached at different densities, and - as the tapping is carried on - the "equilibrium" density slowly changes and its evolution depends on many previous instants and not on the very last tap, i.e. is history dependent. This non-locality in time cannot be described by a set of partial differential equations, therefore the hydrodynamic description here again fails.

2.5.2   Inelastic collapse

The situation discussed in the previous example can be even more dramatic in the case of inelastic collapse. The simplest example involves just three particles, as shown in Fig. 2.4 [16, 123]. The two outer particles move monotonically toward each other and the one in the middle bounces between them. One can easily show that, after the two collisions shown in the figure, the relation between the final and initial velocities is $\mathbf{u}' = \mathcal{M}\mathbf{u}$ where $\mathbf{u} = (\mathbf{u_1}, \mathbf{u_2}, \mathbf{u_3})^{\mathbf{T}}$ and $\mathcal{M}$ is a 3x3 matrix whose entries are quadratic polynomials in r. If this matrix has one real eigenvalue in the interval $(0, 1)$, the cycle shown in Figure endlessly repeats with geometrically smaller space and time scales at each successive cycle. This requires $r = r_c < 7 - 4\sqrt{3} \approx 0.0718$ to happen. In this case an infinite number of collision happens in a finite time. When $r > r_c$, inelastic collapse can still occur, but with the collective participation of more than three particles, or with the presence of an inelastic wall (because of symmetry, this is equivalent to an interaction between four inelastic particles), as discussed in the figure. As the coefficient of restitution r increases toward 1, the number of particles required for collapse increases. For instance, with $r = 0.8$, it is required that $N = 16$ particles bounce off an inelastic wall. Rough estimates suggest (in agreement with numerical calculations) that $N_{min}(r) \approx ln(4/(1 - r))/(1 - r)$ as $r \to 1$.
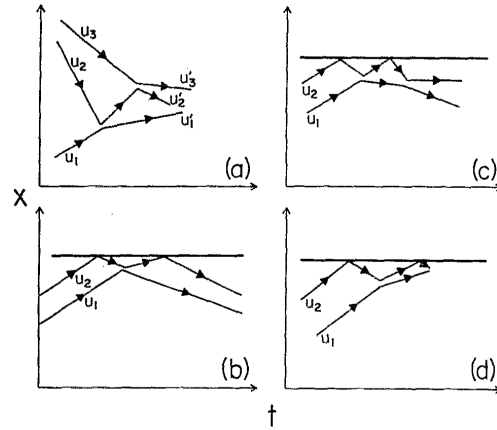
Figure 2.4: Examples of particles' trajectories with or without a wall: (a) three particles collapse ($r < 7 - 4\sqrt{3} \approx 0.0718$); (b) two particles bouncing off an inelastic wall: when $r > 0.346015$ they finally leaves the wall and never come back; (c) critical value $r = 0.346015$, the inner ball remains stationary after two collisions with the other particle; (d) when $r < 3 - 2\sqrt{2} \approx 0.17157$ there is inelastic collapse.

The simulation of cooling granular gases have also interested L. P. Kadanoff in his excursus of the

limits of hydrodynamics. The clustering instabilities and the inelastic collapse are clear signatures of the failure of macroscopic description. Moreover, in the inelastic collapse Kadanoff and Zhou [176] have pointed out (see Fig. 2.5) that there is a correlation between velocity directions of the particles involved in the collapse: in particular collapse is favored by parallel velocities (because they cannot escape in perpendicular directions). This situation implies a dramatic breakdown of Molecular Chaos assumption and gives evidence of the fact that Inelastic Collapse cannot be described even by a Boltzmann equation.
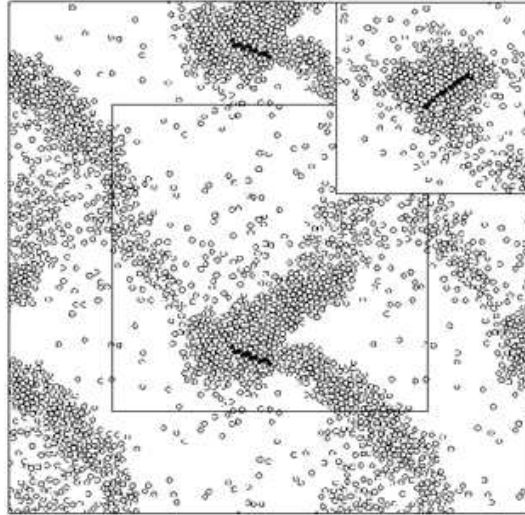
Figure 2.5: A snapshot from a MD simulation of cooling inelastic hard spheres [176]. The particles in black are those that have participated in the last collisions, just before a collapse

Lecture 3

The granular Boltzmann equation

3.1   The Liouville and the pseudo-Liouville equations

In order to discuss the behavior of a system of N identical hard spheres (of diameter σ and mass m) it is natural to introduce the phase space, i.e., a $6N-$dimensional space where the coordinates are the $3N$ components of the N position vectors of the sphere centers $\mathbf{r}_i$ and the $3N$ components of the N velocities $\mathbf{v}_i$. The state of the system is represented by a point in this space. We call $\mathbf{z}$ the $6N$-dimensional position vector of this point. If the positions $\mathbf{r}_i$ of the spheres are restricted in a space region Ω, then the full phase space is given by the product $\Omega^N \times \Re^{3N}$

If the state is not known with absolute accuracy, we must introduce a probability density $P(z, t)$ which is defined by

$$Prob(z \in \mathbf{D} \quad \text{at time } t) = \int_{\mathbf{D}} P(\mathbf{z}, t) d\mathbf{z} \tag{3.1}$$

where $d\mathbf{z}$ is the Lebesgue measure in phase space and we implicitly assume that the probability is a measure absolutely continuous with respect to the Lebesgue measure.

The mean value of a dynamical observable $A(\mathbf{z})$ can be calculated from either the following expressions:

$$\int_{\infty} d\mathbf{z} P(\mathbf{z}, 0) A(\mathbf{z}(t)) = \int_{\infty} d\mathbf{z} P(\mathbf{z}, t) A(\mathbf{z}) \tag{3.2}$$

which are respectively the Lagrangian and Eulerian averages (analogous to the Heisemberg and Schroedinger averages in quantum mechanics). In Eq. (3.2) the time dependence of the observable A and of the distribution P is due to the time evolution operator S_t (also called *streaming operator*, that is $A(\mathbf{z}(t)) \equiv S_t(\mathbf{z}) A(\mathbf{z})$. Considering the equivalence in Eq. (3.2) as an inner product implies that

$$P(\mathbf{z}, t) = S_t^{\dagger} P(\mathbf{z}, 0) \tag{3.3}$$

where $S_t^{\dagger}$ is the adjoint of S_t.

In a general system (not necessarily made of hard spheres) with conservative and additive interactions, the force between the particle pair (ij) is $\mathbf{F}_{ij} = -\partial V(r_{ij})/\partial \mathbf{r}_{ij}$ so that the time evolution operator is given by:

$$S_t(\mathbf{z}) = \exp[tL(\mathbf{z})] = \exp\left[t \sum_i L_i^0 - t \sum_{i<j} \Theta(ij) \right] \tag{3.4}$$

where the *Liouville operator* $L(\mathbf{z})... \equiv \{H(\mathbf{z}), ...\}$ is the Poisson bracket with the Hamiltonian, so that

$$L_i^0 = \mathbf{v}_i \cdot \frac{\partial}{\partial \mathbf{r}_i} \tag{3.5a}$$

$$\Theta(ij) = \frac{1}{m} \frac{\partial V(r_{ij})}{\partial \mathbf{r}_{ij}} \cdot \left(\frac{\partial}{\partial \mathbf{v}_i} - \frac{\partial}{\partial \mathbf{v}_j} \right) \tag{3.5b}$$

and $S_t(\mathbf{z})$ is a unitary operator, $S_t^\dagger = S_{-t}$, while $L^\dagger = -L$. In Eq. (3.4) the evolution operator S_t has been divided into a free streaming operator $S_t^0 = \exp[t \sum_i L_i^0]$ which generates the free particle trajectories, plus a term containing the binary interactions among the particles.

Finally the Liouville equation is obtained writing explicitly Eq. (3.3):

$$\frac{\partial}{\partial t} P(\mathbf{z}, t) = \left(- \sum_i L_i^0 + \sum_{i<j} \Theta(ij) \right) P(\mathbf{z}, t) \tag{3.6}$$

which is an expression of the incompressibility of the flow in phase space.

In the specific case of identical hard spheres, the interaction among particles is defined by Eq. (2.12). It can be shown that this kind of interaction carries no contraction of phase space at collision, i.e.

$$P(\mathbf{z}', t) = P(\mathbf{z}, t) \tag{3.7}$$

where $\mathbf{z}'$ and $\mathbf{z}$ are the phase space points before and after a collision. This can be considered a form of detailed balance law. It is important to stress that $\mathbf{z}' \neq \mathbf{z}$: a collision represents a time discontinuity in the velocity section of phase space. In particular we use the elastic collision model defined in this list of prescriptions (it coincides with the collision rule for smooth hard spheres, see Eq. (2.14)):

$$|\mathbf{r}_i - \mathbf{r}_j| = \sigma \tag{3.8a}$$

$$\hat{\mathbf{n}}_{ij} = (\mathbf{r}_i - \mathbf{r}_j)/\sigma \tag{3.8b}$$

$$\mathbf{V}_{ij} = \mathbf{v}_i - \mathbf{v}_j \tag{3.8c}$$

$$\mathbf{V}_{ij} \cdot \hat{\mathbf{n}}_{ij} < 0 \tag{3.8d}$$

$$\mathbf{z} \equiv (\mathbf{r}_1, \mathbf{v}_1, \mathbf{r}_2, \mathbf{v}_2, ..., \mathbf{r}_i, \mathbf{v}_i, ..., \mathbf{r}_j, \mathbf{v}_j, ..., \mathbf{r}_N, \mathbf{v}_N) \tag{3.8e}$$

$$\mathbf{z}' \equiv (\mathbf{r}_1, \mathbf{v}_1, \mathbf{r}_2, \mathbf{v}_2, ..., \mathbf{r}_i', \mathbf{v}_i', ..., \mathbf{r}_j', \mathbf{v}_j', ..., \mathbf{r}_N, \mathbf{v}_N) \tag{3.8f}$$

$$\mathbf{r}_i' = \mathbf{r}_i \tag{3.8g}$$

$$\mathbf{r}_j' = \mathbf{r}_j \tag{3.8h}$$

$$\mathbf{v}_i' = \mathbf{v}_i - \hat{\mathbf{n}}_{ij}(\hat{\mathbf{n}}_{ij} \cdot \mathbf{V}_{ij}) \tag{3.8i}$$

$$\mathbf{v}_j' = \mathbf{v}_j + \hat{\mathbf{n}}_{ij}(\hat{\mathbf{n}}_{ij} \cdot \mathbf{V}_{ij}) \tag{3.8j}$$

$$\tag{3.8k}$$

these relations conserve the total momentum and the total energy of the system.

To derive the Boltzmann equation, the collisions events $\mathbf{z} \to \mathbf{z}'$ are considered as boundary conditions and the Liouville Equation (3.6) is restricted to the interior of the phase space region $\Lambda \equiv \Omega^N \times \Re^{3N} - \Lambda_{ov}$ where

$$\Lambda_{ov} = \left\{ \mathbf{z} \in \Omega^N \times \Re^{3N} \mid \exists\, i, j \in \{1, 2, ..., N\} \, (i \neq j) : |\mathbf{r}_i - \mathbf{r}_j| < \sigma \right\} \tag{3.9}$$

is the set of phase space points such that one or more pairs of spheres are overlapping. With this conditions, the Liouville equation reads:

$$\frac{\partial}{\partial t} P(\mathbf{z}, t) = \left(-\sum_i \mathbf{v}_i \cdot \frac{\partial}{\partial \mathbf{r}_i} \right) P(\mathbf{z}, t) \quad (\mathbf{z} \in \Lambda) \tag{3.10a}$$

$$P(\mathbf{z}, t) = P(\mathbf{z}', t) \quad (\mathbf{z} \in \partial\Lambda) \tag{3.10b}$$

This version of the Liouville equation is time-discontinuous: this means that formal perturbation expansions used in usual many-body theory methods cannot be applied to it.

An alternative master equation for the probability density function in the phase space can be derived [56]. The streaming operator S_t for hard spheres is not defined for any point of the phase space $\mathbf{z} \in \Lambda_{ov}$. In the calculation of the average (3.2) of physical observables, this is not a problem, as the streaming operators appears multiplied by $P(\mathbf{z}, 0)$ which is proportional to the characteristic function $X(\mathbf{z})$ of the set Λ (the characteristic function is 1 for points belonging to the set and 0 for points outside of it). In perturbation expansions it is safer to have a streaming operator defined for every point of the configurational space. A standard representation, defined for all points in the phase space, has been developed for elastic hard spheres and is based on the binary collision expansion of $S_t(\mathbf{z})$ in terms of binary collision operators. The binary collision operator is defined in terms of two-body dynamics through the following representation of the streaming operator for the evolution of two particles:

$$S_t(1, 2) = S_t^0(1, 2) + \int_0^t d\tau\, S_\tau^0(1, 2) T_+(1, 2) S_{t-\tau}^0(1, 2) \tag{3.11}$$

with $S_t^0 = \exp(tL_0)$ the free flow operator and a collision operator

$$T_+(1, 2) = \sigma^2 \int_{\mathbf{V}_{12} \cdot \hat{\mathbf{n}} < 0} d\hat{\mathbf{n}} |\mathbf{V}_{12} \cdot \hat{\mathbf{n}}| \delta(\sigma\hat{\mathbf{n}} - (\mathbf{r}_1 - \mathbf{r}_2))(b_c - 1) \tag{3.12}$$

where b_c is a substitution operator that replaces $\mathbf{v}_1, \mathbf{v}_2$ with $\mathbf{v}_1', \mathbf{v}_2'$ (see Eqs. (3.8)).

The Eq. (3.11) is a representation of the evolution of two particles as a convolution of free flow and collisional events. Noting that $T_+(1, 2) S_\tau^0(1, 2) T_+(1, 2) = 0$ for $\tau > 0$ (two hard spheres cannot collide more than once), Eq. (3.11) can be put in the form

$$S_t(1, 2) = \exp\left\{t[L_0(1, 2) + T_+(1, 2)]\right\} \tag{3.13}$$

that can be generalized to the N-particle streaming operator (here considered for the case of an infinite volume):

$$S_{\pm t}(\mathbf{z}) = \exp\left\{\pm t[L_0(\mathbf{z}) \pm \sum_{i<j} T_\pm(i, j)]\right\} \tag{3.14}$$

where

$$T_-(1, 2) = \sigma^2 \int_{\mathbf{V}_{12} \cdot \hat{\mathbf{n}} > 0} d\hat{\mathbf{n}} |\mathbf{V}_{12} \cdot \hat{\mathbf{n}}| \delta(\mathbf{r}_1 - \mathbf{r}_2 - \sigma\hat{\mathbf{n}})(b_c - 1) \tag{3.15}$$

Equation (3.14) defines the so-called *pseudo-streaming operator*. In order to write an analogue of the Liouville Equation (3.6), the adjoint of $S_{\pm t}$ is needed: its definition is identical to that in Eq. (3.14) but for the binary collision operators which must be replaced by their adjoints:

$$\overline{T}_\pm(1, 2) = \sigma^2 \int_{\mathbf{V}_{12} \cdot \hat{\mathbf{n}} \lessgtr 0} d\hat{\mathbf{n}} |\mathbf{V}_{12} \cdot \hat{\mathbf{n}}| [\delta(\mathbf{r}_1 - \mathbf{r}_2 - \sigma\hat{\mathbf{n}}) b_c - \delta(\mathbf{r}_1 - \mathbf{r}_2 + \sigma\hat{\mathbf{n}})] \tag{3.16}$$

Finally the pseudo-Liouville equation can be written:

$$\frac{\partial}{\partial t}P(\mathbf{z},t)=\left(-\sum_i L_i^0 + \sum_{i<j}\overline{T}_-(ij)\right)P(\mathbf{z},t). \tag{3.17}$$

This equation is the analogue of Eq. (3.6) for the case of hard core potential (hard spheres). In this sense it replaces Eq. (3.10) and will be used in the following, precisely in paragraph 3.7, to derive kinetic equations different from the ones discussed just below.

3.2　The BBGKY hierarchy

We define the reduced (marginal) probability densities P_s as

$$P_s(\mathbf{r}_1,\mathbf{v}_1,\mathbf{r}_2,\mathbf{v}_2,...,\mathbf{r}_s,\mathbf{v}_s,t)=\int_{\Omega^{N-s}\times\Re^{3(N-s)}}P(\mathbf{r}_1,\mathbf{v}_1,\mathbf{r}_2,\mathbf{v}_2,...,\mathbf{r}_N,\mathbf{v}_N,t)\prod_{j=s+1}^N d\mathbf{r}_j d\mathbf{v}_j \quad (3.18)$$

In order to derive an evolution equation for P_s the first step is to integrate Eq. (3.10) with respect to the variables $\mathbf{r}_j$ and $\mathbf{v}_j$ $(s+1\le j\le N)$ over $\Omega^{N-s}\times\Re^{3(N-s)}$, obtaining:

$$\frac{\partial P_s}{\partial t}+\sum_{i=1}^s\int_{\Lambda_s}\mathbf{v}_i\cdot\frac{\partial P}{\partial\mathbf{r}_i}\prod_{j=s+1}^N d\mathbf{r}_j d\mathbf{v}_j+\sum_{k=s+1}^N\int_{\Lambda_s}\mathbf{v}_k\cdot\frac{\partial P}{\partial\mathbf{r}_k}\prod_{j=s+1}^N d\mathbf{r}_j d\mathbf{v}_j=0 \tag{3.19}$$

where the integration space Λ_s extends to the entire $\Re^{3(N-s)}$ for the velocity variables, while it extends to Ω^{N-s} deprived of the spheres $|\mathbf{r}_i-\mathbf{r}_j|<\sigma$ $(i=1,...,N,i\ne j)$ with respect to the position variables.

The typical term in the first sum contains the integral of a derivative with respect to a variable $\mathbf{r}_i$ over which one does not integrate, but in the exchange of order between integration and derivation one must take into account the domain boundaries which depend on $\mathbf{r}_i$, writing:

$$\int_{\Lambda_s}\mathbf{v}_i\cdot\frac{\partial P}{\partial\mathbf{r}_i}\prod_{j=s+1}^N d\mathbf{r}_j d\mathbf{v}_j=\mathbf{v}_i\cdot\frac{\partial P_s}{\partial\mathbf{r}_i}-\sum_{k=s+1}^N\int_{\Lambda_s}P_{s+1}\mathbf{v}_i\cdot\hat{\mathbf{n}}_{ik}d\sigma_{ik}d\mathbf{v}_k \tag{3.20}$$

where $\hat{\mathbf{n}}_{ik}$ is the outer normal to the sphere $|\mathbf{r}_i-\mathbf{r}_k|=\sigma$, $d\sigma_{ik}$ is the surface element on the same sphere and P_{s+1} has k as its $(s+1)-th$ index.

The typical term in the second sum in Eq. (3.19) can be immediately integrated by means of the Gauss theorem, since it involves the integration of a derivative taken with respect to one of the integration variables (and assuming that the boundary of Ω is a specular reflecting wall or a periodical boundary condition):

$$\int_{\Lambda_s}\mathbf{v}_k\cdot\frac{\partial P}{\partial\mathbf{r}_k}\prod_{j=s+1}^N d\mathbf{r}_j d\mathbf{v}_j$$

$$=\sum_{i=1}^s\int P_{s+1}\mathbf{v}_k\cdot\hat{\mathbf{n}}_{ik}d\sigma_{ik}d\mathbf{v}_k+\sum_{i=s+1,i\ne k}^N\int P_{s+2}\mathbf{v}_k\cdot\hat{\mathbf{n}}_{ik}d\sigma_{ik}d\mathbf{v}_k d\mathbf{r}_i d\mathbf{v}_i \quad (3.21)$$

The last term in the above equation, when summed over $s+1\le k\le N$ vanishes: this fact directly stems from the equivalence (3.10b) (we do not enter in the few steps of this simple proof). Moreover, in both above equations the integral containing the term P_{s+1} is the same no matter what the value of the dummy index k is, so that we can drop the index and write $\mathbf{r}_*,\mathbf{v}_*$ instead of $\mathbf{r}_k,\mathbf{v}_k$.

As a matter of fact, Eq. (3.19) finally reads:

$$\frac{\partial P_s}{\partial t} + \sum_{i=1}^{s} \mathbf{v}_i \cdot \frac{\partial P_s}{\partial \mathbf{r}_i} = (N-s) \sum_{i=1}^{s} \int P_{s+1} \mathbf{V}_i \cdot \hat{\mathbf{n}}_i d\sigma_i d\mathbf{v}_* \qquad (3.22)$$

where $\mathbf{V}_i = \mathbf{v}_i - \mathbf{v}_*$, $\hat{\mathbf{n}}_i = (\mathbf{r}_i - \mathbf{r}_*)/\sigma$ and the arguments of P_{s+1} are $(\mathbf{r}_1, \mathbf{v}_1, \mathbf{r}_2, \mathbf{v}_2, ..., \mathbf{r}_s, \mathbf{v}_s, \mathbf{r}_*, \mathbf{v}_*, t)$. Integrations in Eq. (3.22) are performed over the 1-particle velocity space $\Re^3$ and over the sphere S^i (given by the condition $|\mathbf{r}_i - \mathbf{r}_*| = \sigma$) with surface elements $d\sigma_i$.

Eq. (3.22) states that the evolution of the reduced probability density P_s is governed by the free evolution operator of the s-particles dynamics, which appears in the left hand side, with corrections due to the effect of the interaction with the remaining $(N-s)$ particle. The effect of this interaction is described by the right-hand side of this equation.

Usually Eq. (3.22) is written in a different form, obtained using some symmetries of the problem. In particular one can separate the sphere S^i of integration in the right-hand side, in the two hemispheres S^i_+ and S^i_- defined respectively by $\mathbf{V_i} \cdot \hat{\mathbf{n}}_i > 0$ and $\mathbf{V_i} \cdot \hat{\mathbf{n}}_i < 0$ (considering also that $d\sigma_i = \sigma^2 d\hat{\mathbf{n}}_i$):

$$\int P_{s+1} \mathbf{V}_i \cdot \hat{\mathbf{n}}_i d\sigma_i d\mathbf{v}_* = \sigma^2 \int_{\Re^3} \int_{S^i_+} P_{s+1} |\mathbf{V}_i \cdot \hat{\mathbf{n}}_i| d\hat{\mathbf{n}}_i d\mathbf{v}_* - \sigma^2 \int_{\Re^3} \int_{S^i_-} P_{s+1} |\mathbf{V}_i \cdot \hat{\mathbf{n}}_i| d\hat{\mathbf{n}}_i d\mathbf{v}_* \quad (3.23)$$

and observe that in the S^i_+ integration are included all phase space points such that particle i and particle $*$ (the $(s+1) - th$ generic particle) are coming out from a collision: this means that on the sphere S^i_+ we can write the substitution

$$P_{s+1}(\mathbf{r}_1, \mathbf{v}_1, ..., \mathbf{r}_i, \mathbf{v}_i, ...\mathbf{r}_s, \mathbf{v}_s, \mathbf{r}_i - \sigma\hat{\mathbf{n}}_i, \mathbf{v}_*)$$
$$\rightarrow P_{s+1}(\mathbf{r}_1, \mathbf{v}_1, ..., \mathbf{r}_i, \mathbf{v}_i - \hat{\mathbf{n}}_i(\hat{\mathbf{n}}_i \cdot \mathbf{V}_i), ...\mathbf{r}_s, \mathbf{v}_s, \mathbf{r}_i - \sigma\hat{\mathbf{n}}_i, \mathbf{v}_* + \hat{\mathbf{n}}_i(\hat{\mathbf{n}}_i \cdot \mathbf{V}_i)). \quad (3.24)$$

Moreover we can make the change of variable in the second integral (that on the sphere S^i_-) $\hat{\mathbf{n}}_i \rightarrow -\hat{\mathbf{n}}_i$ which only changes the integration range $S^i_- \rightarrow S^i_+$. Finally, replacing $\hat{\mathbf{n}}_i$ with simply $\hat{\mathbf{n}}$ (and therefore $S^i_+ \rightarrow S_+$) we have:

$$\frac{\partial P_s}{\partial t} + \sum_{i=1}^{s} \mathbf{v}_i \cdot \frac{\partial P_s}{\partial \mathbf{r}_i} = (N-s)\sigma^2 \sum_{i=1}^{s} \int_{\Re^3} \int_{S_+} (P'_{s+1} - P_{s+1}) |\mathbf{V}_i \cdot \hat{\mathbf{n}}| d\hat{\mathbf{n}} d\mathbf{v}_* \qquad (3.25)$$

where we have defined

$$P'_{s+1} = P_{s+1}(\mathbf{r}_1, \mathbf{v}_1, ..., \mathbf{r}_i, \mathbf{v}_i - \hat{\mathbf{n}}_i(\hat{\mathbf{n}}_i \cdot \mathbf{V}_i), ...\mathbf{r}_s, \mathbf{v}_s, \mathbf{r}_i - \sigma\hat{\mathbf{n}}_i, \mathbf{v}_* + \hat{\mathbf{n}}_i(\hat{\mathbf{n}}_i \cdot \mathbf{V}_i)) \qquad (3.26)$$

The system of equations (3.25) is usually called the BBGKY hierarchy for the hard sphere gas.

3.3 The Boltzmann hierarchy and the Boltzmann equation

In a rarefied gas N is a very large number and σ is very small; let us say, to fix ideas, that we have a box whose volume is $1 \quad cm^3$ at room temperature and atmospheric pressure. Then $N \simeq 10^{20}$ and $\sigma \simeq 10^{-8}cm$ and (from Eq. (3.25)) for small s we have $(N-s)\sigma^2 \simeq N\sigma^2 \simeq 1m^2$; at the same time the difference between $\mathbf{r}_i$ and $\mathbf{r}_i + \sigma\hat{\mathbf{n}}$ can be neglected and the volume occupied by the particles $(N\sigma^3 \simeq 10^{-4}cm^3)$ is very small so that the collision between two selected particles is a rather rare event. In this spirit, the Boltzmann-Grad limit has been suggested as a procedure to obtain a closure for Eq. (3.25): $N \rightarrow \infty$ and $\sigma \rightarrow 0$ in such a way that $N\sigma^2$ remains finite. We stress the fact that (as seen in section 2.3) the total number of collisions in the unit of time is given by the total scattering cross section multiplied by N, which for a system of hard spheres gives $N\pi\sigma^2$. The Boltzmann-Grad limit, therefore, states that the single particle collision probability must vanish, but the total number of collisions remains of order 1.

Within this limit, the BBGKY hierarchy reads:

$$\frac{\partial P_s}{\partial t} + \sum_{i=1}^{s} \mathbf{v}_i \cdot \frac{\partial P_s}{\partial \mathbf{r}_i} = N\sigma^2 \sum_{i=1}^{s} \int_{\Re^3} \int_{S_+} (P'_{s+1} - P_{s+1})|\mathbf{V}_i \cdot \hat{\mathbf{n}}|d\hat{\mathbf{n}}d\mathbf{v}_* \tag{3.27}$$

where the arguments of P'_{s+1} and of P_{s+1} are the same as above, except that the position of the $(s+1)-th$ particle ($\mathbf{r}'_*$ and $\mathbf{r}_*$) is equal to $\mathbf{r}_i$ (as $\sigma \to 0$). Eq. (3.27) gives a complete description of the time evolution of a Boltzmann gas (i.e. the ideal gas obtained in the Boltzmann-Grad limit), usually called *the Boltzmann hierarchy*.

Finally the Boltzmann equation is obtained if the *molecular chaos assumption* is taken into account:

$$P_2(\mathbf{r}_1, \mathbf{v}_1, \mathbf{r}_2, \mathbf{v}_2, t) = P_1(\mathbf{r}_1, \mathbf{v}_1)P_1(\mathbf{r}_2, \mathbf{v}_2) \tag{3.28}$$

for particles that are about to collide (that is when $\mathbf{r}_2 = \mathbf{r}_1 - \sigma\hat{\mathbf{n}}$ and $\mathbf{V}_{12} \cdot \hat{\mathbf{n}} < 0$). This assumption naturally stems from the Boltzmann-Grad limit, as it is reasonable that, in the limit of vanishing single-particle collision rate, two colliding particles are uncorrelated. The lack of correlation of colliding particles is the essence of the molecular chaos assumption. We underline that nothing is said about correlation of particles that have just collided.

With the assumption (3.28) we can rewrite the first equation of the hierarchy (3.27), omitting the $_1$ subscript for simplicity:

$$\frac{\partial P(\mathbf{r}, \mathbf{v})}{\partial t} + \mathbf{v} \cdot \frac{\partial P(\mathbf{r}, \mathbf{v})}{\partial \mathbf{r}} = N\sigma^2 \int_{\Re^3} \int_{S_+} (P(\mathbf{r}, \mathbf{v}')P(\mathbf{r}, \mathbf{v}'_*) - P(\mathbf{r}, \mathbf{v})P(\mathbf{r}, \mathbf{v}_*))|\mathbf{V} \cdot \hat{\mathbf{n}}|d\mathbf{v}_*d\hat{\mathbf{n}} \tag{3.29}$$

with $\mathbf{v}' = \mathbf{v} - \hat{\mathbf{n}}(\mathbf{V} \cdot \hat{\mathbf{n}})$, $\mathbf{v}'_* = \mathbf{v}_* + \hat{\mathbf{n}}(\mathbf{V} \cdot \hat{\mathbf{n}})$, $\mathbf{V} = \mathbf{v} - \mathbf{v}_*$. This represents the Boltzmann equation for hard spheres. We also observe that the integral in Eq. (3.29) is extended to the hemisphere S_+ but could be equivalently extended to the entire sphere S^2 provided a factor $1/2$ is inserted in front of the integral itself, as changing $\hat{\mathbf{n}} \to -\hat{\mathbf{n}}$ does not change the integrand.

From a rigorous point of view, the molecular chaos has to be assumed and cannot be proved. However it has been demonstrated that if the Boltzmann hierarchy has a unique solution for data that satisfy for $t = 0$ a generalized form of chaos assumption:

$$P_s(\mathbf{r}_1, \mathbf{v}_1, ..., \mathbf{r}_s, \mathbf{v}_s, t) = \prod_{j=1}^{s} P_1(\mathbf{r}_j, \mathbf{v}_j, t) \tag{3.30}$$

than Eq. (3.30) holds at any time and therefore the Boltzmann equation is fully justified. Otherwise it has also been proved that if Eq. (3.30) is satisfied at $t = 0$ and the Boltzmann equation (3.29) admits a solution for the given initial data, then the Boltzmann hierarchy (3.27) has at least a solution which satisfy (3.30) at any time t.

3.4   Collision invariants and H-theorem

The integral appearing in the right-hand side of Eq. (3.29) is usually called collision integral:

$$Q(P, P) = \int_{\Re^3} \int_{S_+} (P'P'_* - PP_*)|\mathbf{V} \cdot \hat{\mathbf{n}}|d\mathbf{v}_*d\hat{\mathbf{n}} \tag{3.31}$$

where we have used an intuitive contracted notation (the prime or $*$ must be considered applied to the velocity vector in the argument of the function P). In the collision integral, the position $\mathbf{r}$ is the same wherever the function P appears, and therefore it can be considered a parameter of $Q(P, P)$.

Let us have a look to the integral

$$\int_{\Re^3} Q(P, P)\phi(\mathbf{v})d\mathbf{v} = \int_{\Re^3} \int_{\Re^3} \int_{S_+} (P'P'_* - PP_*)\phi(\mathbf{v})|\mathbf{V} \cdot \hat{\mathbf{n}}|d\mathbf{v}_*d\hat{\mathbf{n}}d\mathbf{v} \tag{3.32}$$

which can be transformed in many alternative forms, using its symmetries. In particular one can exchange primed and unprimed quantities, as well as starred and unstarred quantities. With manipulations of this sort, it is immediate to get the following alternative form of Eq. (3.32):

$$\int_{\Re^3} Q(P,P)\phi(\mathbf{v})d\mathbf{v} = \frac{1}{8}\int_{\Re^3}\int_{\Re^3}\int_{S_+}(P'P'_* - PP_*)(\phi + \phi_* - \phi' - \phi'_*)|\mathbf{V}\cdot\hat{\mathbf{n}}|d\mathbf{v}_*d\hat{\mathbf{n}}\phi(\mathbf{v})d\mathbf{v} \quad (3.33)$$

From this equation it comes that if

$$\phi + \phi_* = \phi' + \phi'_* \quad (3.34)$$

almost everywhere in velocity space, then the integral of Eq. (3.33) is zero independent of the particular function P. Many authors have proved under different assumptions that the most general solution of Eq. (3.34) is given by

$$\phi(\mathbf{v}) = C_1 + \mathbf{C}_2\cdot\mathbf{v} + C_3|\mathbf{v}|^2 \quad (3.35)$$

Furtherly, if $\phi = \log P$, from Eq. (3.33) it follows that

$$\int_{\Re^3} Q(P,P)\phi(\mathbf{v})d\mathbf{v} = \frac{1}{8}\int_{\Re^3}\int_{\Re^3}\int_{S_+}(P'P'_* - PP_*)\log(PP_*/P'P'_*)|\mathbf{V}\cdot\hat{\mathbf{n}}|d\mathbf{v}_*d\hat{\mathbf{n}}\phi(\mathbf{v})d\mathbf{v} \leq 0 \quad (3.36)$$

which follows from the elementary inequality $(z - y)\log(y/z) \leq 0$ if $y, z \in \Re^+$. This becomes an equality if and only if $y = z$, therefore the equality sign holds in Eq. (3.36) if and only if

$$P'P'_* = PP_* \quad (3.37)$$

This is equivalent to two important facts:

- $\phi + \phi_* = \phi' + \phi'_*$ (taking the logarithms of both sides of Eq. (3.37)), so that we can use the result (3.35) obtaining $P = \exp(C_1 + \mathbf{C}_2\cdot\mathbf{v} + C_3|\mathbf{v}|^2) = C_0\exp(-\beta|\mathbf{v} - \mathbf{v}_0|^2)$ where we have defined $C_0 = \exp(C_1)$, $\beta = -C_3$ and $\mathbf{v}_0 = \mathbf{C}_2/2\beta$; this function is called Maxwell-Boltzmann distribution or simply Maxwellian;

- $Q(P,P) \equiv 0$, i.e. the collision integral identically vanishes.

Equation (3.36) is a fundamental result of the Boltzmann theory (it is often called Boltzmann Inequality) and can be fully appreciated with the following discussion: we rewrite the Boltzmann Equation (3.29) with a simplified notation:

$$\frac{\partial P}{\partial t} + \mathbf{v}\cdot\frac{\partial P}{\partial\mathbf{r}} = N\sigma^2 Q(P,P). \quad (3.38)$$

We multiply both sides by $\phi = \log P$ and integrate with respect to $\mathbf{v}$, obtaining a transport equation for the quantity ϕ:

$$\frac{\partial H}{\partial t} + \frac{\partial}{\partial\mathbf{r}}\cdot\mathbf{j}_H = S_H \quad (3.39a)$$

$$H = \int_{\Re^3} P\log P d\mathbf{v} \quad (3.39b)$$

$$\mathbf{j}_H = \int_{\Re^3}\mathbf{v}P\log P d\mathbf{v} \quad (3.39c)$$

$$S_H = N\sigma^2\int_{\Re^3}\log PQ(P,P)d\mathbf{v}. \quad (3.39d)$$

Then Eq. (3.36) states that $S_H \leq 0$ and $S_H = 0$ if and only if P is a Maxwellian. For example, if we look for a space homogeneous solution of the Boltzmann equation, it happens that

$$\frac{\partial H}{\partial t} = S_H \leq 0 \tag{3.40}$$

that is the famous H-Theorem. It simply states that there exists a macroscopic quantity (H in this case) that decreases as the gas evolves in time and eventually goes to zero when (if and only if) the distribution P becomes a Maxwellian. When the homogeneity is not achievable (due to non-homogeneous boundary conditions) rigorous results are more complicated, but we are still tempted to say that the Maxwellian represents the local asymptotic equilibrium, with the spatial dependence carried by the parameters of this distribution function.

For a discussion of the H-Theorem and the consequent paradoxes (irreversibility obtained starting from reversibility), see the reference "Qualche osservazione su irreversibilita', equazione di Boltzmann e Teorema H" by Angelo Vulpiani.

3.5   The Maxwell molecules

The collisional integral of Boltzmann equation for hard spheres, Eq. (3.31), contains a term $g = |\mathbf{V} \cdot \hat{\mathbf{n}}|$ which multiplies the probabilities of particles entering or coming out from a collision. In general the collisional integral must contain the differential collision rate $dR/D\Omega$ for particle coming at a certain relative velocity (in modulus g and direction $\hat{\mathbf{n}}$, or equivalently scattering angle χ centered in the solid angle $d\Omega$), which may be expressed in terms of the scattering cross section s (see for example Eq. (2.20)):

$$\frac{dR}{d\Omega} = gs(g, \chi)P_2(\mathbf{r}, \mathbf{r} + \sigma\hat{\mathbf{n}}, \mathbf{v}_1, \mathbf{v}_2, t)d\mathbf{v}_2 \tag{3.41}$$

We discussed in paragraph 2.3 the fact that the scattering cross section depends strongly on the kind of interaction between the molecules of the gas. For power law repulsive interaction potential $V(r) \sim r^{-(a-1)}$, the scattering angle χ depends on the relative energy $g^2/2$ and on the impact parameter b only through the combination $(g^2 b^{a-1})$. This means that there exists a function $\gamma(\chi)$ such that:

$$b = g^{-2/(a-1)}\gamma(\chi) \tag{3.42}$$

and this means that from relation (2.22) one obtains:

$$gs(g, \chi) \sim g^{1-4/(a-1)}\frac{\gamma(\chi)}{\sin\chi}\frac{d\gamma}{d\chi} \tag{3.43}$$

which holds in $d = 3$. The extension to generic dimension of the last equation is:

$$gs(g, \chi) \sim g^{1-2(d-1)/(a-1)}\frac{\gamma^{d-2}}{(\sin\chi)^{d-2}}\frac{d\gamma}{d\chi} \sim g^{1-2(d-1)/(a-1)}\alpha(\cos\chi) \tag{3.44}$$

Therefore when $a = 1 + 2(d-1)$ (i.e. $a = 5$ for $d = 3$ and $a = 3$ for $d = 2$) the collision rate $gs(g, \chi)$ *does not depend upon* g. This property defines the so-called Maxwell molecules [55]. Interaction with $a < 1 + 2(d-1)$ are called soft interactions (e.g. the electrostatic or gravitational interaction). Interactions with $a > 1 + 2(d-1)$ are called hard interactions. Hard spheres ($a \to \infty$) belongs to this set of interactions, with $gs(g, \chi) \sim g$. It has been also studied the Very Hard Particles model, which is characterized by $gs(g, \chi) \sim g^2$, which is not attainable with an inverse power potential, as it requires an interaction harder than the hard sphere interaction.

The obvious advantage of Maxwell molecules is that the Boltzmann equation greatly simplifies, as g does not appear in the collision integral. A further simplification of the Boltzmann equation came from Krook and Wu [92], who studied the Boltzmann equation of Maxwell molecules with an isotropic scattering cross-section, i.e $\alpha = const$, often called Krook and Wu model. A very large literature

exists for linear and non-linear model-Boltzmann equations (for a review see [55]). The importance of the Maxwell molecules model is the possibility of obtaining solutions for it: the general method (extended to other model-Boltzmann equations) is to obtain an expansion in orthogonal polynomial where the expansion coefficients are polynomial moments of the solution distribution function. For Maxwell molecules the moments satisfy a recursive system of differential equations that can be solved sequentially. Given an initial distribution, one can solve the problem if the series expansion converges. Bobylev [18] has shown that if one searches for *similarity* solutions (i.e. solutions with scaling form $P(\mathbf{v}, t) \equiv e^{-\alpha t} F(e^{-\alpha t} \mathbf{v})$), then the solution can be found solving a recursive system of algebraic equation.

The Maxwell molecules model has been subject of study also in the framework of the kinetic theory of granular gases [10].

3.6 The Enskog correction

The Boltzmann-Grad limit (see paragraph 3.3) restricts the validity of the Boltzmann equation to rarefied gases. This conditions is necessary to consider valid the *Molecular Chaos* which states the independence of colliding particles. In principle, in fact, two colliding particles can be correlated due to an intersection of their collisional histories: one simple possibility is that they may have collided some time before or, alternatively, they may have collided with particles that have collided before. Moreover, the spatial extension of particles (i.e. the fact that they are not really pointlike) restricts the possibilities of motion and as a consequence the degree of independence (this is the so called *excluded volume effect*). All these kinds of correlations become relevant when the gas is not in the situation considered by the Boltzmann-Grad limit, that is when the gas is not rarefied but (either moderately or highly) dense.

The first approach to the problem of not rarefied gases was introduced by Enskog [40]: he did not consider the effects of velocity correlations due to common collisional histories, but simply added to the Boltzmann equation an heuristic correction to take into account short range correlations on positions only. In general the two-body probability distribution function can be written in terms of the one-body functions:

$$P_2(\mathbf{r}_1, \mathbf{v}_1, \mathbf{r}_2, \mathbf{v}_2, t) = g_2(\mathbf{r}_1, \mathbf{v}_1, \mathbf{r}_2, \mathbf{v}_2) P_1(\mathbf{r}_1, \mathbf{v}_1) P_1(\mathbf{r}_2, \mathbf{v}_2) \tag{3.45}$$

where g_2 is the pair correlation function. The Molecular Chaos assumption states that $g_2(\mathbf{r}_1, \mathbf{r}_1 + \sigma \hat{\mathbf{n}}, \mathbf{v}_1, \mathbf{v}_2) \equiv 1$.

In the Enskog theory the Molecular Chaos assumption is modified in the following way:

$$P_2(\mathbf{r}_1, \mathbf{v}_1, \mathbf{r}_1 + \sigma \hat{\mathbf{n}}, \mathbf{v}_2, t) = \Xi(\sigma, n(\mathbf{r}_1)) P_1(\mathbf{r}_1, \mathbf{v}_1) P_1(\mathbf{r}_1 + \sigma \hat{\mathbf{n}}, \mathbf{v}_2) \tag{3.46}$$

i.e. $g_2 \equiv \Xi(\sigma, n)$ for particles entering or coming out from a collision, and the existence of a well defined coarse-grained density $n(\mathbf{r}_1)$ is assumed. The term $\Xi(\sigma, n)$ becomes a multiplicative constant in front of the collisional integral $Q(P, P)$, giving place to the so-called Boltzmann-Enskog equation. Of course, in a general non-homogeneous situation, the density is a spatially and temporally non-uniform quantity which can be described by a macroscopic field: one may assume (as it is in kinetic theory) that this field changes slowly in space-time, so that the Boltzmann-Enskog equation can be locally solved with constant n as it was a Boltzmann equation with an effective total scattering cross section $\Xi(\sigma, n) N \sigma^2$.

For elastic hard disks or hard spheres, spatial correlations are described by the formulas of Carnahan and Starling [39]:

$$\Xi(\sigma, n) = \frac{1 - 7\phi/16}{(1 - \phi)^2} \ (d = 2) \tag{3.47a}$$

$$\Xi(\sigma, n) = \frac{1 - \phi/2}{(1 - \phi)^3} \ (d = 3) \tag{3.47b}$$

$$\tag{3.47c}$$

where ϕ is the solid fraction ($\phi = n\pi\sigma^2/4$ in $d = 2$, $\phi = n\pi\sigma^3/6$ in $d = 3$). This formula is expected to work well with solid fractions below ϕ_c, where a phase transition takes place [3], with $\phi_c = 0.675$ in $d = 2$.

The Enskog correction produces, for example, important corrections to the transport coefficients and to the pressure term in the hydrodynamic description.

.

3.7   The ring kinetics equations for hard spheres

The BBGKY hierarchy for hard spheres can be obtained by integration of the Eq. (3.17). Here we report the first two equations of the hierarchy derived in this way. Note that here a slightly different notation is used, where $P_i(1, 2...i)$ is used to denote the reduced i-particles distribution, with $(1, 2..., i)$ indicating phase-space (position and velocity) of particles 1, 2, ... i respectively. Moreover, we are using a normalization such that $\int d(1)..d(i)P_i$ returns the number of possible choices of i different particles (this normalization is widely used in the granular gas literature).

$$\left(\frac{\partial}{\partial t} + L_1^0 \right) P_1(1) = \int dr_2 \int d\mathbf{v}_2 \overline{T}_-(1, 2)P_2(1, 2) \tag{3.48a}$$

$$\left[\frac{\partial}{\partial t} + L_1^0 + L_2^0 - \overline{T}_-(1, 2) \right] P_2(1, 2) = \int dr_3 \int d\mathbf{v}_3 [\overline{T}_-(1, 3) + \overline{T}_-(2, 3)]P_3(1, 2, 3) \tag{3.48b}$$

This set of equations is an open hierarchy which expresses the time evolution of the s-particle distribution function in terms of the $(s + 1)$-th function.

Using again the Molecular Chaos assumption (Eq. (3.28)), the Boltzmann Equation (3.29) is immediately recovered from Eq. (3.48a).

Using the Enskog correction to the Molecular Chaos, Eq. (3.46), the Boltzmann-Enskog Equation is obtained.

As the density increases, the contributions of correlated collision sequences to the collision term become more and more important. At moderate densities, a simple way to take these correlations into account has been found in a cluster expansion of the $s-$particle distribution functions, defined recursively as

$$P_2(1, 2) = P_1(1)P_1(2) + g_2(1, 2) \tag{3.49a}$$

$$P_3(1, 2, 3) = P_1(1)P_1(2)P_1(3) + P_1(1)g_2(2, 3) + P_1(2)g_2(1, 3) + P_1(3)g_2(1, 2) + g_3(1, 2, 3) \tag{3.49b}$$

etc., where $g_2(1, 2) = P_2(1, 2) - P_1(1)P_1(2)$ accounts for pair correlations, $g_3(1, 2, 3)$ for triplet correlations, etc. The molecular chaos assumption implies $g_2(1, 2) = 0$. The basic assumption to obtain the ring kinetic equations is that the pair correlations are dominant and higher order ones can be neglected, i.e. $g_3 = g_4 = ... = 0$ in the above cluster expansion. The ring kinetic equations, obtained in this way, read:

$$\left(\frac{\partial}{\partial t} + L_1^0\right) P_1(1) = \int d\mathbf{r}_2 \int d\mathbf{v}_2 \overline{T}_-(1,2)(P_1(1)P_1(2) + g_2(1,2)) \tag{3.50a}$$

$$\left[\frac{\partial}{\partial t} + L_1^0 + L_2^0 - \overline{T}_-(1,2)\right] g_2(1,2) - \left[(1 + \mathcal{X}(1,2)) \int d\mathbf{r}_3 \int d\mathbf{v}_3 \overline{T}_-(1,3)(1 + \mathcal{X}(1,3))P_1(3)\right] g_2(1,2)$$
$$= \overline{T}_-(1,2)[P_1(1)P_1(2) + g_2(1,2)] \tag{3.50b}$$

with $\mathcal{X}(i,j)$ the operator that interchanges the particle labels i and j. With further algebra and approximation one can derive the generalized Boltzmann equation in ring approximation. We do not give here this derivation, as it is not the aim of this work to review the entire ring kinetic theory in details, but just to give its basic ideas (which are the binary collision expansion Eqs. (3.11) and the cluster expansion, Eqs. (3.49)).
.

3.8 The Boltzmann equation for granular gases

The binary collision operator $\overline{T}_-(1,2)$, for inelastic particles, must be changed [164] according to the inelastic collision rules, Eqs. (2.31) and Eqs. (2.32). It must be noted that when $r = 1$ (elastic collisions), the two set of equations coincide, i.e. the direct or inverse collision are identical transformation. This is not true if $r < 1$. Therefore, in the definition of the inverse binary collision operators at the end of section 3.1, that is $T_-(1,2)$ and $\overline{T}_-(1,2)$, we have put the same operator b_c that appears in the direct binary collision operators $T_+(1,2)$ and $\overline{T}_+(1,2)$, while in general it must be used the operator b_c' that replaces velocities with precollisional velocities (using the transformation given in Eqs. (2.32)). The adjoint of inverse binary inelastic collision operator(the only one needed in the following) therefore reads:

$$\overline{T}_-(1,2) = \sigma^2 \int_{\mathbf{V}_{12}\cdot\hat{\mathbf{n}}>0} d\hat{\mathbf{n}} |\mathbf{V}_{12} \cdot \hat{\mathbf{n}}| \left[\frac{1}{r^2}\delta(\mathbf{r}_1 - \mathbf{r}_2 - \sigma\hat{\mathbf{n}})b_c' - \delta(\mathbf{r}_1 - \mathbf{r}_2 + \sigma\hat{\mathbf{n}})\right] \tag{3.51}$$

Deriving from this the BBGKY hierarchy (analogue of (3.48)) and putting in the first equation of it the Molecular Chaos assumption, the Boltzmann Equation for granular gases is obtained [25, 164]:

$$\left(\frac{\partial}{\partial t} + L_1^0\right) P(\mathbf{r}_1, \mathbf{v}_1, t) = \sigma^2 \int d\mathbf{v}_2 \int_{\mathbf{V}_{12}\cdot\hat{\mathbf{n}}>0} d\hat{\mathbf{n}} |\mathbf{V}_{12} \cdot \hat{\mathbf{n}}|$$
$$\times \left[\frac{1}{r^2}P(\mathbf{r}_1, \mathbf{v}_1', t)P(\mathbf{r}_1, \mathbf{v}_2', t) - P(\mathbf{r}_1, \mathbf{v}_1, t)P(\mathbf{r}_1, \mathbf{v}_2, t)\right] \tag{3.52}$$

where the primed velocities are defined in Eqs. (2.32).

This equation has been studied in the spatially homogeneous case (no spatial gradients, $L_1^0 = 0$), with the Enskog correction (i.e. a multiplying factor $\Xi(\sigma, n)$ in front of the collision integral) by Goldshtein and Shapiro [72] and by Ernst and van Noije [162]. The equation is

$$\frac{\partial}{\partial t} F(\mathbf{v}_1, t) = \Xi(\sigma, n)\sigma^2 \int d\mathbf{v}_2 \int_{\mathbf{V}_{12}\cdot\hat{\mathbf{n}}>0} d\hat{\mathbf{n}} |\mathbf{V}_{12} \cdot \hat{\mathbf{n}}|$$
$$\times \left[\frac{1}{r^2}F(\mathbf{v}_1', t)F(\mathbf{v}_2', t) - F(\mathbf{v}_1, t)F(\mathbf{v}_2, t)\right] \tag{3.53}$$

where $F(\mathbf{v}, t) = \int d\mathbf{r} P(\mathbf{r}, \mathbf{v}, t)$.

Lecture 4

Non-equilibrium thermostats

In this chapter we are mainly interested in *spatially homogeneous* situations.

4.1   Average energy loss

We rewrite here the Boltzmann Equation for a 3D cooling granular gas [27, 164] (see paragraph 3.8):

$$\left(\frac{\partial}{\partial t} + L_1^0\right) P(\mathbf{r}_1, \mathbf{v}_1, t) = \sigma^2 \int d\mathbf{v}_2 \int_{\mathbf{V}_{12} \cdot \hat{\mathbf{n}} > 0} d\hat{\mathbf{n}} |\mathbf{V}_{12} \cdot \hat{\mathbf{n}}|$$

$$\times \left[\frac{1}{r^2} P(\mathbf{r}_1, \mathbf{v}_1', t) P(\mathbf{r}_1, \mathbf{v}_2', t) - P(\mathbf{r}_1, \mathbf{v}_1, t) P(\mathbf{r}_1, \mathbf{v}_2, t)\right] = \sigma^2 Q(P, P) \quad (4.1)$$

It is useful to define a rescaled distribution, under the assumption of *spatial homogeneity*:

$$P(\vec{v}, t) = \frac{n}{v_T^3} \tilde{f}(\vec{v}/v_T) \quad (4.2)$$

with $T(t) = \frac{1}{2} m v_T^2(t)$ e $\vec{c} = \vec{v}/v_T$ and n the average number density.

We may replace $Q \to n^2 v_T^{-2} \tilde{Q}$ where

$$\tilde{Q} = \int d\vec{c}_2 \int_+ d\hat{n} |\vec{c}_{12} \cdot \hat{n}| \left[\frac{1}{r^2} \tilde{f}(\vec{c}_1', t) \tilde{f}(\vec{c}_2', t) - \tilde{f}(\vec{c}_1) \tilde{f}(\vec{c}_2)\right]. \quad (4.3)$$

The main contribution to the time derivative of temperature is given by the effect of inelastic collisions: in homogeneous situations, where collisions reduce the kinetic energy by a quantity proportional to the kinetic energy itself, we expect to find $\dot{T} \sim \omega T$ where ω is the average collision rate. The rigorous calculations reads

$$\frac{d}{dt}\left(\frac{3}{2} n T\right)\bigg|_{coll} = \int d\vec{v} \frac{m v^2}{2} \frac{\partial}{\partial t} P(\vec{v}, t)|_{coll} = \int d\vec{v} \frac{m v^2}{2} \sigma^2 Q(P, P)$$

$$= \sigma^2 n^2 v_T \frac{m v_T^2}{2} \int d\vec{c}_1 c_1^2 \tilde{Q} = -\sigma^2 n^2 v_T T \mu_2 \quad (4.4)$$

with

$$\mu_p = -\int d\vec{c}_1 c_1^p \tilde{Q} \quad (4.5)$$

so that

$$\frac{dT}{dt}|_{coll} = -\zeta(t) T \quad (4.6)$$

where

$$\zeta(t) = \frac{2\sqrt{2}}{3} n\sigma^2 \mu_2 \sqrt{\frac{T}{m}}. \tag{4.7}$$

Computation of μ_2, and therefore of ζ, requires the knowledge of $\tilde{f}(c,t)$.

4.2   Sonine polynomials

It is useful to introduce a polynomial expansion in polynomials which reveals useful in standard kinetic theory as well as in granular kinetic theory: in fact it serves the purpose of describing small corrections to the Maxwellian. Such small corrections appear in homogeneous granular gases, as well as in all (granular or elastic) dilute gases in spatially non-homogeneous situations. The expansion reads:

$$\tilde{f}(\vec{c}) = \phi(\vec{c}) \left[1 + \sum_{p=1}^{\infty} a_p S_p(c^2) \right] \tag{4.8}$$

with the basic Maxwellian given by

$$\phi(c) = \pi^{-3/2} exp(-c^2). \tag{4.9}$$

The polynomials S_p are said "Sonine" polynomials (they are in fact assocaited Laguerre polynomials $S_p^{(m)}$ with $m = d/2 - 1$) and constitute a complete set of orthogonal functions:

$$\int d\vec{c}\phi(c) S_p(c^2) S_{p'}(c^2) = \frac{2(p+1/2)!}{\sqrt{\pi}p!}\delta_{pp'} = \mathcal{N}_p\delta_{pp'} \tag{4.10}$$

In granular homogeneous situations one finds good fit by using expression (4.8) stopping the expansion at $p = 2$. In dimension $d = 3$ the first polynomials read

$$S_0(x) = 1 \tag{4.11}$$
$$S_1(x) = -x + 3/2 \tag{4.12}$$
$$S_2(x) = \frac{x^2}{2} - \frac{5x}{2} + \frac{15}{8} \tag{4.13}$$

It is easy to verify that

$$\langle c^2 \rangle = \frac{3}{2}(1 - a_1) \tag{4.14}$$

and

$$\langle c^4 \rangle = \frac{15}{4}(1 + a_2). \tag{4.15}$$

Note also that

$$\int d\vec{v}\frac{mv^2}{2}P(r,v,t) = \frac{mv_t^2}{2}n\int d\vec{c}c^2\tilde{f}(\vec{c}) = \langle c^2 \rangle \frac{mv_t^2}{2}n \tag{4.16}$$

and

$$\int d\vec{v}\frac{mv^2}{2}P(r,v,t) = n\frac{m\langle v^2 \rangle}{2} = \frac{3}{2}nT = \frac{3}{2}n\frac{mv_T^2}{2} \tag{4.17}$$

so that $\langle c^2 \rangle = 3/2$ and therefore $a_1 = 0$: the first non trivial coefficient is a_2.

Equations for a_2 are found once a model (boundary conditions) is specified.

4.2.1 Approximation of μ_2

The explicit expression for μ_2 reads

$$\mu_2 = -\int d\vec{c}_1 c_1^2 \int d\vec{c}_2 \int_+ d\hat{n} |\vec{c}_{12} \cdot \hat{n}| \left[\frac{1}{r^2}\tilde{f}(\vec{c}_1', t)\tilde{f}(\vec{c}_2', t) - f(\vec{c}_1)f(\vec{c}_2)\right] \tag{4.18}$$

By using the Sonine expansion truncated at $p = 2$, with lot of algebra and changes of variables, one finally gets

$$\mu_2 = \sqrt{2\pi}(1 - r^2)\left(1 + \frac{3}{16}a_2 + O(a_2^2)\right). \tag{4.19}$$

4.3 The Homogeneous Cooling State

This is the simplest granular regime: it is assumed spatial homogeneity and absence of any energy injection. The system is initialized with some starting velocity distribution.

The rescaled distribution implies the appearance of additional contribution to the time-derivative:

$$\frac{\partial P}{\partial t} = \frac{n}{v_T^3}\frac{\partial \tilde{f}}{\partial t} + \left(-\frac{3n}{v_T^4}\tilde{f} + \frac{n}{v_T^3}\frac{\partial \tilde{f}}{\partial c_1}\frac{\partial c_1}{\partial v_T}\right)\frac{dv_T}{dt}. \tag{4.20}$$

One finally gets to the following time evolution equation:

$$\frac{1}{v_T}\frac{\partial \tilde{f}}{\partial t} - \frac{1}{v_T^2}\frac{\partial(\vec{c}_1 \tilde{f})}{\partial \vec{c}_1}\frac{dv_T}{dt} = \sigma^2 n\tilde{Q}. \tag{4.21}$$

Recalling the expression for $\dot{T}(t) = -\zeta(t)T(t)$ as well as for $\zeta(t)$, we can see that

$$\frac{1}{v_T^2}\frac{dv_T}{dt}\bigg|_{coll} = \frac{1}{2v_T T}\frac{dT}{dt} = -\frac{1}{3}\sigma^2 n\mu_2 \tag{4.22}$$

is time-independent.

We make the hypothesis that a scaling function exists $\tilde{f} \to \tilde{f}_{HC}$ with $\frac{\partial \tilde{f}_{HC}}{\partial t} = 0$. If it exists, it must satisfy

$$\frac{\mu_2}{3}\frac{\partial(\vec{c}_1 \tilde{f}_{HC})}{\partial \vec{c}_1} = \tilde{Q}. \tag{4.23}$$

This is the kinetic definition of Homogeneous Cooling State.

The solution of the temperature equation reads:

$$T(t) = \frac{T(0)}{(1 + \frac{\zeta(0)t}{2})^2} \tag{4.24}$$

Eq. (4.24) is known as Haff's law [73]

Using the Sonine approximation truncated at the second polynomial one has

$$\zeta(t) = \frac{4\sqrt{\pi}}{3}n\sigma^2\sqrt{\frac{T(t)}{m}}(1 - r^2)\left(1 + \frac{3}{16}a_2 + O(a_2^2)\right) = \frac{1 - r^2}{3}\omega_c(t). \tag{4.25a}$$

with

$$\omega_c = 4\sqrt{\pi}n\sigma^2\sqrt{\frac{T(t)}{m}}\left(1 + \frac{3}{16}a_2 + O(a_2^2)\right) \tag{4.26}$$

the collision frequency.

4.3.1   The Gaussian thermostat

After the Haff's law, it is immediate to realize that

$$\omega_c \sim \frac{1}{1 + \zeta(0)t/2} \tag{4.27}$$

which means that the *cumulated number of collisions* goes as $\tau_c(t) \sim \ln(1 + \zeta(0)t/2)$. This observation suggests to introduce a new time-scale

$$\tau = \tau_0 \ln(1 + \zeta(0)t/2) \tag{4.28}$$

with arbitrary τ_0, getting

$$\frac{\partial}{\partial t} = \frac{\tau_0 \zeta(0)/2}{1 + \zeta(0)t/2} \frac{\partial}{\partial \tau}. \tag{4.29}$$

This is interesting, since it shows that

$$\frac{1}{v_T(t)} \frac{\partial}{\partial t} = \frac{\tau_0 \zeta(0)/2}{v_t(0)} \frac{\partial}{\partial \tau}. \tag{4.30}$$

Finally, with the new time-cale, we have

$$\frac{\partial \tilde{f}}{\partial \tau} + \frac{n\sigma^2 \mu_2}{3} \frac{\partial(\vec{c}_1 \tilde{f})}{\partial \vec{c}_1} = \sigma^2 n \tilde{Q} \tag{4.31}$$

equivalent to the Boltzmann equation for particles under the effect of a force

$$F = \frac{n\sigma^2 \mu_2 \vec{c}}{3} \tag{4.32}$$

which is equivalent to a *positive* viscosity!

All this equivalence makes sense until the state remains homogeneous. We will see in lecture 6 that the homogeneous cooling state is unstable for large wavelength perturbations.

4.3.2   High velocity tails

Ernst and van Noije [162] have given estimates for the tails of the velocity distribution, using an asymptotic method employed by Krook and Wu [92]. This method assumes that for a fast particle the dominant contributions to the collision integral come from collisions with thermal (bulk) particles and that the gain term of the integral can be neglected with respect to the loss term.

The loss term in the Boltzmann equation reads

$$-\int dc_2 \int_+ d\hat{n} |c_{12}\hat{n}| \tilde{f}(c_1)\tilde{f}(c_2) \approx -\pi c_1 \tilde{f}(c_1). \tag{4.33}$$

If $\tilde{f}$ is isotropic, then $\vec{c}\frac{d}{d\vec{c}}\tilde{f} = c\frac{d}{dc}\tilde{f}$. Then it remains

$$\mu_2 \tilde{f} + \frac{1}{3}\mu_2 c \frac{d}{dc}\tilde{f} = -\pi c \tilde{f} \tag{4.34}$$

and for large c one finds

$$\tilde{f} \sim \exp\left(-\frac{3\pi}{\mu_2} c\right). \tag{4.35}$$

It must be recalled that $\mu_2 \sim (1 - r^2)$, which means that this estimate is valid when $c > 1/(1 - r^2)$.

4.4 An example of bulk driving

4.4.1 Equations of motion and collisions

The randomly driven granular gas (introduced by Puglisi et al. [140, 141]) consists of an assembly of N identical hard objects (spheres, disks or rods) of mass m and diameter σ. We put, for simplicity, $m = 1$ and $k_B = 1$ (the Boltzmann constant).

The grains move in a box of volume $V = L^d$ (L is the length of the sides of the box), with periodic boundary conditions, i.e. opposite borders of the box are identified.

The mean free path (calculated exactly in Eq. (2.29) for the case of an homogeneous gas of 3D hard spheres with a Maxwellian distribution of velocities) can be roughly estimated as

$$\lambda = \frac{1}{nS} \tag{4.36}$$

where, $n = N/V$ is the mean number density and S is the total scattering cross section. We stress the fact that S has the dimensions of a surface in $d = 3$ ($S \sim \sigma^2$), of a line in $d = 2$ ($S \sim \sigma$) and no dimensions in $d = 1$ (this is consistent with the fact that the diameter, in $d = 1$ is irrelevant).

The dynamics of the gas is obtained as the byproduct of three physical phenomena: friction with the surroundings, random accelerations due to external driving, inelastic collisions among the grains. We model the first two ingredients in the shape of a Langevin equation with exact fulfillment of the Einstein relation (see for example[93]), for the evolution of the velocities of the grains in the free time between collisions. The inelastic collisions follow the usual inelastic rule. The equations of motion for a particle i that is not colliding with any other particle, are:

$$m\frac{d}{dt}\mathbf{v}_i(t) = -\gamma_b \mathbf{v}_i(t) + \sqrt{2\gamma_b T_b}\boldsymbol{\eta}_i(t) \tag{4.37a}$$

$$\frac{d}{dt}\mathbf{x}_i(t) = \mathbf{v}_i(t) \tag{4.37b}$$

We call the parameters $\tau_b = m/\gamma_b$ and T_b *characteristic time of the bath* and *temperature of the bath* respectively. The function $\boldsymbol{\eta}_i(t)$ is a stochastic process with average $< \boldsymbol{\eta}_i(t) >= 0$ and correlations $< \eta_i^\alpha(t)\eta_j^\beta(t') >= \delta(t - t')\delta_{ij}\delta_{\alpha\beta}$ (α and β being component indexes) i.e. a standard white noise.

4.4.2 Characteristic times, elastic limit, collisionless limit, cooling limit: the two stationary regimes

In the dynamics of the N particles, as defined in Eqs. (4.37) and by the inelastic hard core collision rules, the most important parameters are:

- the coefficient of normal restitution r, which determines the degree of inelasticity;

- the ratio $\rho = \tau_b/\tau_c$ between the characteristic time of the bath and the "global" mean free time between collisions;

On the basis of these two parameters, we can define three fundamental limits of the dynamics of our model:

- the elastic limit: $r \to 1^-$;

- the collisionless limit: $\rho \to 0$ ($\tau_c \gg \tau_b$);

- the cooling limit: $\rho \to \infty$ ($\tau_c \ll \tau_b$);

The *elastic limit* is smooth in dimensions $d > 1$, so that we can consider it equivalent to put $r = 1$. In this case the collisions mix up the components leaving constant the energy (in the center of mass frame as well in the absolute frame). We can assume that, in this limit, the effect of the collisions is that of homogenizing the positions of the particles and making their velocity distribution relax toward the Maxwellian with temperature $T_g = \langle v^2 \rangle / d = \langle v_x^2 \rangle$ (this temperature is equal to the starting kinetic energy, but is modified by the relaxation toward T_b due to the Langevin Eqs. (4.37)). In one dimension this mixing effect (toward a "Maxwellian") is no more at work, as the elastic collisions exactly conserve the starting velocity distribution (the collisions can be viewed as exchanges of labels and the particles as non-interacting walkers).

In the *collisionless limit* we have $\tau_c \gg \tau_b$ and therefore, the collisions are very rare events with respect to the characteristic time of the bath. In this case we can consider the model as an ensemble of non-interacting Brownian walkers, each following the Eqs. (4.37). Therefore, whatever r is, and in any dimension, the distribution of velocities relaxes in a time τ_b toward a Maxwellian with temperature $T_g = \langle v^2 \rangle / d = T_b$ with a homogeneous density.

Finally, in the *cooling limit*, the collisions are almost the only events that act on the distribution of velocities, while between collisions the particles move almost ballistically. In this limit (if $r < 1$) the gas can be considered stationary only on observation times very long with respect to the time of the bath τ_b, where the effect of the external driving (the Langevin equation) emerges. For observation times larger than the mean free time τ_c but shorter than τ_b, the gas appears as a *cooling granular gas*.

To conclude this brief discussion on the expected behavior of the randomly driven granular gas model, we sketch a scenario with the presence of two fundamental stationary regimes:

- the "collisionless" stationary regime: when $\rho \ll 1$, i.e. approaching the *collisionless* limit; in this regime we expect, after a transient time of the order of τ_b, the stationary statistics of an ensemble of non-interacting Brownian particles (homogeneous density and Maxwell distribution of velocities, absence of correlations);

- the "colliding" stationary regime: when $\rho \gg 1$, i.e. approaching the *cooling* limit, but observing the system on times larger than τ_b; here we expect to see anomalous statistical properties.

4.4.3 Boltzmann equation

For this model, the Boltzmann equation includes two additional contributions which are equivalent to the "Fokker-Planck" operators which evolve the velocity distribution in a Langevin equation. The equation therefore reads:

$$\frac{\partial P}{\partial t} = \sigma^2 Q + \frac{\gamma_b}{m} \frac{\partial \vec{v} P}{\partial \vec{v}} + \frac{\gamma_b}{m} \frac{T_b}{m} \nabla_v P \tag{4.38}$$

Using the definition of rescaled distribution (4.2), and obviously $\dot{v}_T = 0$ (we are in a statistically stationary state), one gets

$$\frac{\partial \tilde{f}}{\partial t} = v_T n \sigma^2 \tilde{Q} + \frac{\gamma_b}{m} \frac{\partial \vec{c} \tilde{f}}{\partial \vec{c}} + \frac{\gamma_b}{2m} \frac{T_b}{T_g} \nabla_c \tilde{f}. \tag{4.39}$$

4.4.4 Stationary granular temperature

From the definition, it follows that

$$T = \frac{m}{dim} \langle v^2 \rangle \tag{4.40}$$

and therefore

$$\langle v \dot{v} \rangle = \frac{\dot{T}}{2m} = -\frac{\gamma_b}{m} \langle v^2 \rangle + \frac{\gamma_b}{m} \frac{T_b}{m} - \zeta \frac{T}{2m}. \tag{4.41}$$

Imposing $\dot{T} = 0$, in the stationary state, we get

$$T - T_b = \zeta \tau_b T \tag{4.42}$$

which can be (numerically) solved to obtain T (we remind that $\zeta \propto (1 - r^2) T^{1/2}$).

It is worth noting that r e τ_b appear through a factor $(1 - r^2) \tau_b$.

4.4.5 High velocity tails

For the heated case, assuming that at large velocities $\tilde{Q} \sim -\pi c \tilde{f}$, one finds

$$-\pi v_T n\sigma^2 c\tilde{f} + \frac{\gamma_b}{2m}\frac{T_b}{T_g}\left(\frac{d^2}{dc^2} + \frac{2}{c}\frac{d}{dc}\right)\tilde{f} + \frac{\gamma_b}{m}\left(3 + c\frac{d}{dc}\right)\tilde{f} = 0. \qquad (4.43)$$

This has two different "solutions"

- in the limit $\gamma \to 0$ (with $T_b \to \infty$ with finite γT_b), one has $\tilde{f} \sim \exp(-c^{3/2})$

- when $\gamma > 0$ one apparently finds $\tilde{f} \sim \exp(-c^2)$ but in this case the approximations (in particular having neglected the gain term in the collisional integral) are no guaranteed.

Lecture 5

Granular kinetic theory

Fluids are, in general, in spatially non-homogeneous situations: this can be an effect of non-equilibrium initial conditions (the experimentalist sets up the system far from the final situations, and then observes the system relaxing toward it), or an effect of forcing boundary conditions which keep the system in a non-equilibrium stationary state ("ness"). For granular fluids, there always exists an *intrinsic* energy "sink" which keeps the system out of equilibrium and one can - eventyally - apply an external forcing in order to keep the fluid in a stationary state. An example of homogeneous forcing has been discussed in the previous lecture. In this lesson we study non-homogeneous situations. An example - due to non-homogeneous forcing (coming from only one boundary) - is shown in Figure 5.1. The theory sketched in this lecture is however valid independently of the origin of non-homogeneity, as long as it satisfies the criterion of "small gradients". It will be useful, for example, to describe the departure from homogeneity in the cooling regime (where no external driving is present).
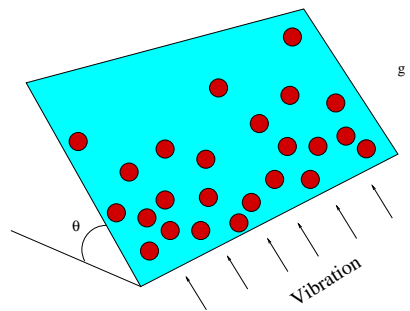
Figure 5.1: A sketch of an experiment where the granular assembly is driven by gravity plus a (periodically or stochastic) vibrating wall

5.1 A sketch of the program of Chapman-Enskog kinetic theory

The Chapman-Enskog procedure is a way of construct a non-homogeneous solution, for weak gradients, of the Boltzmann equation.

- define densities and fluxes for "slow" variables

- write continuity equations (always valid) for the "slow" quantities

- first assumption: $P(v, r, t)$ depends on r and t only through the above "slow" quantities; this means that the Boltzmann equation is replaced by a local boltzmann equation plus equations for the slow parameters

- second assumption: mean free path λ is small with respect to linear size of gradients L (which is of comparable order to linear size of the experiment); $\epsilon = \lambda/L \ll 1$ is called "Knudsen" number

- for small ϵ expand fluxes and take only up to linear order in the gradients: "transport coefficients" remain to be determined

- for consistency $P \rightarrow f^{(0)} + \epsilon f^{(1)} + \epsilon^2 f^{(2)} + \dots$ and all spatial and time derivatives are "expanded" in growing powers of ϵ

- these expansions, put into the Boltzmann equation and its supplementary "slow" equations, leads to families of equations at different order which can be solved separately

- at order 0 one has the homogeneous solution (Euler equation for elastic fluids) and find $f^{(0)}$

- at order 1 one can find $f^{(1)}$ through its coefficients of the linear expansion in gradients; the transport coefficients are functions of these coefficients

- hydro equations at order 2 are closed now (if solved, they could be used to find $f^{(2)}$)

5.2   Densities and fluxes

We assume that a phase space distribution function can be defined:

$$N(t, \mathbf{r}, \mathbf{v}) = P(t, \mathbf{r}, \mathbf{v})d^3r d^3v \tag{5.1}$$

where $N(t, \mathbf{r}, \mathbf{v})$ is the number of particles found at time t near the point $\mathbf{r}, \mathbf{v}$ of the phase space. P is assumed to be the solution of the Boltzmann Equation (3.29).

The particle number density is defined as

$$n(t, \mathbf{r}) = \iiint_\infty d^3v P(t, \mathbf{r}, \mathbf{v}) \tag{5.2}$$

The average molecular velocity is defined as

$$\mathbf{u}(t, \mathbf{r}) = \frac{1}{n(t, \mathbf{r})} \iiint_\infty d^3v \mathbf{v} P(t, \mathbf{r}, \mathbf{v}) \tag{5.3}$$

and this allows to introduce the random velocity vector

$$\mathbf{V}(t, \mathbf{r}) = \mathbf{v} - \mathbf{u}(t, \mathbf{r}) \tag{5.4}$$

which depends on time and position (while $\mathbf{v}$ is independent of t and $\mathbf{r}$) and has zero average:

$$\iiint_\infty d^3c V_i P(t, \mathbf{r}, \mathbf{V}) = 0 \tag{5.5}$$

The average fluxes of the molecular quantity $W(\mathbf{v})$ can be expressed as velocity moments of the phase space distribution function:

$$j_W^i(t, \mathbf{r}) = \iiint_\infty d^3v v_i W(\mathbf{v}) P(t, \mathbf{r}, \mathbf{v}) \tag{5.6}$$

When $W = m$ one has the mass flux:

$$j_m^i = mn(t, \mathbf{r})u_i(t, \mathbf{r}). \tag{5.7}$$

When $W = mv_j$ one has the momentum flux:

$$j^i_{mv_j} = mn(t, \mathbf{r})\langle v_i v_j \rangle = mnu_i u_j + mn\langle V_i V_j \rangle \tag{5.8}$$

which is a 3×3 symmetric matrix. In the last form two contributions can be recognized, that is the flux due to the bulk (organized) motion and the flux resulting from the random (thermal) motion of the gas particles. This second term is usually called the *pressure tensor* $\mathcal{P}_{ij} = mn\langle V_i V_j \rangle$. One can define, from this discussion, two quantities that are the *scalar pressure* p and the *vector temperature* T_i:

$$p = \frac{1}{3}(\mathcal{P}_{xx} + \mathcal{P}_{yy} + \mathcal{P}_{zz}) \tag{5.9}$$

$$\frac{1}{2}k_B T_i = \frac{1}{2}m\langle V_i^2 \rangle = \frac{1}{2}\frac{\mathcal{P}_{ii}}{n} \tag{5.10}$$

and in the isotropic case $T_i = T$ so that $p = nk_B T$. It can be also defined the stress tensor $\mathcal{T}$ as:

$$\mathcal{T}_{ij} = \delta_{ij} p - \mathcal{P}_{ij} \tag{5.11}$$

which expresses the deviation of the pressure tensor from the equilibrium Maxwellian case (for which $\mathcal{P}_{ij} = p\delta_{ij}$).

Finally, the flux of the quantity $W = mv_j v_k$ is given by:

$$j^i_{mv_j v_k} = mnu_i u_j u_k + u_i \mathcal{P}_{jk} + u_j \mathcal{P}_{ik} + u_k \mathcal{P}_{ij} + \mathcal{Q}_{ijk} \tag{5.12}$$

where $\mathcal{Q}_{ijk} = mn\langle V_i V_j V_k \rangle$ is the generalized heat flow tensor and describes the transport of random energy $V_j V_k$ due to thermal motion V_i of the molecules (for all the permutations of i, j, k).

In equation (5.12) three contributions can be recognized: the first term describes the bulk transport of the bulk flux of momentum; the second, third and fourth terms describe the a combination of bulk and random momentum fluxes; the last term is the transport of random energy component due to the random motion itself. Often a "classical" heat flow vector is introduced, more intuitive than the generalized heat flow tensor:

$$q_i = \frac{\mathcal{Q}_{ikk}}{2} = n\left\langle V_i \frac{mc^2}{2} \right\rangle. \tag{5.13}$$

5.3 Equations for the densities

Multiplying the Boltzmann equation by 1, v and v^2 and integrating over v, one gets equations for the slow variables:

$$\frac{\partial n}{\partial t} + \nabla \cdot (n\vec{u}) = 0 \tag{5.14}$$

$$\frac{\partial \vec{u}}{\partial t} + \vec{u} \cdot \nabla \vec{u} + (nm)^{-1}\nabla \cdot \mathcal{P} = 0 \tag{5.15}$$

$$\frac{\partial T}{\partial t} + \vec{u} \cdot \nabla T + \frac{2}{3n}\left[\mathcal{P} : (\nabla \vec{u}) + \nabla \vec{q}\right] + \zeta T = 0 \tag{5.16}$$

$$\tag{5.17}$$

These are the continuity equations and are always valid. The only term which does not appear in the continuity equation for elastic gases is, obviously, the ζT term (indeed $\zeta \equiv 0$ for elatic collisions).

5.4 Chapman-Enskog closure

The purpose is to close the continuity equations for small gradients. It consists in

1. change spatial scale $r \to \epsilon r$ where $\epsilon = \lambda/L$, i.e. if old positions where measured in terms of mean free path λ, now the new ones are measured in terms of the characteristic length L which is the macroscopic scale (macroscopic boundary conditions impose spatial variations at this scale); all gradients are transformed as $\nabla \to \epsilon \nabla$;

2. for small ϵ the fluxes can be approximated as linear in the gradients

$$\mathcal{P}_{ij} = p\delta_{ij} - \eta\epsilon\left(\nabla_i u_j + \nabla_j u_i - \frac{2}{3}\delta_{ij}\nabla \cdot \vec{u}\right) \tag{5.18}$$

$$\vec{q} = -\kappa\epsilon\nabla T - \mu\epsilon\nabla n \tag{5.19}$$

the main missing ingredients are, therefore, the coefficients η, κ and μ

3. we get the "linear" continuity equations

$$\frac{\partial n}{\partial t} = -\epsilon\nabla \cdot (n\vec{u}) \tag{5.20}$$

$$\frac{\partial \vec{u}}{\partial t} = -\epsilon\left(\vec{u} \cdot \nabla\vec{u} - \frac{1}{nm}\nabla p\right) + \epsilon^2\frac{\eta}{mn}\left(\nabla^2\vec{u} + \frac{1}{3}\nabla(\nabla \cdot \vec{u})\right) \tag{5.21}$$

$$\frac{\partial T}{\partial t} = -\zeta T - \epsilon\left(\vec{u} \cdot \nabla T + \frac{2}{3n}p(\nabla \cdot \vec{u})\right) + \epsilon^2 G \tag{5.22}$$

$$\tag{5.23}$$

with

$$G = \frac{2\eta}{3n}\left[(\nabla_i u_j)(\nabla_j u_i) + (\nabla_j u_i)(\nabla_j u_i) - \frac{2}{3}(\nabla \cdot \vec{u})^2\right] + \frac{2}{3n}(\kappa\nabla^2 T + \mu\nabla^2 n) \tag{5.24}$$

4. a "normal form" is assumed for the distribution $P(v, r, t) \to f[V|n(r,t), u(r,t), T(r,t)]$, (we recall that $V = v - u$), so that derivatives read

$$\frac{\partial f}{\partial t} = \frac{\partial f}{\partial n}\frac{\partial n}{\partial t} + \frac{\partial f}{\partial \vec{u}} \cdot \frac{\partial \vec{u}}{\partial t} + \frac{\partial f}{\partial T}\frac{\partial T}{\partial t}. \tag{5.25}$$

5. for consistency with the above expansions (and the assumption of "normal" form) we can introduce time-scales which measure the time-variations associated to growing powers of ϵ (i.e. happening at different spatial scales):

$$\frac{\partial}{\partial t} = \frac{\partial^{(0)}}{\partial t} + \epsilon\frac{\partial^{(1)}}{\partial t} + \epsilon^2\frac{\partial^{(2)}}{\partial t} + \dots \tag{5.26}$$

6. for the same reason, a spatially non-uniform f can be expanded as

$$f = f^{(0)} + \epsilon f^{(1)} + \epsilon^2 f^{(2)} + \dots \tag{5.27}$$

7. all these expansions are put into the original Boltzmann equation which (because of the assumed "normal" form) must be supplemented by Eqs. (5.20) for the slow variables; terms at the same order in ϵ can be solved separately: this must be executed in order of growing powers of ϵ since at each order the solution at smaller order is needed.

5.4.1   Zero order

At the smallest (zero) order in ϵ, the Boltzmann equation with its *supplementary* equations for slow parameters read:

$$\frac{\partial^{(0)} f^{(0)}}{\partial t} = Q(f^{(0)}, f^{(0)}) \tag{5.28}$$

$$\frac{\partial^{(0)} n}{\partial t} = 0 \tag{5.29}$$

$$\frac{\partial^{(0)} \vec{u}}{\partial t} = 0 \tag{5.30}$$

$$\frac{\partial^{(0)} T}{\partial t} = -\zeta^{(0)} T \tag{5.31}$$

It describes of course a spatially homogeneous situation. The solution of these equations has been already discussed in the previous lesson, it is the Homogeneous Cooling State, i.e. $f^{(()}0) = \tilde{f}_{HC}$:

$$f^{(0)} = \frac{n}{v_T^3} \tilde{f}^{(0)} \left(\frac{\vec{V}}{v_T} \right) \tag{5.32}$$

with

$$\zeta^{(0)} = -\frac{m}{3nT} \int d\vec{v}_1 v_1^2 Q(f^{(0)}, f^{(0)}) = \frac{2}{3} n\sigma^2 \sqrt{\frac{2T}{m}} \mu_2. \tag{5.33}$$

5.4.2   First order

$$\frac{\partial^{(0)} f^{(1)}}{\partial t} + \left(\frac{\partial^{(1)}}{\partial t} + \vec{v} \cdot \nabla \right) f^{(0)} = Q(f^{(0)}, f^{(1)}) + Q(f^{(1)}, f^{(0)}) \tag{5.34}$$

$$\frac{\partial^{(1)} n}{\partial t} = -\nabla(n\vec{u}) \tag{5.35}$$

$$\frac{\partial^{(1)} \vec{u}}{\partial t} = -\vec{u} \cdot \nabla \vec{u} - \frac{1}{nm} \nabla p \tag{5.36}$$

$$\frac{\partial^{(1)} T}{\partial t} = -\vec{u} \cdot \nabla T - \frac{2}{3} T \nabla \cdot \vec{u} - \zeta^{(1)} T \tag{5.37}$$

Putting $f^{(0)} + f^{(1)}$ in the expression for ζ and keeping the first order in ϵ one has

$$\zeta^{(1)} = 2 \frac{(1 - r^2) m \pi \sigma^2}{24nT} \int d\vec{v}_1 d\vec{v}_2 v_{12}^3 f^{(0)} f^{(1)} \tag{5.38}$$

The above equations are the Euler equations if $r = 1$ (elastic collisions). In elastic case, they describe transport without dissipation (i.e. no viscosity or heat conductivity).

Knowledge (even formal) of $f^{(0)}$ allows to write an equation for $f^{(1)}$ only. It is necessary to express $\frac{\partial^{(1)} f^{(0)}}{\partial t}$ as

$$\frac{\partial^{(1)} f^{(0)}}{\partial t} = \frac{\partial f^{(0)}}{\partial n} \frac{\partial^{(1)} n}{\partial t} + \frac{\partial f^{(0)}}{\partial \vec{u}} \cdot \frac{\partial^{(1)} \vec{u}}{\partial t} + \frac{\partial f^{(0)}}{\partial T} \frac{\partial^{(1)} T}{\partial t} \tag{5.39}$$

The terms in $\frac{\partial^{(1)}}{\partial t}$ are taken from the continuity equations at 1st order. Prefactors are known: $\frac{\partial f^{(0)}}{\partial n} = f^{(0)}/n$, $\frac{\partial f^{(0)}}{\partial \vec{u}} = -\frac{\partial f^{(0)}}{\partial \vec{V}}$, $\frac{\partial f^{(0)}}{\partial T} = -\frac{1}{2T} \frac{\partial(\vec{V} f^{(0)})}{\partial \vec{V}}$; analogously one can also write down the "streaming" term $\vec{v} \cdot \nabla$, recalling that $p = nT$, getting to

$$\frac{\partial^{(0)} f^{(1)}}{\partial t} + J(f^{(0)}, f^{(1)}) - \zeta^{(1)} T \frac{\partial f^{(0)}}{\partial T} = \vec{A} \cdot \nabla \ln T + \vec{B} \cdot \nabla \ln n + C_{ij} \nabla_j u_i \tag{5.40}$$

with $J = -Q(0,1) - Q(1,0)$.

R.h.s. depends upon three coefficients which depend only on $f^{(0)}$ and on "slow" fields

$$\vec{A} = \vec{V} \left[\frac{T}{m} \left(\frac{mV^2}{2T} - 1 \right) \frac{1}{V} \frac{\partial}{\partial V} + \frac{3}{2} \right] f^{(0)} \tag{5.41}$$

$$\vec{B} = -\vec{V} \left(\frac{T}{m} \frac{1}{V} \frac{\partial}{\partial V} + 1 \right) f^{(0)} \tag{5.42}$$

$$C_{ij} = \left(V_i V_j - \frac{1}{3} \delta_{ij} V^2 \right) \frac{1}{V} \frac{\partial f^{(0)}}{\partial V} \tag{5.43}$$

The most general scalar function depending linearly on vectorial and tensorial gradients is

$$f^{(1)} = \vec{\alpha} \cdot \nabla \ln T + \vec{\beta} \cdot \nabla \ln n + \gamma_{ij} \nabla_j u_i \tag{5.44}$$

with coefficients that depend only on V and on space-time through the slow fields.

Putting this form into the Boltzmann equation and comparing terms with same gradients, one obtaines equations for the coefficients of $f^{(1)}$ $\vec{\alpha}$, $\vec{\beta}$ and γ_{ij}.

The missing transport coefficient η, κ e μ can be expressed as functions of the above coefficents of $f^{(1)}$

$$\eta = -\frac{1}{10} \int D_{ij} \gamma_{ji} d\vec{V} \tag{5.45}$$

$$\kappa = -\frac{1}{3T} \int \vec{S} \cdot \alpha d\vec{V} \tag{5.46}$$

$$\mu = -\frac{1}{3n} \int \vec{S} \cdot \beta d\vec{V} \tag{5.47}$$

where we have used $\vec{S}(V) = \left(mV^2/2 - 5/2T \right) \vec{V}$ e $D_{ij} = m \left(V_i V_j - \frac{1}{3} \delta_{ij} V^2 \right)$.

5.4.3   Elastic case

In the elastic case $f^{(0)}$ is the Maxwellian f_M or ϕ when rescaled to have unitary variance. In this case it is found that $\vec{B} = 0$ and therefore $\vec{\beta} = 0$, leading finally to $\mu = 0$ (Fourier's law).

One finally gets

$$\eta = -\frac{5}{2\sigma^2} \sqrt{mT/2} \frac{1}{\Omega_\eta[\phi(c_1), \phi(c_2)]} \tag{5.48}$$

$$\kappa = -\frac{75}{16\sigma^2} \sqrt{2T/(m)} \frac{1}{\Omega_\kappa[\phi(c_1), \phi(c_2)]} \tag{5.49}$$

with the following "pure" numbers

$$\Omega_\eta = \int d\vec{c}_1 \int d\vec{C}_2 \int d\hat{n} \Theta(-\vec{c}_{12} \cdot \hat{n}) |\vec{c}_{12} \cdot \hat{n}| \phi_1(c_1) \phi_2(c_2)$$
$$\times \left[(\vec{c}_1' \cdot \vec{c}_2)^2 + (\vec{c}_2' \cdot \vec{c}_2)^2 - (\vec{c}_1 \cdot \vec{c}_2)^2 - (\vec{c}_2 \cdot \vec{c}_2)^2 - \frac{1}{3} c_2^2 \Delta(c_1^2 + c_2^2) \right] \tag{5.50}$$

and

$$\Omega_\kappa = \int d\vec{c}_1 \int d\vec{C}_2 \int d\hat{n} \Theta(-\vec{c}_{12} \cdot \hat{n}) |\vec{c}_{12} \cdot \hat{n}| \phi_1(c_1) \phi_2(c_2)$$
$$\times \left(c_2^2 - \frac{5}{2} \right) \left[(\vec{c}_1' \cdot \vec{c}_2)(c_1')^2 + (\vec{c}_2' \cdot \vec{c}_2)(c_2')^2 - (\vec{c}_1 \cdot \vec{c}_2) c_1^2 - (\vec{c}_2 \cdot \vec{c}_2) c_2^2 \right] \tag{5.51}$$

obtaining finally:

$$\eta = \frac{5}{16\sigma^2}\sqrt{mT/\pi} \tag{5.52}$$

$$\kappa = \frac{75}{64\sigma^2}\sqrt{T/(m\pi)} \tag{5.53}$$

$$f(V) = f_M(V)\left(1 - \frac{2m\kappa}{5nT^3}\vec{S}\cdot\nabla T - \frac{\eta}{nT^2}D_{ij}\nabla_j u_i\right) \tag{5.54}$$

5.4.4 Inelastic case

In the inelastic case $f^{(0)}$ is not known analytically, but can be expressed as an expansion in Sonine polynomials, and the coefficients can always be calculated (at any order), for instance stopping at the 2nd order, recalling that $\vec{c} = \vec{V}/v_T$:

$$f^{(0)} = \left(\frac{n}{v_T^3}\right)\phi(c)[1 + a_2 S_2(c^2)] \tag{5.55}$$

with

$$S_2(x) = \frac{1}{2}x^2 - \frac{5}{2}x + \frac{15}{8}. \tag{5.56}$$

For consistency, in the coefficients Ω now one must insert $\Omega[(1 + a_2 S_2)\phi(c_1), \phi(c_2)]$. One finally gets to

$$\eta = \frac{15}{2(1+r)(13-r)\sigma^2}\left(1 + \frac{3}{8}\frac{4-3r}{13-r}a_2\right)\sqrt{mT/\pi} \tag{5.57}$$

$$\kappa = \frac{75}{2(1+r)(9+7r)\sigma^2}\left(1 + \frac{1}{32}\frac{797+211r}{9+7r}\right)\sqrt{T/(\pi m)} \tag{5.58}$$

$$\mu = \frac{750(1-r)}{(1+r)(9+7r)(19-3r)n\sigma^2}(1 + q(r)a_2)\sqrt{T^3/(\pi m)} \tag{5.59}$$

$$\tag{5.60}$$

with $q(r)$ a quite lengthy function of the restitution coefficient r.

It is therefore obtained the solution of the Boltzmann equation at first order in the gradients: e per finire

$$f^{(1)}(V) = -\frac{1}{nT^2}[\frac{2m}{5T}\vec{S}\cdot(\kappa\nabla T + \mu\nabla n) + \eta D_{ij}\nabla_j u_i]f_M \tag{5.61}$$

We conclude this lecture noting that the above procedure (sketched in great generality) leads to a "solution" for the $f^{(i)}(V)$ at order i in the gradients, as well as to closed equations for the slow fields $n(r,t)$, $\mathbf{u}(\mathbf{r},\mathbf{t})$, $\mathbf{T}(\mathbf{r},\mathbf{t})$, which include fluxes at order i in the gradients, and therefore (since continuity is given by divergence of fluxes), are at order $i+1$ in the gradients.

Lecture 6

Failures and successes of hydrodynamics

6.1 Linear stability analysis of the homogeneous cooling state

A granular gas prepared with a homogeneous density and no macroscopic flow, at a given temperature $T(0)$, reaches the Homogeneous Cooling State in a few free times t_0. To study the behavior of small (macroscopic, i.e. for wave vectors of low magnitude $k \ll \min\{2\pi/l_0, 2\pi/\sigma\}$) fluctuations around this state, a linear stability study of hydrodynamics equations has been performed by several authors (Goldhirsch and Zanetti [71], Deltour and Barrat [50], van Noije et al. [165]). We follow the detailed discussion of [163], reviewing their result for the linearized hydrodynamics of rescaled fields. The rescaled fluctuation fields are defined as

$$\delta\tilde{n}(\mathbf{r}, \tau) = \delta n(\mathbf{r}, t)/n \tag{6.1a}$$

$$\tilde{\mathbf{u}}(\mathbf{r}, \tau) = \mathbf{u}(\mathbf{r}, t)/v_0(t) \tag{6.1b}$$

$$\delta\tilde{T}(\mathbf{r}, \tau) = \delta T(\mathbf{r}, t)/T(t) \tag{6.1c}$$

Their Fourier transforms are given by $\delta\tilde{a}(\mathbf{k}, \tau) = \int d\mathbf{r} \exp(-i\mathbf{k} \cdot \mathbf{r}) \delta\tilde{a}(\mathbf{r}, \tau)$, where a is one of $(n, \mathbf{u}, T)$.

The vector $\tilde{\mathbf{u}}(\mathbf{k}, \tau)$ can be decomposed in $(d-1)$ vectors perpendicular to $\mathbf{k}$, called indistinctly $\tilde{\mathbf{u}}_\perp$, and one vector parallel to $\mathbf{k}$, called $\tilde{\mathbf{u}}_\parallel$.

The linearized hydrodynamics for these fluctuations is given (in Fourier space) by the following equation:

$$\frac{\partial}{\partial\tau}\delta\tilde{\mathbf{a}}(\mathbf{k}, \tau) = \tilde{\mathcal{M}}(\mathbf{k})\delta\tilde{a}(\mathbf{k}, \tau) \tag{6.2}$$

where

$$\tilde{\mathbf{a}} = \begin{cases} (n, u_\perp, u_\parallel, T) \ (d=2) \\ (n, u_\perp, u'_\perp, u_\parallel, T) \ (d=3) \end{cases} \tag{6.3}$$

The matrix $\tilde{\mathcal{M}}$ is given (in $d=2$) by:

$$\tilde{\mathcal{M}} = \begin{pmatrix} 0 & 0 & -ikl_0 & 0 \\ 0 & \gamma_0(1-k^2\xi_\perp^2) & 0 & 0 \\ -ikl_0\left(\frac{1}{2nT\chi_T}\right) & 0 & \gamma_0(1-k^2\xi_\parallel^2) & -ikl_0\left(\frac{p}{2nT}\right) \\ -\gamma_0 g(n) & 0 & -ikl_0\left(\frac{2p}{dnT}\right) & -\gamma_0(1+k^2\xi_T^2) \end{pmatrix} \tag{6.4}$$
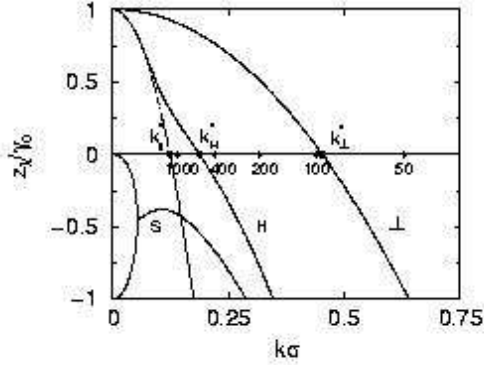
Figure 6.1: Growth rates ζ_λ/γ_0 for shear ($\lambda =\perp$), heat ($\lambda = H$) and sound ($\lambda = \pm$) modes versus $k\sigma$ for inelastic hard disks with $r = 0.9$ at a packing fraction $\phi = 0.4$. The dashed line indicate the imaginary parts of the sound modes that vanish for $k \ll \gamma_0/l_0$. (From Orza et al. [136])

with $\gamma_0 = \frac{1-r^2}{2d}$

Here we have introduced the correlation lengths $\xi_\perp$, $\xi_\parallel$ and ξ_T that depend on the transport coefficients (shear and bulk viscosity and heat conductivity), on the isothermal compressibility $\chi_T = (\partial n/\partial p)_T/n$ and on the pair distribution function $g(n)$ already mentioned. We refer to [163] for detailed calculations of these correlation lengths.

We report in Fig. 6.1 a plot published in several articles from van Noije and co-workers [136], that displays the linear dispersion relations, i.e. the exponential growth rates of the modes as functions of the wave number.

Several facts must be noted. The first is that (in this linear analysis) the evolution of fluctuations of normal velocity components (shear modes, $\tilde{\mathbf{u}}_\perp$) are not coupled with any other fluctuating component. At the same time, all the other components are coupled together. The study of eigenvalues and eigenvectors confirms the fact that the shear modes are not coupled with the other modes. The eigenvectors of the matrix define, beyond the shear modes, three other modes: one heat mode and two sound modes, denoted in the following with the subscripts H and $+$ or $-$ respectively. The associated eigenvalues are $\zeta_\perp(k)$, $\zeta_H(k)$, $\zeta_+(k)$ and $\zeta_-(k)$. It is immediate to see that $\zeta_\perp(k) = \gamma_0(1 - k^2\xi_\perp^2)$. At low values of k (in the dissipative range defined below) also the heat mode is "pure", as it is given by the longitudinal velocity mode $\tilde{\mathbf{u}}_\parallel$ only, with eigenvalue $\zeta_H(k) \simeq \gamma_0(1 - \xi_\parallel^2 k^2)$; in this range the sound modes are combination of density and temperature fluctuations.

The most important result of this analysis is that $\zeta_\perp(k)$ and $\zeta_H(k)$ are *positive* below the threshold values $k_\perp^* = 1/\xi_\perp \sim \sqrt{\epsilon}$ and $k_H^* \simeq 1/\xi_\parallel \sim \epsilon$ respectively, indicating two linearly unstable modes with exponential (in τ) growth rates. Here $\epsilon = 1 - r^2$.

The shear and heat instabilities are well separated at low inelasticity, as $k_\perp^* \sim \sqrt{\epsilon}$ while $k_H^* \sim \epsilon$, so that $k_\perp^* \gg k_H^*$. It is also important to note that the linear total size L of the system can suppress the various instability, as the minimum wave number $k_{min} = 2\pi/L$ can be larger than k_H^* or even than $k_\perp^*$.

Moreover, the study of the eigenvalues of the linear stability matrix, shows that several regimes in the k-space are present:

- for $2\pi/L \ll k \ll \gamma_0/l_0$ (*dissipative range*), all the eigenvalues are real, so that propagating modes are absent;

- for $\gamma_0/l_0 \ll k \ll \sqrt{\gamma_0}/l_0$ (*standard range*), the eigenvalues corresponding to sound modes are complex conjugates, so that the sound modes propagate;

- for $\sqrt{\gamma_0}/l_0 \ll k \ll \min\{2\pi/l_0, 2\pi/\sigma\}$ (*elastic range*) the heat conduction become dominant; in this range the dispersion relations resemble those of an elastic fluid.

The above picture, of course, requires the scale separation $\gamma_0 \ll \sqrt{\gamma_0}$ (valid at low inelasticity).

6.2 Hydrodynamic of the inclined plane model

We follow Brey et al. [23] and write down the hydrodynamics for the Inclined Plane Model presented in this paper (gravity in one direction and vibrating bottom wall, i.e. $\mathbf{g} = (0, g_e)$ and $g_e < 0$), with the following assumptions: the fields do not depend upon x (the coordinate parallel to the bottom wall), i.e. $\partial/\partial x = 0$, and the system is in a steady state, i.e. $\partial/\partial t = 0$. The continuity equation then reads $\frac{\partial}{\partial y}(n(y)u_y(y)) = 0$ and this can be compatible with the bottom and top walls (where $nv_y = 0$) only if $n(y)v_y(y) = 0$, that is in the absence of macroscopic vertical flow. The equations are written for the dimensionless fields $\tilde{T}(\tilde{y}) = k_B T(y)/(-g_e m \sigma)|_{y=\sigma\tilde{y}}$ and $\tilde{n}(\tilde{y}) = n(y)\sigma^2|_{y=\sigma\tilde{y}}$, while the position y is made dimensionless using $\tilde{y} = y/\sigma$. Finally for the pressure we put $p(y) = \mathcal{P}_{22} = n(y)k_B T(y)$. With the assumption discussed above the equations of Brey et al read:

$$\frac{d}{d\tilde{y}}(\tilde{n}(\tilde{y})\tilde{T}(\tilde{y})) = -\tilde{n}(\tilde{y}) \tag{6.5}$$

$$\frac{1}{\tilde{n}(\tilde{y})}\frac{d}{d\tilde{y}}Q_r(\tilde{y}) - C(r)\tilde{n}(\tilde{y})\tilde{T}(\tilde{y})^{3/2} = 0 \tag{6.6}$$

where $Q_r(\tilde{y})$ is the granular heat flux expressed by

$$Q_r(\tilde{y}) = A(r)\tilde{T}(\tilde{y})^{1/2}\frac{d}{d\tilde{y}}\tilde{T}(\tilde{y}) + B(r)\frac{\tilde{T}(\tilde{y})^{3/2}}{\tilde{n}(\tilde{y})}\frac{d}{d\tilde{y}}\tilde{n}(\tilde{y}) \tag{6.7}$$

In the above equations $A(r)$, $B(r)$ and $C(r)$ are dimensionless monotone coefficients, all with the same sign (positive), explicitly given in the Appendix B. In particular $B(1) = 0$ and $C(1) = 0$, i.e. in the elastic limit there is no dissipation and the heat transport is due only to the temperature gradients, while when $r < 1$ a term dependent upon $\frac{d}{d\tilde{y}}\ln(\tilde{n}(\tilde{y}))$ appears in $Q_r(\tilde{y})$. The use of dimensionless fields eliminates the explicit $\mathbf{g}$ dependence from the equations, that remains hidden in their structure (the right hand term of equation 6.5, that is due to the gravitational pressure gradient, disappears in the equation for $g = 0$).

6.2.1 The solution of the equations

A change of coordinate can be applied to Eqs. (6.5),(6.6) in order to obtain a simpler form:

$$\tilde{y} \to l(\tilde{y}) = \int_0^{\tilde{y}} \tilde{n}(y')dy' \tag{6.8}$$

It follows that when y spans the range $[0, L_y]$, the coordinate l spans the range $[0, \sigma/L_x]$. With this change of coordinate it happens that

$$\frac{d}{d\tilde{y}} \to \tilde{n}(l)\frac{d}{dl} \tag{6.9}$$

and the first equation (6.5) reads:

$$\frac{d}{dl}(\tilde{n}(l)\tilde{T}(l)) = -1 \tag{6.10}$$

from which is immediate to see that

$$H = \tilde{n}(l)\tilde{T}(l) + l \tag{6.11}$$

is a constant, i.e. $\frac{d}{dl}H = 0$. This is equivalent to observe that

$$p(y) - g \int_0^y n(y')dy' \qquad (6.12)$$

is constant which is nothing more than the Bernoulli theorem for a fluid in the gravitational field with the density depending upon the height.

The relation (6.11) is verified by the model simulated in this work for almost all the height of the container, apart of the boundary layer near the bottom driving wall.

Using the coordinate l introduced in (6.8) and the elimination of $\tilde{n}(l)$ using the recognized constant, that is

$$\tilde{n}(l) = \frac{H - l}{\tilde{T}(l)} \qquad (6.13)$$

the second equation (6.6), after some simplifications, and after a second change of coordinate $l \to s(l) = H - l$, becomes:

$$\frac{\alpha(r)s}{\tilde{T}(s)^{1/2}} \frac{d^2}{ds^2}\tilde{T}(s) - \frac{\alpha(r)s}{2\tilde{T}(s)^{3/2}} \left(\frac{d}{ds}\tilde{T}(s)\right)^2 + \frac{\beta(r)}{\tilde{T}(s)^{1/2}}\frac{d}{ds}\tilde{T}(s) - s\tilde{T}(s)^{1/2} = 0 \qquad (6.14)$$

where $\alpha(r) = (A(r) - B(r))/C(r)$, $\beta(r) = (A(r) - \frac{1}{2}B(r))/(C(r))$ are numerically checked to be positive (α is positive for values of r not too low, about $r > 0.3$) and are divergent in the limit $r \to 1$.

The correspondence with the solution of Brey et al. [26] is given by:

$$k^* \to A \qquad (6.15a)$$
$$\mu^* \to B \qquad (6.15b)$$
$$\zeta^* \to \frac{C}{\pi} \qquad (6.15c)$$
$$l \to 2\sqrt{2}s - p_L^* \qquad (6.15d)$$
$$C \to 2\sqrt{2} \qquad (6.15e)$$
$$a(r) \to \frac{1}{4\sqrt{2}\alpha} \qquad (6.15f)$$
$$b(r) \to \frac{\beta}{\alpha} \qquad (6.15g)$$
$$\xi \to \frac{s}{\sqrt{2\alpha}} \qquad (6.15h)$$
$$\nu \to \frac{1}{2}\frac{\beta - \alpha}{\alpha} \qquad (6.15i)$$

The equation (6.14) become a linear equation in $\tilde{T}(s)$ as soon as the change of variable $z(s) = \tilde{T}(s)^{1/2}$ is performed:

$$2\alpha(r)s\frac{d^2}{ds^2}z(s) + 2\beta(r)\frac{d}{ds}z(s) - sz(s) = 0 \qquad (6.16)$$

giving the solution:

$$z(s) = \mathcal{A}s^{-\nu(r)}I_{\nu(r)}(s/\sqrt{2\alpha}) + \mathcal{B}s^{-\nu(r)}K_{\nu(r)}(s/\sqrt{2\alpha}) \qquad (6.17)$$

where I_ν and K_ν are the modified Bessel functions of the first kind and the second kind respectively, $\nu(r) = B(r)/(4(A(r) - B(r)))$ is real and positive for all the values of r greater than the zero of the function $A(r) - B(r)$ (about $r \simeq 0.3$), with $\nu(1) = 0$, while $\mathcal{A}$ and $\mathcal{B}$ are constants that must be determined with assigning the boundary conditions.

Then we can derive the expressions for $\tilde{T}(l)$ and $\tilde{n}(l)$:

$$\tilde{T}(l) = (H - l)^{-2\nu(r)}(\mathcal{A}I_{\nu(r)}((H - l)/\sqrt{2\alpha(r)}) + \mathcal{B}K_{\nu(r)}((H - l)/\sqrt{2\alpha(r)}))^2 \qquad (6.18)$$

$$\tilde{n}(l) = \frac{(H - l)^{1+2\nu(r)}}{(\mathcal{A}J_{\nu(r)}((H - l)/\sqrt{2\alpha(r)}) + \mathcal{B}N_{\nu(r)}((H - l)/\sqrt{2\alpha(r)}))^2} \qquad (6.19)$$

To calculate the expressions of $\tilde{T}$ and $\tilde{n}$ as a function of the original coordinate $\tilde{y}$ one needs to solve the equation

$$\frac{d}{dl}\tilde{y}(l) = \frac{1}{\tilde{n}(l)} \qquad (6.20)$$

putting in it the solution (6.19). However one can obtain a comparison with the numerical simulations using the new coordinate l. For a discussion of the boundary conditions needed to eliminate the constants H, $\mathcal{A}$ and $\mathcal{B}$ we refer the reader to the paper of Brey et al.[26]. In this paper the authors show that the solution fit very well a large region in the bulk but cannot work on the boundary regions near the vibrating bottom and near the open surface. The authors show also that a minimum of the temperature is compatible with the proposed equations.

6.3   The problem of scale separation

I. Goldhirsch [71, 70, 69, 67, 68] takes in consideration all the recent literature on rapid granular flows, putting in evidence the points where the hydrodynamics description is at risk. The limits of hydrodynamics have been intensively probed by means of simulations and experiments, and it seems that a range of good validity can be found (perhaps it is more difficult to predict it!). However Goldhirsch points out that even these successes are somehow lacking a rigorous foundation, or using is words that "the notion of a hydrodynamic, or macroscopic description of granular materials is based on unsafe grounds and it requires further study". He addresses two fundamental issues:

1. in granular materials a reference equilibrium state is missing;

2. in granular materials the spatial and temporal scales of the dynamics of the particles are not well separated from the relevant macroscopic scales;

The first problem is more evident than the second. If a molecular gas is left to itself it comes to an equilibrium state given by the stationary solution of the corresponding kinetic equation (rarefied gases follow the Boltzmann equation, dense gases follow the Enskog-Boltzmann equation or better the ring kinetic equations). If such an equilibrium state is well defined, perturbations around it can be used as solutions of non-equilibrium problems. Moreover, if external time scales are much larger than the microscopic time scale of relaxation to equilibrium, most of the degrees of freedom of the gas are rapidly averaged and only a few variables are needed for the description of the out of equilibrium dynamics, which obey to macroscopic equations such as Euler or Navier-Stokes equations. If a granular gas is left to itself, instead, the only equilibrium state is an asymptotic death of the motion of all the particles, but before it different kinds of correlations arise leading to strong inhomogeneities (clustering, vortices, shocks, collapse, and so on). In this sense the relaxation to equilibrium has a characteristic time which is infinite and *many other characteristic times* given by different instabilities, due to the non-conservative nature of the collisions. What reference state can be used in a perturbative method like the Chapman-Enskog expansion? In the first derivations of granular hydrodynamics the Maxwell-Boltzmann equilibrium was used, in the latest derivations a more rigorous Chapman-Enskog expansion has been followed using solutions of the Enskog-Boltzmann equation by means of a Sonine expansion (which again must be performed around a Maxwell distribution). Goldhirsch has observed however that the limit $(1 - r) \to 0$ and $Kn \to 0$ (the Knudsen number, indicating the intensity of the gradients) is smooth and non singular for the granular Boltzmann equation, since the relaxation to local equilibrium

takes place in a few collisions per particle, while the effect of (low) inelasticity is relevant on the order of hundreds or thousands of collisions. This means that a perturbative (in $1 - r^2$ and Kn) expansion may be applied to the Boltzmann equation around a well suited "elastic" equilibrium, but it is expected to breakdown as $(1 - r)$ or Kn are of order ~ 1.

In a stationary state the only hope is that the system fluctuates around a well defined "most probable state" (described by a well defined n-particles distribution function, hopefully $n = 1$) and again an expansion around it can be performed. This program has not yet been realized: till now all hydrodynamic theories assume that the equilibrium reference state does not depend on the boundary conditions (e.g. the form of the external driving) and that both cooling and driven regimes can be described by the same set of equations.

The second issue raised by Goldhirsch stems from a more quantitative discussion. He stresses the fact that the lack of scales separation is not only a mere experimental problem: one can in principle think of experiments with an Avogadro number of grains and very large containers. Instead the lack of separation of scales is of fundamental nature in the framework of granular materials. This problem has been already recognized in molecular gases: indeed, when molecular gases are subject to large shear rates or large thermal gradients (i.e. when the velocity field or the temperature field changes significantly over the scale of a mean free path or the time defined by the mean free time) there is no scale separation between the microscopic and macroscopic scales and the gas can be considered mesoscopic. In this case the Burnett and super-Burnett corrections (and perhaps beyond) are of importance and the gas exhibits differences of the normal stress (e.g. $\mathcal{P}_{xx} \neq \mathcal{P}_{yy}$) and other properties characteristic of granular gases. Even if clusters are not expected in molecular gases, strongly sheared gases do exhibit ordering which violates the molecular-chaos assumption. In granular gases this kind of *mesoscopicity* is generic and not limited to strong forcing. Moreover, phenomena like clustering, collapse (and of course avalanches or oscillon excitations) pertain only to granular gases. In mesoscopic systems fluctuations are expected to be stronger and the ensemble averages need not to be representative of their typical values. Furthermore, like in turbulent systems or systems close to second-order phase transitions, in which scale separation is non-existent, one expects constitutive relations to be scale dependent, as it happens in granular gases.

The quantitative demonstration of the intrinsic mesoscopic nature of (cooling) granular gases follows from the relation [71]

$$T = C \frac{\gamma^2 l_0^2}{1 - r^2} \tag{6.21}$$

that relates the local granular temperature with the local shear rate γ and the mean free path l_0. The above relation holds until γ can be considered a slow varying (decaying) quantity in respect to the much more rapid decay of the temperature fluctuations (this can be observed by a linear stability analysis and also by the fact that shear modes decay slowly for small wave-numbers - a result of momentum conservation). From the Eq. (6.21) follows that the ratio between the change of macroscopic velocity over a distance of a mean free path $l_0\gamma$ and the thermal speed $\sqrt{T}$ is $\sqrt{1 - r^2}/\sqrt{C}$, e.g. $\simeq 0.44$ for $r = 0.9$, that is not small. Thus, except for very low values of $1 - r^2$, the shear rate is always large and the Chapman-Enskog expansion should therefore carried out beyond the Navier-Stokes order. The above consideration is a simple consequence of the supersonic nature of granular gases [68]. It is clear that a collision between two particles moving in (almost) the same direction reduces the relative velocity, i.e. velocity fluctuations, but not the sum of their momenta, so that in a number of these collisions the magnitude of the velocity fluctuations may become very small with respect to the macroscopic velocities and their differences over the distance of a mean free path. Also the notion of mean free path may become useless: l_0 is defined as a Galilean invariant, i.e. as the product between the thermal speed $\sqrt{T}$ and the mean free time τ; but in a shear experiment the average squared velocity of a particle is given by $\gamma^2 y^2 + T$ (y is the direction of the increasing velocity field), so when $y \gg \sqrt{T}/\gamma$, the distance covered by the particle in the mean free time τ is $l(y) = y l_0 \gamma/\sqrt{T} = y \sqrt{1 - r^2}/\sqrt{C}$ and therefore can become much larger that the "equilibrium" mean free path l_0 and even of the length of the system in the streamwise direction.

Furtherly, the ratio between the mean free time $\tau = l_0/\sqrt{T}$ and the macroscopic characteristic time of the problem $1/\gamma$, using expression (6.21), reads again $\sqrt{1 - r^2}/\sqrt{C}$. This means that also the

separation between microscopic and macroscopic time scales is guaranteed only for $r \rightarrow 1$. And this result is irrespective of the size of the system or the size of the grains. This lack of separation of time scales poses two serious problem: (a) the fast local equilibration that allows to use local equilibrium as zeroth order distribution function is not obvious; (b) the stability studies are usually performed linearizing hydrodynamic equations, but the characteristic times related to the (stable and unstable) eigenvalues must be of the order of the characteristic "external" time (e.g. $1/\gamma$) which, in this case, is of the order of the mean free time (as just derived), leading to the paradoxical conclusion that the hydrodynamic equations predict instabilities on time scales which they are not supposed to resolve.

Goldhirsch [68] has also shown that the lack of separation of space and time scales leads to scale dependence of fields and fluxes. In particular he has shown that the pressure tensor depends on the scale of the coarse graining used to take space-time averages. This is similar to what happens, for example, in turbulence, where the "eddy viscosity is scale dependent. Pursuing this analogy, Goldhirsch has noted that an intermittent behavior can be observed in the time series of experimental and numerical measures of the components pressure tensor: single collisions, which are usually averaged over in molecular systems, appear as "intermittent events" in granular systems as they are separated by macroscopic times.

Lecture 7

Granular mixtures

Important note: *in chapters 7, 8 and 9 I have replaced the symbol r with the symbol α to denote the restitution coefficient*

7.1 Two possible driven models

We shall consider a dilute inelastic gas constituted of N_1 particles of mass m_1 and N_2 particles of mass m_2 subject to some kind of external driving (this will be specified in the following). We suppose that the interactions between the grains can be described by the smooth inelastic hard sphere model, thus we specify only the radius of the spheres, their masses and the fraction of the kinetic energy dissipated at each collision. This can be done by defining three different restitution coefficients α_{ij}, i.e. α_{11}, α_{22}, and $\alpha_{12} = \alpha_{21}$, which account for normal dissipation in collisions among particles of type i and j. No internal degrees of freedom (e.g. rotations) are included.

One can describe the velocity changes induced by the instantaneous inelastic collisions of smooth disks labeled 1 and 2 of diameter σ_1 and σ_2 by the following equations:

$$\mathbf{v}'_1 = \mathbf{v}_1 - \frac{1 + \alpha_{\kappa_1 \kappa_2}}{2} \frac{m_{\kappa_2}}{m_{\kappa_1} + m_{\kappa_2}} ((\mathbf{v}_1 - \mathbf{v}_2) \cdot \hat{\mathbf{n}}) \hat{\mathbf{n}} \tag{7.1a}$$

$$\mathbf{v}'_2 = \mathbf{v}_2 + \frac{1 + \alpha_{\kappa_1 \kappa_2}}{2} \frac{m_{\kappa_1}}{m_{\kappa_1} + m_{\kappa_2}} ((\mathbf{v}_1 - \mathbf{v}_2) \cdot \hat{\mathbf{n}}) \hat{\mathbf{n}} \tag{7.1b}$$

where $\hat{\mathbf{n}} = 2(\mathbf{x_1} - \mathbf{x_2})/(\sigma_{\kappa_1} + \sigma_{\kappa_2})$ is the unit vector along the line of centers $\mathbf{x}_1$ and $\mathbf{x}_2$ of the colliding disks at contact and κ_1, κ_2 are the species (1 or 2) to whom particles 1 and 2 belong. An elementary collision conserves the total momentum and reduces the relative kinetic energy by an amount proportional to $(1 - \alpha^2_{\kappa_1 \kappa_2})/4$. The collision rule we have adopted excludes the presence of tangential forces, and hence the rotational degrees of freedom do not contribute to the description of the dynamics.

Since the particles suffer mutual collisions and loose kinetic energy, in order to achieve a steady state, one needs to supply from the exterior some energy. Here we assume that the particles experience a uniform stochastic force and a viscous damping (see Lecture 4). The presence of the velocity-dependent term in addition to the random forcing, not only is motivated by the idea of preventing the energy of a driven elastic system ($\alpha_{\kappa_1 \kappa_2} \to 1$), to increase indefinitely, but also mimics the presence of friction of the particles with the container. A fluctuation dissipation relation is assumed between the viscous force and the intensity of the noise. Even in extended systems with small inelasticity the absence of friction may cause some problems of stability.

Since we consider throughout only sufficiently low density systems successive binary collisions are effectively uncorrelated and Boltzmann equation can be used to describe the non equilibrium dynamics.

In order to see the effect of the heat bath let us consider the system in the absence of collisions. In this case, the evolution of the velocity of each particle is described by an Ornstein-Uhlenbeck process. If

we require that the two components must reach the same granular temperature in the limit of vanishing inelasticity we have two different possibilities to fix the heat bath parameters:

$$\partial_t \mathbf{x}_i(t) = \mathbf{v}_i(t) \tag{7.2}$$

$$m_i \partial_t \mathbf{v}_i(t) = -\gamma \mathbf{v}_i(t) + \sqrt{2\gamma T_b}\, \xi_i(t) \tag{7.3a}$$

$$m_i \partial_t \mathbf{v}_i(t) = -m_i \eta \mathbf{v}_i(t) + \sqrt{2 m_i \eta T_b}\, \xi_i(t) \tag{7.3b}$$

where $i = 1, 2$ and T_b is the heat bath temperature and $\xi(t)$ is a Gaussian noise with the following properties:

$$< \xi_i(t) > = 0 \tag{7.4a}$$

$$< \xi_i(t_1)\xi_j(t_2) > = \delta(t_1 - t_2)\delta_{ij} \tag{7.4b}$$

The associated Fokker-Planck equations for the two cases are respectively:

$$\partial_t f_i(\mathbf{r}, \mathbf{v}, t) = \frac{\gamma}{m_i} \nabla_v (\mathbf{v} f_i(\mathbf{r}, \mathbf{v}, t)) + \frac{\gamma T_b}{m_i^2} \nabla_v^2 f_i(\mathbf{r}, \mathbf{v}, t) \mathbf{v} \nabla_r f_i(\mathbf{r}, \mathbf{v}, t) \tag{7.5a}$$

$$\partial_t f_i(\mathbf{r}, \mathbf{v}, t) = \eta \nabla_v (\mathbf{v} f_i(\mathbf{r}, \mathbf{v}, t)) + \frac{\eta T_b}{m_i} \nabla_v^2 f_i(\mathbf{r}, \mathbf{v}, t) + \mathbf{v} \nabla_r f_i(\mathbf{r}, \mathbf{v}, t) \tag{7.5b}$$

7.1.1 Spatially Uniform solutions

When we take into account collisions among particles equations (7.5) become two coupled Boltzmann equations modified by the presence of a diffusion term due to the thermal noise. In order to derive the temperature of each species in the homogeneous stationary state, we shall first neglect the spatial dependence of the distribution functions f_i. This can be regarded as a mean field approximation to the Boltzmann equation. In other words we let collisions to occur regardless their spatial separation. First, indicating by $n_i = N_i/V$ the partial density of species i, we notice that both eqs. (7.5) possess the same equilibrium solution:

$$f_i(\mathbf{v}) = n_i \left(\frac{m_i}{2\pi T_b} \right)^{\frac{d}{2}} e^{-\frac{m_i v^2}{2T_b}} \tag{7.6}$$

but their relaxation properties are different. Only upon adding the inelastic collision term the two species display different temperatures. The resulting Boltzmann equation for a granular mixture is:

$$\partial_t f_i(\mathbf{v}_1; t) = \sum_j J_{ij}[\mathbf{v}_1 | f_i, f_j] + \frac{\xi_{0i}^2}{2} \nabla_v^2 f_i + \eta_i \nabla_v \cdot (\mathbf{v}_1 f_i) \tag{7.7}$$

where we have used a compact notation to represent the two different choices of heat bath:

- **Case 1**

$$\begin{aligned} \xi_{0i}^2 &\to \frac{2\gamma T_b}{m_i^2} \\ \eta_i &\to \frac{\gamma}{m_i} \end{aligned} \tag{7.8}$$

- **Case 2**

$$\begin{aligned} \xi_{0i}^2 &\to \frac{2\eta T_b}{m_i} \\ \eta_i &\to \eta \end{aligned} \tag{7.9}$$

and $J_{ij}[v_1|f_i, f_j]$ is the collision integral:

$$J_{ij}[v_1|f_i, f_j] \equiv \sigma_{ij}^2 \int d\mathbf{v}_2 \int d\hat{\sigma} \Theta(\hat{\sigma} \cdot \mathbf{g}_{12})(\hat{\sigma} \cdot \mathbf{g}_{12})[\alpha_{ij}^{-2} f_i(\mathbf{v_1'})f_j(\mathbf{v_2'}) - f_i(\mathbf{v_1})f_j(\mathbf{v_2})] \qquad (7.10)$$

The primed velocities are pre-collisional states, which can be obtained by inverting eqs. (7.1)

Due to the presence of the heat bath terms the system reaches asymptotically a steady state, characterized by time independent pdf's. By requiring stationarity and integrating over $\mathbf{v_1}$ the eq. for $v_i^2 f_i$ we obtain:

$$\sum_j \int d\mathbf{v}_1 v_1^2 J_{ij}[\mathbf{v}_1|f_i, f_j] + \frac{\xi_{0i}^2}{2} \int d\mathbf{v}_1 v_1^2 \nabla_v^2 f_i + \eta_i \int d\mathbf{v}_1 v_1^2 \nabla_v \cdot (\mathbf{v}_1 f_i) = 0 \qquad (7.11)$$

After simplifying the second and the third integral by integration by parts and using the normalization property $\int f_i dv_i = n_i$ we find:

$$\sum_j \int d\mathbf{v_1} v_1^2 J_{ij}[\mathbf{v_1}|f_i, f_j] + n_i d\xi_{0i}^2 - 2\eta_i \int d\mathbf{v}_1 v_1^2 f_i(\mathbf{v}_1) = 0 \qquad (7.12)$$

The partial temperature is defined as:

$$n_i T_i \equiv \frac{1}{d} \int d\mathbf{v_1} m_i v_1^2 f_i \qquad (7.13)$$

so that eq. (7.12) can be recast as:

$$T_i = \frac{m_i}{2d\eta_i} \left(\frac{1}{n_i} \sum_j \int d\mathbf{v_1} v_1^2 J_{ij}[v_1|f_i, f_j] + d\xi_{0i}^2 \right) \qquad (7.14)$$

Eq. (7.14) determines the partial temperatures once the f_i are known. In practice one can obtain an estimate of T_i by substituting two Maxwell distributions:

$$f_i(v) = n_i \left(\frac{m_i}{2\pi T_i} \right)^{\frac{d}{2}} e^{-\frac{m_i v_1^2}{2T_i}}.$$

After performing the remaining integrals one gets:

$$\frac{d\Gamma(d/2)}{m_i \pi^{(d-1)/2}} 2\eta_i(T_b - T_i) = \sigma_{ii}^{d-1} n_i \frac{2(1 - \alpha_{ii}^2)}{m_i^{3/2}} T_i^{3/2}$$

$$+ \sigma_{ij}^{d-1} n_j \mu_{ji} \left[\mu_{ji}(1 - \alpha_{ij}^2) \left(\frac{2T_i}{m_i} + \frac{2T_j}{m_j} \right) + 4(1 + \alpha_{ij}) \frac{T_i - T_j}{m_1 + m_2} \right] \left(\frac{2T_i}{m_i} + \frac{2T_j}{m_j} \right)^{1/2} \qquad (7.15)$$

where $\mu_{ij} = m_i/(m_i + m_j)$. One obtains the steady values of the partial temperatures in the spatially homogeneous situation, by solving numerically the nonlinear system of eqs. (7.15).

7.1.2 Comparison between the two heat-baths

In figs. 7.1 and 7.2 we report the temperature ratio $\frac{T_1}{T_2}$ as a function of a common restitution coefficient α, having chosen equal coefficients $\alpha_{11} = \alpha_{22} = \alpha_{12} = \alpha$. Assuming identical concentrations, and varying the mass ratio $\frac{m_1}{m_2}$, we considered cases 1 and 2.

In the first case the species with the largest mass is "colder". In fact both components receive the same energy from the heat-bath, but the heavier species dissipates more energy due to collisions.

We notice that, on the contrary, with the second recipe (case 2) the temperature ratio is, on the contrary, an increasing function of the mass ratio m_1/m_2. The experimental observation [64] suggest that the trend of case 2 is physically more relevant. In case 2 both the friction term and the power supplied are proportional to the mass of the two species.
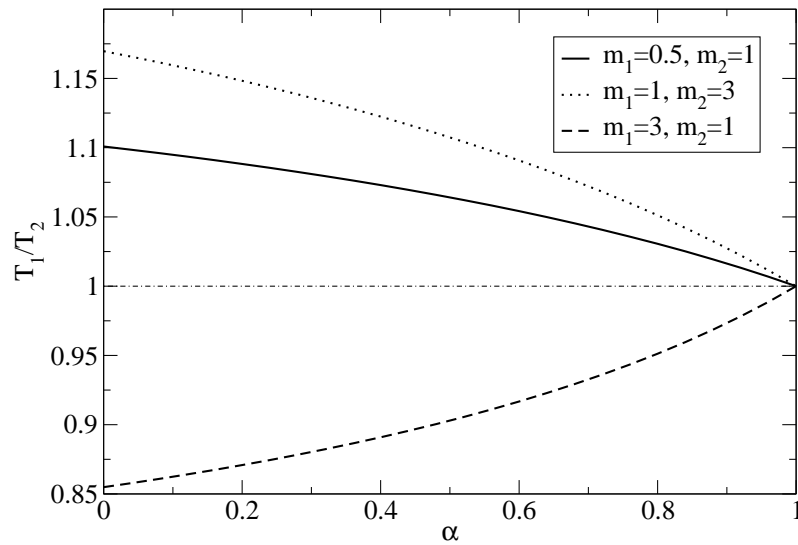
Figure 7.1: Homogeneous driving. Granular temperature ratio T_1/T_2 vs. α obtained with the heat bath of case 1 using $T_b = 1$, $\gamma = 0.1$ and different mass ratios.
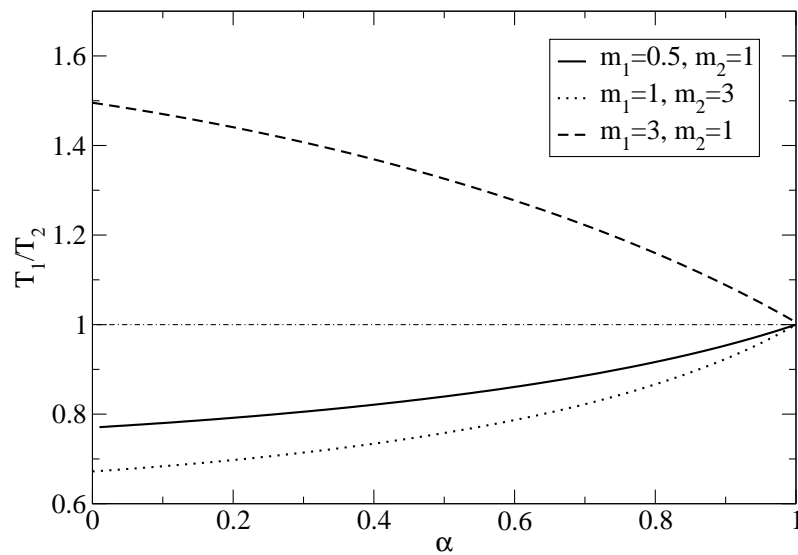

Figure 7.2: Homogeneous driving of case 2. Granular temperature ratio T_1/T_2 vs. α with $T_b = 1$, $\eta = 0.1$ and various mass ratios.

7.2 Tracer limit: the Markovian case

Here we consider the case of two species 1 and 2, with the species 1 constituted by N particles and the species 2 by only one particle: they are also called the "gas" and the "intruder" respectively. The gas particles have mass m and diameter $2r$, while the intruder has mass M and diameter R. We also define the following quantities which will be useful: $\epsilon = \sqrt{m/M}$ and $\chi = n(r + R)^{d-1}$ (with n the gas density).

Let us start by writing the coupled Boltzmann equations for the probability distributions $P(\mathbf{V}, t)$ (for the intruder) and $p(\mathbf{v}, t)$ (for the gas), denoting - for simplicity - with $\mathbf{V}$ and $\mathbf{v}$ the intruder velocity and the gas velocity, respectively

$$
\begin{aligned}
\frac{\partial P(\mathbf{V}, t)}{\partial t} &= \int d\mathbf{V}'[W_{tr}(\mathbf{V}|\mathbf{V}')P(\mathbf{V}', t) - W_{tr}(\mathbf{V}'|\mathbf{V})P(\mathbf{V}, t)] + \mathcal{B}_{tr}P(\mathbf{V}, t) \\
\frac{\partial p(\mathbf{v}, t)}{\partial t} &= \int d\mathbf{v}'[W_g(\mathbf{v}|\mathbf{v}')p(\mathbf{v}', t) - W_g(\mathbf{v}'|\mathbf{v})p(\mathbf{v}, t)] + \mathcal{B}_g p(\mathbf{v}, t) \\
&+ \chi Q[\mathbf{v}|p, p],
\end{aligned}
\tag{7.16}
$$

where $\mathcal{B}_{tr}$ and $\mathcal{B}_g$ take into account the interactions with the thermal bath. In these equations the collision operators appear, for the tracer and the gas particles, respectively

$$
\begin{aligned}
W_{tr}(\mathbf{V}|\mathbf{V}') &= \chi \int d\mathbf{v}' \int d\hat{\sigma} p(\mathbf{v}', t)\Theta\left[-(\mathbf{V}' - \mathbf{v}') \cdot \hat{\sigma}\right](\mathbf{V}' - \mathbf{v}') \cdot \hat{\sigma} \\
&\times \delta^{(d)}\left\{\mathbf{V} - \mathbf{V}' + \frac{\epsilon^2}{1 + \epsilon^2}(1 + \alpha)\left[(\mathbf{V}' - \mathbf{v}') \cdot \hat{\sigma}\right]\hat{\sigma}\right\}
\end{aligned}
\tag{7.17}
$$

and

$$
\begin{aligned}
W_g(\mathbf{v}|\mathbf{v}') &= \frac{\chi}{N} \int d\mathbf{V}' \int d\hat{\sigma} P(\mathbf{V}', t)\Theta\left[-(\mathbf{V}' - \mathbf{v}') \cdot \hat{\sigma}\right](\mathbf{V}' - \mathbf{v}') \cdot \hat{\sigma} \\
&\times \delta^{(d)}\left\{\mathbf{v} - \mathbf{v}' + \frac{1}{1 + \epsilon^2}(1 + \alpha)\left[(\mathbf{v}' - \mathbf{V}') \cdot \hat{\sigma}\right]\hat{\sigma}\right\},
\end{aligned}
\tag{7.18}
$$

where $\Theta(x)$ is the Heaviside step function and $\delta^{(d)}(x)$ is the Dirac delta function in d; in the expressions (7.17) and (7.18) we have assumed that the probability $P_2(\mathbf{V}, \mathbf{v}, t)$ that a collision between the intruder and a gas particle occurs, when they have velocities $\mathbf{V}$ and $\mathbf{v}$ respectively, is given by the Molecular-Chaos approximation

$$
P_2(\mathbf{V}, \mathbf{v}, t) = P(\mathbf{V}, t)p(\mathbf{v}, t);
\tag{7.19}
$$

the terms describing the action of the termal bath read

$$
\mathcal{B}_{tr}P(\mathbf{V}, t) = \frac{\gamma_b}{M}\frac{\partial}{\partial\mathbf{V}}\left[\mathbf{V}P(\mathbf{V}, t)\right] + \frac{\gamma_b T_b}{M}\Delta_V[P(\mathbf{V}, t)]
\tag{7.20}
$$

$$
\mathcal{B}_g p(\mathbf{v}, t) = \frac{\gamma_b}{m}\frac{\partial}{\partial\mathbf{v}}\left[\mathbf{v}p(\mathbf{v}, t)\right] + \frac{\gamma_b T_b}{m}\Delta_v[p(\mathbf{v}, t)],
\tag{7.21}
$$

where Δ_v is the Laplacian operator with respect to the velocity; finally, the Boltzmann collision operator for the particle-particle interactions $Q[\mathbf{v}|p, p]$ is discussed in Lecture 3. In view of the fact that it is not relevant for the rest of the paper, we omit its explicit expression.

7.2.1 Decoupling the gas from the tracer: Gaussian case

The system of Boltzmann equations (7.16) is simplified when the quantities $P(\mathbf{V}, t)$ and $p(\mathbf{v}, t)$ significantly change on well-separated characteristic time scales, which happens if $N \gg 1$. Then one assumes that the probability distribution function $p(\mathbf{v})$ is constant and, following numerical evidence (verified below) it is approximated with a Gaussian function with variance T_g/m:

$$
p(\mathbf{v}) = \frac{1}{\sqrt{(2\pi T_g/m)^d}} \exp\left[-\frac{m\mathbf{v}^2}{2T_g}\right].
\tag{7.22}
$$

or by its first Sonine non-trivial correction (the second polynomial), when necessary.

The assumption of constant $p(\mathbf{v})$ implies that the first equation of the mixture (the evolution of the intruder probability) is decoupled from the second one and it is *linear* in $P(\mathbf{V})$: it becomes a Master Equation for a Markov process with transition rate W_{tr}.

7.2.2 The transition rate

When $p(\mathbf{v})$ is constant, one can calculate the transition rate for the intruder.

We first discuss in detail what happens in a collision (assume for simplicity equal masses) and then give a rigorous derivation of the master equation. The collision rule for inelastic hard spheres reads:

$$\mathbf{v}_1' = \mathbf{v}_1 - \frac{1+\alpha}{2}(\mathbf{v}_{12} \cdot \hat{\boldsymbol{\sigma}})\hat{\boldsymbol{\sigma}} \tag{7.23}$$

where $\hat{\boldsymbol{\sigma}}$ is the direction joining the centers of the two colliding particles. There are some consequences of the collision rules which have to be remarked. For simplicity we assume to be in dimension $d = 2$.

- $\Delta\mathbf{v}_1 = \mathbf{v}_1' - \mathbf{v}_1$ is parallel to $\hat{\sigma}$, i.e. $\theta = \arctan\frac{\Delta v_{1y}}{\Delta v_{1x}}$ where $\hat{\sigma}_x = \cos\theta$ and $\hat{\sigma}_y = \sin\theta$. This is equivalent to recognize that the velocity $\mathbf{v}_1$ changes only in the direction $\hat{\sigma}$. The fact that $\mathbf{v}_{12\sigma}$ must be negative determines completely the angle θ, i.e. the unitary vector $\hat{\sigma}$. From here on, we call $\Delta v_1 \equiv \Delta v_{1\sigma} \equiv \Delta\mathbf{v}_1 \cdot \hat{\sigma}$.

- $v_{2\sigma} \equiv \mathbf{v}_2 \cdot \hat{\sigma} = \frac{2}{1+\alpha}\Delta v_1 + v_{1\sigma} = \frac{2}{1+\alpha}v_{1\sigma}' - \frac{1-\alpha}{1+\alpha}v_{1\sigma}$.

- From the previous two remarks, it is clear that Δv_1 determines univocally $\hat{\sigma}$ and $v_{2\sigma}$. The component of $\mathbf{v}_2$ which is not determined by Δv_1 is the one orthogonal to $\hat{\sigma}$. We call $\hat{\tau}$ the direction perpendicular to $\hat{\sigma}$, i.e. the vector of component $(-\sin\theta, \cos\theta)$. We define $v_{2\tau} = \mathbf{v}_2 \cdot \hat{\tau}$.

From the above discussion, it is easy to understand that the transition probability for the particle 1 to change velocity during a collision, going from $\mathbf{v}_1$ to $\mathbf{v}_1'$ must be

$$W_{tr}(\mathbf{v}_1 \to \mathbf{v}_1') = C(\mathbf{v}_1, \mathbf{v}_1') \int \mathrm{d}v_{2\tau} P(\mathbf{v}_2) \tag{7.24a}$$

$$\mathbf{v}_2 = v_{2\sigma}\hat{\sigma} + v_{2\tau}\hat{\tau} \tag{7.24b}$$

$$\hat{\sigma} = (\cos\theta, \sin\theta) \tag{7.24c}$$

$$\hat{\tau} = (-\sin\theta, \cos\theta) \tag{7.24d}$$

$$\theta = \arctan\frac{\Delta v_{1y}}{\Delta v_{1x}} \tag{7.24e}$$

$$\hat{\sigma} \parallel \mathbf{v}_1' - \mathbf{v}_1 \tag{7.24f}$$

$$v_{2\sigma} = \frac{2}{1+\alpha}\Delta v_1 + v_{1\sigma} \tag{7.24g}$$

where $P(\mathbf{v})$ is the 1-particle probability density function for the velocity in the bulk gas. The constant of proportionality C must be of dimensions $1/length$ so that W_{tr} has dimensions $1/(velocity^d time)$ which is expected because W_{tr} is a rate of change of the velocity pdf (in d dimensions).

Now, we want to obtain the complete result, that is rigorously compare the usual linear Boltzmann equation for inelastic models to a Master Equation for a single-particle Markov process. The comparison immediately leads to

$$W_{tr}(\mathbf{v}_1 \to \mathbf{v}_1') = \chi \int \mathrm{d}\mathbf{v}_2 \int \mathrm{d}\hat{\boldsymbol{\omega}} \Theta(\mathbf{v}_{12} \cdot \hat{\boldsymbol{\omega}})|\mathbf{v}_{12} \cdot \hat{\boldsymbol{\omega}}|p(\mathbf{v}_2)\delta\left\{\mathbf{v}_1' - \mathbf{v}_1 + k(\epsilon,\alpha)[\mathbf{v}_{12} \cdot \hat{\boldsymbol{\omega}}]\hat{\boldsymbol{\omega}}\right\}. \tag{7.25}$$

where $p(v)$ is the velocity pdf of the bulk gas and $k(\epsilon,\alpha) = (1+\alpha)\epsilon^2/(1+\epsilon^2)$. Using that for a generic d-dimensional vector $\mathbf{r} = r\hat{\mathbf{r}}$ one has $\delta(\mathbf{r} - \mathbf{r}_0) = \frac{1}{r_0^{d-1}}\delta(r - r_0)\delta(\hat{\mathbf{r}} - \hat{\mathbf{r}}_0)$, the previous expression can

be rewritten as:

$$W_{tr}(\mathbf{v}_1 \rightarrow \mathbf{v}'_1) = \chi \int d\mathbf{v}_2 \int d\hat{\boldsymbol{\omega}}\Theta(\mathbf{v}_{12}\cdot\hat{\boldsymbol{\omega}})\frac{|\mathbf{v}_{12}\cdot\hat{\boldsymbol{\omega}}|}{\Delta v^{d-1}}p(\mathbf{v}_2)\delta(\hat{\boldsymbol{\sigma}}+\hat{\boldsymbol{\omega}})\delta\left(\Delta v + k(\epsilon,\alpha)|\mathbf{v}_{12}\cdot\hat{\boldsymbol{\omega}}|\right) \quad , \quad (7.26)$$

where Δv and $\hat{\boldsymbol{\sigma}}$ are defined by $\mathbf{v}'_1 - \mathbf{v}_1 = \Delta v\, \hat{\boldsymbol{\sigma}}$. Then, performing the angular integration over $\hat{\boldsymbol{\omega}}$, one obtains:

$$W_{tr}(\mathbf{v}_1 \rightarrow \mathbf{v}'_1) = \chi \int d\mathbf{v}_2\Theta(\mathbf{v}_{12}\cdot\hat{\boldsymbol{\sigma}})\frac{|\mathbf{v}_{12}\cdot\hat{\boldsymbol{\sigma}}|}{\Delta v^{d-1}}p(\mathbf{v}_2)\delta\left(\Delta v + k(\epsilon,\alpha)|\mathbf{v}_{12}\cdot\hat{\boldsymbol{\sigma}}|\right) \quad . \qquad (7.27)$$

Denoting by $v_{2\sigma}$ the component of $\mathbf{v}_2$ parallel to $\hat{\boldsymbol{\sigma}}$, and by $\mathbf{v}_{2\tau}$ the $(d-1)$-dimensional vector in the hyper-plane perpendicular to $\hat{\boldsymbol{\sigma}}$, the above equation is rewritten as;

$$W_{tr}(\mathbf{v}_1 \rightarrow \mathbf{v}'_1) = \chi \int dv_{2\sigma}d\mathbf{v}_{2\tau}\Theta(\mathbf{v}_{12}\cdot\hat{\boldsymbol{\sigma}})\frac{|\mathbf{v}_{12}\cdot\hat{\boldsymbol{\sigma}}|}{\Delta v^{d-1}}p(v_{2\sigma},\mathbf{v}_{2\tau})\delta\left(\Delta v + k(\epsilon,\alpha)|\mathbf{v}_{12}\cdot\hat{\boldsymbol{\sigma}}|\right) \quad . \quad (7.28)$$

Finally, integrating over $dv_{2\sigma}$, one gets the following formula:

$$W_{tr}(\mathbf{v},\mathbf{v}') = \frac{1}{k(\epsilon,\alpha)^2}\chi|\Delta\mathbf{v}|^{2-d}\int d\mathbf{v}_{2\tau}P[\mathbf{v}_2(\mathbf{v},\mathbf{v}',\mathbf{v}_{2\tau})], \qquad (7.29)$$

where $\Delta\mathbf{v} = \mathbf{v}' - \mathbf{v}$ denotes the change of velocity of the test particle after a collision. The vectorial function $\mathbf{v}_2$ is defined as

$$\mathbf{v}_2(\mathbf{v},\mathbf{v}',\mathbf{v}_{2\tau}) = v_{2\sigma}(\mathbf{v},\mathbf{v}')\hat{\boldsymbol{\sigma}}(\mathbf{v},\mathbf{v}') + \mathbf{v}_{2\tau}, \qquad (7.30)$$

where $\hat{\boldsymbol{\sigma}}(\mathbf{v},\mathbf{v}')$ is the unitary vector parallel to $\Delta\mathbf{v}$, while $\mathbf{v}_{2\tau}$ is entirely contained in the $(d-1)$-dimensional space perpendicular to $\Delta\mathbf{v}$ (i.e. $\mathbf{v}_{2\tau} \cdot \Delta\mathbf{v} = 0$). This implies that the integral in expression (7.29) is $(d-1)$-dimensional. Finally, to fully determine the transition rate (7.29), the expression of $v_{2\sigma}$ is needed:

$$v_{2\sigma}(\mathbf{v},\mathbf{v}') = \frac{1}{k(\epsilon,\alpha)}|\Delta\mathbf{v}| + \mathbf{v}\cdot\hat{\boldsymbol{\sigma}} \quad . \qquad (7.31)$$

If $P(\mathbf{v}) = \frac{1}{(2\pi T_g)^{d/2}}\exp\left(-\frac{v^2}{2T_g}\right)$, it then immediately follows that the transition rate $W_{tr}(\mathbf{v},\mathbf{v}')$ reads:

$$W_{tr}(\mathbf{v},\mathbf{v}') = \left(\frac{1}{k(\epsilon,\alpha)}\right)^2\chi\,|\Delta v|^{2-d}\frac{1}{\sqrt{2\pi T_g}}e^{-\frac{v_{2\sigma}^2}{2T_g}} \quad . \qquad (7.32)$$

From now on we specialize to the two dimensional case, where the above equation simplifies to

$$\begin{aligned} W_{tr}(\mathbf{V}'|\mathbf{V}) &= \chi\frac{1}{\sqrt{2\pi T_g/m}k(\epsilon,\alpha)^2} \\ &\times \exp\left\{-m\left[V'_\sigma - V_\sigma + k(\epsilon,\alpha)V_\sigma\right]^2/(2T_g k(\epsilon,\alpha)^2)\right\}. \end{aligned} \qquad (7.33)$$

As discussed in details below, with the assumption of well-separated characteristic time scales, the dynamics of the tracer alone is Markovian, and it is known that such transition rates (which do not take into account the external driving) satisfy detailed balance with respect to a Gaussian invariant probability $P(\mathbf{V})$ [145, 121].

For T_g (see Lecture 4), given density, radii of particles, restitution coefficient and the parameters of the external bath, one has the implicit equation

$$T_g = T_b - \chi\frac{\sqrt{\pi m}(1-\alpha^2)}{2\gamma_b}T_g^{3/2}, \qquad (7.34)$$

which can be solved to obtain T_g.

7.2.3   Sonine correction to the rates

In kinetic theory, one of the most used corrections to the Gaussian is the first non-zero Sonine polynomial approximation. This means assuming that $p(\mathbf{v}) = \frac{1}{(2\pi T)^{d/2}} \exp\left(-\frac{v^2}{2T}\right)(1 + a_2 S_2^d(v^2/2T))$ with $S_2^d(x) = \frac{1}{2}x^2 - \frac{d+2}{2}x + \frac{d(d+2)}{8}$. The calculation of the integral needed to have an explicit expression of the transition rate is straightforward:

$$\int d\mathbf{v}_{2\tau} p(\mathbf{v}_2) = \frac{e^{-\frac{v_{2\sigma}^2}{2T}}}{\sqrt{2\pi T}} \left(1 + a_2 S_2^{d=1}(v_{2\sigma}^2/2T)\right) \quad . \tag{7.35}$$

This leads to

$$W_{tr}(\mathbf{v}, \mathbf{v}') = \left(\frac{1}{k(\epsilon, \alpha)}\right)^2 \chi\, |\Delta v|^{2-d} \frac{1}{\sqrt{2\pi T_g}} e^{-\frac{v_{2\sigma}^2}{2T_g}} \left(1 + a_2 S_2^{d=1}\left(\frac{v_{2\sigma}^2}{2T_g}\right)\right). \tag{7.36}$$

Lecture 8

Granular diffusion and ratchets

8.1 Kramers-Moyal expansion for the tracer-gas collision operator

With the assumption of separation of time-scales discussed above, the system of equations (7.16) is decoupled. That allows us to write the following Master Equation for the tracer

$$\frac{\partial P(\mathbf{V}, t)}{\partial t} = L_{gas}[P(\mathbf{V}, t)] + L_{bath}[P(\mathbf{V}, t)], \tag{8.1}$$

and the Markovian linear operator L_{gas} can be expanded as

$$L_{gas}[P(\mathbf{V}, t)] = \sum_{n=1}^{\infty} \frac{(-1)^n \partial^n}{\partial V_{j_1} \dots \partial V_{j_n}} D_{j_1 \dots j_n}^{(n)}(\mathbf{V}) P(\mathbf{V}, t), \tag{8.2}$$

(the sum over repeated indices is meant) with

$$D_{j_1 \dots j_n}^{(n)}(\mathbf{V}) = \frac{1}{n!} \int d\mathbf{V}'(V_{j_1}' - V_{j_1}) \dots (V_{j_n}' - V_{j_n}) W_{tr}(\mathbf{V}'|\mathbf{V}), \tag{8.3}$$

and

$$L_{bath}[P(\mathbf{V}, t)] = \mathcal{B}_{tr} P(\mathbf{V}, t). \tag{8.4}$$

In the limit of large mass M, i.e. small ϵ, we expect that the interaction between the granular gas and the tracer can be described by means of an effective Langevin equation. In this case, we keep only the first two terms of the expansion [148]

$$L_{gas}[P(\mathbf{V}, t)] = -\frac{\partial}{\partial V_i}[D_i^{(1)}(\mathbf{V}) P(\mathbf{V}, t)] + \frac{\partial^2}{\partial V_i \partial V_j}[D_{ij}^{(2)}(\mathbf{V}) P(\mathbf{V}, t)]. \tag{8.5}$$

A justification of this truncation, in the limit of small ϵ, comes from observing that terms $D_{j_1 \dots j_n}^{(n)}$ are of order ϵ^{2n}: this can be obtained by plugging the collision rule (for the case of the tracer, i.e. $\mathbf{V} \equiv \mathbf{v}_1$) into (8.3).

It is useful at this point to introduce the velocity-dependent collision rate and the total collision frequency

$$r(\mathbf{V}) = \int d\mathbf{V}' W_{tr}(\mathbf{V}'|\mathbf{V}), \tag{8.6}$$

$$\omega = \int d\mathbf{V} \, P(\mathbf{V}) r(\mathbf{V}). \tag{8.7}$$

The former quantity can be exactly calculated in the assumption of Gaussian $p(v)$ and $P(v)$, giving

$$
\begin{aligned}
r(\mathbf{V}) & = \chi\sqrt{\frac{\pi}{2}}\left(\frac{T_g}{m}\right)^{1/2}e^{-\epsilon^2 q^2/4} \\
& \times \left[(\epsilon^2 q^2 + 2)I_0\left(\frac{\epsilon^2 q^2}{4}\right) + \epsilon^2 q^2 I_1\left(\frac{\epsilon^2 q^2}{4}\right)\right],
\end{aligned} \tag{8.8}
$$

where the rescaled variable $\mathbf{q} = \mathbf{V}/\sqrt{T_g/M}$ is introduced in Appendix through Eqs. (8.46) and $I_n(x)$ are the modified Bessel functions. To have an approximation of ω, on the other side, one has to make a position about $P(\mathbf{V})$. Let us take it to be a Gaussian with variance T_{tr}/M. The consistency of this choice will be verified in the following section. With this assumption, the collision rate turns out to be

$$
\omega = \chi\sqrt{2\pi}\sqrt{T_g/m + T_{tr}/M} = \chi\sqrt{2\pi}\left(\frac{T_g}{m}\right)^{1/2}\sqrt{1 + \frac{T_{tr}}{T_g}\epsilon^2} = \omega_0 K(\epsilon), \tag{8.9}
$$

where $\omega_0 = \chi\sqrt{2\pi}\left(\frac{T_g}{m}\right)^{1/2}$ and $K(\epsilon) = \sqrt{1 + \frac{T_{tr}}{T_g}\epsilon^2}$.

8.1.1 Large mass limit

We are then able to compute the terms $D_i^{(1)}$ and $D_{ij}^{(2)}$ appearing in L_{gas}. The result and the details of the computation of these coefficients as functions of ϵ are given in Appendix. Here, in order to be consistent with the approximation in (8.5), from Eqs. (8.47) we report only terms up to $\mathcal{O}(\epsilon^4)$

$$
\begin{aligned}
D_x^{(1)} & = -\chi\sqrt{2\pi}\frac{T_g}{m}q_x(1+\alpha)\epsilon^3 + \mathcal{O}(\epsilon^5) \\
& = -\chi\sqrt{2\pi}\left(\frac{T_g}{m}\right)^{1/2}(1+\alpha)\epsilon^2 V_x + \mathcal{O}(\epsilon^5) \\
& = -\omega_0(1+\alpha)\epsilon^2 V_x + \mathcal{O}(\epsilon^5) \tag{8.10} \\
D_y^{(1)} & = -\omega_0(1+\alpha)\epsilon^2 V_y + \mathcal{O}(\epsilon^5) \tag{8.11} \\
D_{xx}^{(2)} & = D_{yy}^{(2)} = \chi\sqrt{\pi/2}\left(\frac{T_g}{m}\right)^{3/2}(1+\alpha)^2\epsilon^4 + \mathcal{O}(\epsilon^5) \\
& = \frac{\omega_0}{2}\frac{T_g}{m}(1+\alpha)^2\epsilon^4 + \mathcal{O}(\epsilon^5) \tag{8.12} \\
D_{xy}^{(2)} & = \mathcal{O}(\epsilon^6). \tag{8.13}
\end{aligned}
$$

The linear dependence of $D_\beta^{(1)}$ upon V_β (for each component β), allows to define a granular viscosity

$$
\eta_g = \omega_0(1+\alpha)\epsilon^2. \tag{8.14}
$$

In the elastic limit $\alpha \to 1$, one retrieves the classical results: $\eta_g \to 2\omega_0\epsilon^2$ and $D_{xx}^{(2)} = D_{yy}^{(2)} \to 2\omega_0\epsilon^2\frac{T_g}{M}$. In this limit the Fluctuation-Dissipation relation of the second kind is satisfied [93, 120], i.e. the ratio between the noise amplitude and γ_g, associated to the same source (collision with gas particles), is exactly T_g/M. When the collisions are inelastic, $\alpha < 1$, one sees two main effects: 1) the time scale associated to the drag $\tau_g = 1/\eta_g$ is modified by a factor $\frac{1+\alpha}{2}$, i.e. it is weakly influenced by inelasticity; 2) the Fluctuation-Dissipation relation of the second kind is *violated* by the same factor $\frac{1+\alpha}{2}$. This is only a partial conclusion, which has to be re-considered in the context of the full dynamics, including the external bath: this is discussed in the next Lecture.

8.1.2 Langevin equation for the tracer

Putting together the results in Eqs. (8.10-8.13) with Eqs. (8.1-8.5), we are finally able to write the Langevin equation for the tracer

$$
M\dot{\mathbf{V}} = -\Gamma\mathbf{V} + \mathcal{E}, \tag{8.15}
$$

where $\Gamma = \gamma_b + \gamma_g$ and $\mathcal{E} = \boldsymbol{\xi}_b + \boldsymbol{\xi}_g$, with

$$\gamma_g = M\eta_g = M\omega_0(1+\alpha)\epsilon^2 = \omega_0(1+\alpha)m \tag{8.16}$$

$$\langle \mathcal{E}_i(t)\mathcal{E}_j(t') \rangle = 2\left[\gamma_b T_b + \gamma_g \left(\frac{1+\alpha}{2}T_g\right)\right]\delta_{ij}\delta(t-t'), \tag{8.17}$$

concluding that the stationary velocity distribution of the intruder is Gaussian with temperature

$$T_{tr} = \frac{\gamma_b T_b + \gamma_g \left(\frac{1+\alpha}{2}T_g\right)}{\gamma_b + \gamma_g}. \tag{8.18}$$

Equation (8.15) is consistent with the Gaussian ansatz used in computing ω_0. Note that the above expression for T_{tr} is consistent with the large mass expansion obtained in Eqs. (8.13) only if it is dominated by T_g, for instance when $\gamma_g \gg \gamma_b$ (see discussion at the end of 8.2.1). In the opposite limit, the tracer dynamics is dominated by the coupling with the external bath and the typical velocity of the tracer cannot be taken sufficiently small with respect to the typical velocity of gas particles, making the expansion unreliable. In this case, however, if the diameter of the intruder is similar to that of the gas particles, it is reasonable to expect similar collision frequencies: the gas particles will therefore be dominated by the external bath and the whole system will be very near to equilibrium [111, 139].

## 8.2   The granular Brownian ratchet
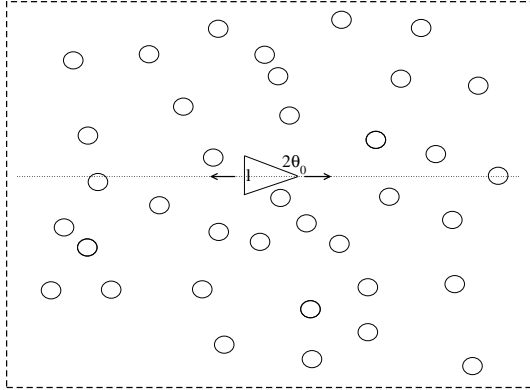
Figure 8.1: Sketch of the 2D model. The triangle is constrained to move only in the $\hat{x}$ (left/right) direction, while its orientation is fixed, i.e. it cannot rotate. Gas particles collide against it and occasionally receive energy from an external bath.

The granular ratchet model, sketched in Fig. 8.1, consists of a triangular particle (the ratchet) of mass M, shaped as an isosceles triangle with base l and angle opposite to the base $2\theta_0$ and surrounded by a gas of N disks of diameter $\sigma = 1$ and mass $m = 1$. The ratchet can only slide, without rotating, along the direction x, perpendicular to its base and the whole system is enclosed in a squared box of side L with periodic boundary conditions. The $N+1$ particles undergo binary instantaneous collisions described by the rule:

$$\mathbf{v}_i = \mathbf{v}'_i - (1+\alpha_{ij})c_{ij}[(\mathbf{v}'_i - \mathbf{v}'_j)\cdot\hat{\mathbf{n}}]\hat{\mathbf{n}}, \tag{8.19}$$

where $\mathbf{v}$ and $\mathbf{v}'$ are the post-collisional and pre-collisional velocities respectively. The quantity $\alpha_{ij} \leq 1$ is the coefficient of restitution for that particular collision, taking value α_d if both objects are disks or value α_r if the ratchet is involved, $\hat{\mathbf{n}}$ is the outward-pointing unit vector normal, in the contact point, to the surface of particle i, and c_{ij} is a coefficient which takes, in the different collisions, the values

$$c_{ij} = \begin{cases} 1/2 & \text{if objects are both disks} \\ 1/(1+\epsilon^2\hat{n}_x^2) & \text{if } j \text{ is the triangle} \\ \epsilon^2/(1+\epsilon^2\hat{n}_x^2) & \text{if } i \text{ is the triangle} \end{cases} \tag{8.20}$$

where $\epsilon^2 = m/M$. Because of the constraint the vertical velocity of the ratchet is always 0. The collision rule (8.19) conserves the total momentum if i and j are disks, and conserves the x-component of the momentum only, when the triangle is involved. If $\alpha_{ij} = 1$ the total kinetic energy is also conserved. Three possible cases may be considered: (i) a pure elastic gas where $\alpha_d = \alpha_r = 1$, (ii) a mixed gas where $\alpha_d = 1$ and $\alpha_r < 1$, (iii) a pure inelastic gas where $\alpha_d < 1$ and $\alpha_r < 1$. In both cases (ii) and (iii) an external driving mechanism is needed to attain a stationary state and avoid indefinite cooling of the system. Here, we do not enter into the details of the external driving mechanism: we only assume that the system is large enough to decouple the Boltzmann equation of the intruder from that of the gas. In this case it will suffice to know the stationary velocity distribution of the gas and plug it into the transition rate expression for the intruder.

8.2.1   Diffusional limit

In the dilute gas limit, it is reasonable to study the ratchet dynamics by means of a linearized Boltzmann equation for its velocity pdf, $P(V,t)$, which can be written as a Master Equation (ME) for a Markov process [43]:

$$\frac{\partial P(V,t)}{\partial t} = \int dV' \ [W(V|V')P(V',t) - W(V'|V)P(V,t)] \tag{8.21}$$

where the transition rate is:

$$W(V|V') = n \int_0^{2\pi} d\theta SF(\theta) \int_{-\infty}^{\infty} dv'_x \int_{-\infty}^{\infty} dv'_y p(v'_x, v'_y)$$
$$(\vec{V}' - \vec{v}') \cdot \hat{\mathbf{n}} \Theta \left[(\vec{V}' - \vec{v}') \cdot \hat{\mathbf{n}} \right] \cdot \delta[V - V_{post}(V', \vec{v}', \alpha_r, \epsilon)] \tag{8.22}$$

with $p(\mathbf{v})$ the gas particle distribution, V_{post} the post-collisional ratchet velocity (see eq. (8.19)), Θ the Heaviside step function, S the perimeter length, $\hat{\mathbf{n}} = (\sin\theta, -\cos\theta)$ and for the triangle

$$SF(\theta) = \frac{l}{2\sin\theta_0} \left\{ 2\sin\theta_0 \delta(\theta - 3\pi/2) + \delta(\theta - \theta_0) + \delta[\theta - (\pi - \theta_0)] \right\}. \tag{8.23}$$

Following numerical evidence we approximate the velocity pdf of the gas, $p(\mathbf{v})$, by a Maxwellian with zero mean and variance T_g. Expression (8.22) is equivalent to a Master Equation (ME) describing a Markov process. It is straightforward to verify that detailed balance, in the form

$$P(V)W(V'|V) = P(-V')W(-V|-V'), \tag{8.24}$$

holds if $\alpha_r = 1$.

As numerical results suggest, the ME describes a driven-diffusive process. In order to gain a deeper insight it is convenient to approximate the ME by a Fokker-Planck equation (FPE), from which we can extract the analytical expression of the drift and diffusion terms. This is achieved by expressing the r.h.s. of eq. (8.21) by means of the Kramers-Moyal (KM) expansion

$$\frac{\partial P(V,t)}{\partial t} = \sum_{n=1}^{\infty} \frac{(-1)^n}{n!} \left(\frac{d}{dV} \right)^n [j_n(V)P(V,t)] \tag{8.25}$$

where $j_n(V) = \int dV'(V' - V)^n W(V'|V)$. By retaining only the first two terms we obtain the sought FPE, which can be still simplified by expanding these terms in the small parameter ϵ. The resulting expressions suggest a simple physical picture, which can be illustrated with the help of the Langevin equation associated with the FPE:

$$\dot{V}(t) = -\gamma V(t) + \frac{F}{M} + \Gamma(t) \tag{8.26}$$

with noise

$$\langle \Gamma(t)\Gamma(t') \rangle = \frac{2\gamma T_r}{M} \delta(t - t') \qquad \langle \Gamma(t) \rangle = 0 \tag{8.27}$$

The quantities γ and F are effective parameters related to the original parameters by

$$\gamma = 4\eta n l \epsilon \sqrt{\frac{T_g}{2\pi M}}(1 + \sin\theta_0) \tag{8.28}$$

$$\frac{F}{M} = -nl\frac{T_g}{M}\epsilon^2(1 - \sin^2\theta_0)\eta(1 - \eta) \tag{8.29}$$

$$1 - \eta = 1 - \frac{T_r}{T_g} = \frac{1 - \alpha_r}{2} \tag{8.30}$$

Hence, for $\alpha_r < 1$ the ratchet drifts with an average negative velocity

$$\langle V(t)\rangle = \frac{F}{M\gamma} = -\frac{1 - \alpha_r}{8}\sqrt{\frac{2\pi T_g}{M}}\epsilon(1 - \sin\theta_0) \tag{8.31}$$

Indeed, the net velocity vanishes linearly with $\epsilon \to 0$ and is very tiny for massive ratchets. It is of interest to observe that in virtue of eq. (8.30) the net driving force is proportional to the temperature difference $T_g - T_r$, so that the tracer and the gas temperatures play role analogous the two reservoir temperatures of the Brownian ratchet model. In principle it is possible that for a purely inelastic system (case iii), for some choice of inelasticity and masses, the difference $T_g - T_r$ can change sign, implying a change of sign of the average ratchet velocity.

From eqs. (8.26)- (8.30) it is also possible to estimate the signal to noise ratio:

$$\sqrt{\frac{\langle V(t)\rangle^2}{\langle V^2(t)\rangle - \langle V(t)\rangle^2}} \simeq \sqrt{2\pi}\frac{1 - \alpha_r}{8}\epsilon(1 - \sin\theta_0). \tag{8.32}$$

The measure of $\langle V\rangle$ can be blurred by thermal noise in the limit of large M/m, a fact that can be avoided with a large number of independent trajectories.

Appendix. Calculation of first two coefficients of the Kramers-Moyal expansion for the symmetric intruder

For larger generality (whose motiviation is discussed in the Conclusions), in this Appendix we discuss the case where the gas surrounding the intruder may have a non-zero average $\mathbf{u}$ [1]:

$$p(\mathbf{v}) = \frac{1}{\sqrt{(2\pi T_g/m)^d}}\exp\left[-\frac{m(\mathbf{v} - \mathbf{u})^2}{2T_g}\right] \tag{8.33}$$

which is a simple task involving only the definition of new shifted variables

$$\mathbf{c} = \mathbf{V} - \mathbf{u} \tag{8.34}$$
$$\mathbf{c}' = \mathbf{V}' - \mathbf{u}. \tag{8.35}$$

We are interested in computing

$$
\begin{aligned}
D_i^{(1)}(\mathbf{V}) &= \int d\mathbf{V}'(V_i' - V_i)W_{tr}(\mathbf{V}'|\mathbf{V}) \\
&= \int d\mathbf{c}'(c_i' - c_i)\chi\frac{1}{\sqrt{2\pi T_g/m}k(\epsilon)^2} \\
&\times \exp\left\{-m\left[c_\sigma' + (k(\epsilon) - 1)c_\sigma\right]^2/(2T_gk(\epsilon)^2)\right\}.
\end{aligned}
\tag{8.36}
$$

---

[1] note that in all the cases discussed in the main text, we have always taken $\mathbf{u} = 0$.
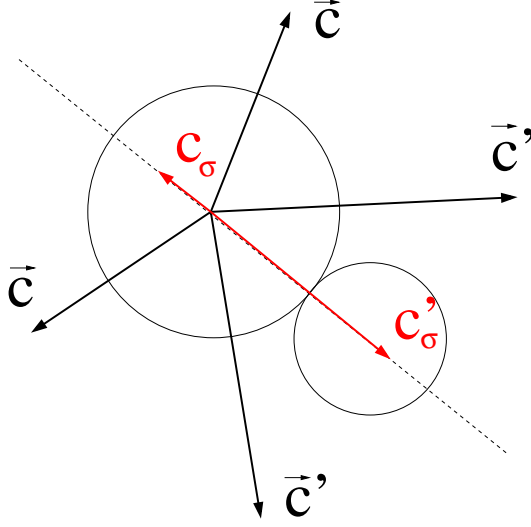
Figure 8.2: An example for the change of variables $(c'_x, c'_y) \rightarrow (c_\sigma, c'_\sigma)$, introduced in Eq. (8.37). Such change of variable, when inverted, has two possible determinations: in this example both represented vectors $\mathbf{c}'$ yield the same (c_σ, c'_σ).

In order to perform the integral, we make the following change of variables (see Fig. 8.2 for an example)

$$
\begin{aligned}
c_\sigma &= c_x \frac{c'_x - c_x}{\sqrt{(c'_x - c_x)^2 + (c'_y - c_y)^2}} + c_y \frac{c'_y - c_y}{\sqrt{(c'_x - c_x)^2 + (c'_y - c_y)^2}} \\
c'_\sigma &= c'_x \frac{c'_x - c_x}{\sqrt{(c'_x - c_x)^2 + (c'_y - c_y)^2}} + c'_y \frac{c'_y - c_y}{\sqrt{(c'_x - c_x)^2 + (c'_y - c_y)^2}}
\end{aligned}
\tag{8.37}
$$

which implies

$$
d\mathbf{c}' = dc'_x dc'_y \rightarrow dc_\sigma dc'_\sigma |J|,
\tag{8.38}
$$

where

$$
|J| = \frac{|c'_\sigma - c_\sigma|}{\sqrt{c_x^2 + c_y^2 - c_\sigma^2}} \Theta(c_x^2 + c_y^2 - c_\sigma^2)
\tag{8.39}
$$

is the Jacobian of the transformation. The collision rate is then

$$
r(\mathbf{V}) = \chi \sqrt{\frac{\pi}{2T_g/m}} e^{-\frac{mc^2}{4T_g}} \left[(c^2 + 2T_g/m) I_0 \left(\frac{mc^2}{4T_g} \right) + c^2 I_1 \left(\frac{mc^2}{4T_g} \right) \right],
\tag{8.40}
$$

where $I_n(x)$ are the modified Bessel functions. For $D_i^{(1)}$ we can write

$$
\begin{aligned}
D_i^{(1)}(\mathbf{V}) &= \chi \int_{-\infty}^{+\infty} dc_\sigma \int_{c_\sigma}^{\infty} dc'_\sigma (c'_i - c_i) |J| \frac{1}{\sqrt{2\pi T_g/m} k(\epsilon)^2} \\
&\times \exp \left\{ -m \left[c'_\sigma + (k(\epsilon) - 1) c_\sigma \right]^2 / (2T_g k(\epsilon)^2) \right\} \\
&= \chi \int_{-c}^{+c} dc_\sigma \int_{c_\sigma}^{\infty} dc'_\sigma (c'_i - c_i) \frac{c'_\sigma - c_\sigma}{\sqrt{c^2 - c_\sigma^2}} \\
&\times \frac{1}{\sqrt{2\pi T_g/m} k(\epsilon)^2} \exp \left\{ -m \left[c'_\sigma + (k(\epsilon) - 1) c_\sigma \right]^2 / (2T_g k(\epsilon)^2) \right\}
\end{aligned}
\tag{8.41}
$$

where we have enforced the constraint of the theta function, namely $c_\sigma \in (-c, +c)$, with $c = \sqrt{c_x^2 + c_y^2}$.
Notice that the integral in dc_σ' is lower bounded by the condition $c_\sigma' \geq c_\sigma$ which follows from the definition of c_σ. In order to compute the integral, we have to invert the transformation (8.37). That yields two determinations for the variables c_x' and c_y' (see Fig. 8.2)

$$(A) \begin{cases} c_x' - c_x = \frac{c_\sigma' - c_\sigma}{c^2} \left(c_\sigma c_x + c_y Sign(c_x) \sqrt{c^2 - c_\sigma^2} \right) \\ c_y' - c_y = \frac{c_\sigma' - c_\sigma}{c^2} \left(c_\sigma c_y - c_x Sign(c_x) \sqrt{c^2 - c_\sigma^2} \right) \end{cases}$$

$$(B) \begin{cases} c_x' - c_x = \frac{c_\sigma' - c_\sigma}{c^2} \left(c_\sigma c_x - c_y Sign(c_x) \sqrt{c^2 - c_\sigma^2} \right) \\ c_y' - c_y = \frac{c_\sigma' - c_\sigma}{c^2} \left(c_\sigma c_y + c_x Sign(c_x) \sqrt{c^2 - c_\sigma^2} \right) \end{cases}$$

Then the integral (8.41) can be written as

$$\begin{aligned} D_x^{(1)}(\mathbf{V}) &= \frac{1}{l_0} \int_{-c}^{c} dc_\sigma \int_{c_\sigma}^{\infty} dc_\sigma' \left[(c_x' - c_x)^{(A)} + (c_x' - c_x)^{(B)} \right] |J| \\ &\times \frac{1}{\sqrt{2\pi T_g/m}k(\epsilon)^2} \exp\left\{ -m \left[c_\sigma' + (k(\epsilon) - 1)c_\sigma \right]^2 / (2T_g k(\epsilon)^2) \right\}, \end{aligned}$$

(8.42)

yielding

$$\begin{aligned} D_x^{(1)} &= -\frac{2}{3} \frac{1}{l_0} k(\epsilon) \sqrt{\frac{m\pi}{2T_g}} c_x e^{-\frac{mc^2}{4T_g}} \left[(c^2 + 3T_g/m)I_0(\frac{mc^2}{4T_g}) + (c^2 + T_g/m)I_1(\frac{mc^2}{4T_g}) \right], \\ D_y^{(1)} &= -\frac{2}{3} \frac{1}{l_0} k(\epsilon) \sqrt{\frac{m\pi}{2T_g}} c_y e^{-\frac{mc^2}{4T_g}} \left[(c^2 + 3T_g/m)I_0(\frac{mc^2}{4T_g}) + (c^2 + T_g/m)I_1(\frac{mc^2}{4T_g}) \right]. \end{aligned}$$

(8.43)

Analogously, for the coefficients $D_{ij}^{(2)}$ one obtains

$$\begin{aligned} D_{xx}^{(2)}(\mathbf{V}) &= \frac{1}{2} \frac{1}{l_0} \int_{-c}^{c} dc_\sigma \int_{c_\sigma}^{\infty} dc_\sigma' \left[\left((c_x' - c_x)^{(A)} \right)^2 + \left((c_x' - c_x)^{(B)} \right)^2 \right] |J| \\ &\times \frac{1}{\sqrt{2\pi T_g/m}k(\epsilon)^2} \exp\left\{ -m \left[c_\sigma' + (k(\epsilon) - 1)c_\sigma \right]^2 / (2T_g k(\epsilon)^2) \right\} \\ &= \frac{1}{2} \frac{1}{l_0} \frac{k(\epsilon)^2}{15} \sqrt{\frac{2m\pi}{T_g}} e^{-\frac{mc^2}{4T_g}} \\ &\times \left\{ \left[c^2(4c_x^2 + c_y^2) + 3T_g(7c_x^2 + 3c_y^2)/m + 15T_g^2/m^2 \right] I_0\left(\frac{mc^2}{4T_g} \right) \right. \\ &\left. + \left[c^2(4c_x^2 + c_y^2) + T_g(13c_x^2 + 7c_y^2)/m + 3T_g^2/m^2 \frac{-c_x^2 + c_y^2}{c^2} \right] I_1\left(\frac{mc^2}{4T_g} \right) \right\}, \end{aligned}$$

(8.44)

$$
\begin{aligned}
D_{xy}^{(2)}(\mathbf{V}) &= \frac{1}{2}\frac{1}{l_0}\int_{-c}^{c}dc_\sigma\int_{c_\sigma}^{\infty}dc'_\sigma\left[(c'_x-c_x)^{(A)}(c'_y-c_y)^{(A)}+(c'_x-c_x)^{(B)}(c'_y-c_y)^{(B)}\right]|J| \\
&\times \frac{1}{\sqrt{2\pi T_g/mk(\epsilon)^2}}\exp\left\{-m\left[c'_\sigma+(k(\epsilon)-1)c_\sigma\right]^2/(2T_gk(\epsilon)^2)\right\} \\
&= \frac{1}{2}\frac{1}{l_0}\frac{k(\epsilon)^2}{5}\sqrt{\frac{2m\pi}{T_g}}e^{-\frac{mc^2}{4T_g}}c_xc_y \\
&\times \left[(c^2+4T_g/m)I_0\left(\frac{mc^2}{4T_g}\right)+\frac{c^4+2c^2T_g/m-2T_g^2/m^2}{c^2}I_1\left(\frac{mc^2}{4T_g}\right)\right].
\end{aligned}
$$

$$(8.45)$$

Then we introduce the rescaled variables

$$
q_x = \frac{c_x}{\sqrt{T_g/m}}\epsilon^{-1} \qquad q_y = \frac{c_y}{\sqrt{T_g/m}}\epsilon^{-1},
$$

$$(8.46)$$

obtaining

$$
\begin{aligned}
D_x^{(1)}(\mathbf{V}) &= -\frac{2}{3}\frac{1}{l_0}\sqrt{\frac{\pi}{2}}\frac{T_g}{m}q_xk(\epsilon)\epsilon e^{-\frac{\epsilon^2q^2}{4}}\left[(\epsilon^2q^2+3)\,I_0(\frac{\epsilon^2q^2}{4})+(\epsilon^2q^2+1)\,I_1(\frac{\epsilon^2q^2}{4})\right], \\
D_{xx}^{(2)}(\mathbf{V}) &= \frac{1}{2}\frac{1}{l_0}\frac{1}{15}\sqrt{2\pi}\left(\frac{T_g}{m}\right)^{3/2}k(\epsilon)^2e^{-\frac{\epsilon^2q^2}{4}} \\
&\times \left\{\left[\epsilon^4q^2(4q_x^2+q_y^2)+3\epsilon^2(7q_x^2+3q_y^2)+15\right]I_0\left(\frac{\epsilon^2q^2}{4}\right)\right. \\
&\left.+\left[\epsilon^4q^2(4q_x^2+q_y^2)+\epsilon^2(13q_x^2+7q_y^2)+3\frac{-q_x^2+q_y^2}{q^2}\right]I_1\left(\frac{\epsilon^2q^2}{4}\right)\right\} \\
D_{xy}^{(2)}(\mathbf{V}) &= \frac{1}{2}\frac{1}{l_0}\frac{1}{5}\sqrt{2\pi}\left(\frac{T_g}{m}\right)^{3/2}q_xq_yk(\epsilon)^2\epsilon^2e^{-\frac{\epsilon^2q^2}{4}} \\
&\times \left[(\epsilon^2q^2+4)\,I_0\left(\frac{\epsilon^2q^2}{4}\right)+\left(\frac{\epsilon^4q^4+2\epsilon^2q^2-2}{\epsilon^2q^2}\right)I_1\left(\frac{\epsilon^2q^2}{4}\right)\right].
\end{aligned}
$$

$$(8.47)$$

Up to this last results we have not introduced any small ϵ approximation. The next step consists in assuming that $q\sim\mathcal{O}(1)$ with respect to ϵ, which is equivalent to assume that $c^2\sim T_g/M$: this assumption must be compared to its consequences, in particular to Eq. (8.18); the assumption is good for not too small values of α and for $\gamma_g\gg\gamma_b$, i.e. when $T_{tr}\sim T_g$. When this is the case, expanding in ϵ and using that $I_0(x)\sim1+x^2/4$ and $I_1(x)\sim x/2$ for small x, one finds Eqs. (8.13).

Lecture 9

Non-equilibrium fluctuations

9.1 Diffusion of the symmetric intruder: an equilibrium-like process

In the previous lecture we have seen that the granular intruder, in the limit of large mass, follows a Langevin equation with white noise and linear drag. Only the parameters of the equation (drag coefficient Γ and noise amplitude $\langle \mathcal{E}^2 \rangle$ are "special" in the sense they represent the joint effect of two different baths, which is peculiar of granular systems. Anyway the linear Langevin equation in itself is not special at all, but represents a standard example of stochastic motion. It was proposed - roughly a century ago - to describe the so-called Brownian motion, i.e. the erratic trajectory of a pollen grain suspended in water. In that case the "bath" is unique (just water) and the system is at equilibrium. If one looks at the motion of the granular intruder any measurement would give the same results as for the pollen grain: in summary, it is not possible to realize that non-equilibrium processes occur, if the intruder position and velocity are the only observables available. We resume here the main consequences of Eq. (8.15), specializing for simplicity to the one-dimensional case:

$$M\dot{V} = -\Gamma V + \mathcal{E} \tag{9.1}$$

with $\langle \mathcal{E} \rangle = 0$ and $\langle \mathcal{E}(t)\mathcal{E}(t') \rangle = 2T_{tr}\Gamma\delta(t - t')$.

The solution of this stochastic equation is

$$V(t) = e^{-t\Gamma/M}\left[V(0) + \int_0^t ds\, e^{s\Gamma/M}\mathcal{E}(s)\right] \tag{9.2}$$

which implies, in the stationary state, that

$$C(t) = \langle V(t)V(0) \rangle = \langle V^2 \rangle e^{-t\Gamma/M}. \tag{9.3}$$

The position of the intruder follows the diffusion equation which implies

$$\langle (x(t) - x(0))^2 \rangle = \left\langle \int_0^t ds \int_0^t ds'\, v(s)v(s') \right\rangle \to_{t\to\infty} 2Dt \tag{9.4}$$

with

$$D = \int_0^\infty dt\, C(t). \tag{9.5}$$

For the granular intruder it is immediately obtained

$$D_{tr} = \int_0^\infty dt \langle V_x(t)V_x(0) \rangle = \frac{T_{tr}}{\Gamma} = \frac{\gamma_b T_b + \gamma_g\left(\frac{1+\alpha}{2}T_g\right)}{(\gamma_b + \gamma_g)^2}. \tag{9.6}$$

Solving numerically the equation (7.34) and substituting the result into the above equation, one can study D_{tr} as a function of the restitution coefficient α (this is done numerically in the next section). When all other parameters are kept constant and α is reduced from 1, the behavior of D_{tr} is non-monotonic, it decreases, has a minimum and then increases for lower values of α. Anyway, this minimum is expected for quite low values of α or high values of the packing fraction ϕ, where the approximations involved in this theory are not good. For this reason, at the values of parameters chosen to have a good comparison with simulations, this non-monotonic behavior is not observed.

It should be also noticed that, in the Homogeneous Cooling State, the self-diffusion coefficient at a given granular temperature increases as α is reduced from 1, i.e. it has an opposite behavior with respect to the present case [24, 28]. Other studies on different models of driven granular gases have found expressions very close to Eq. (8.16), which is not surprising considering the universality of the main ingredient for this quantity, i.e. the collision integral [138, 32].

9.1.1   Linear response

Moreover, if one applies an external time-dependent external force $F(t)$, it appears that

$$\langle \delta V(t) \rangle = \langle V(t) \rangle_{F(t)} - \langle V(t) \rangle_{F \equiv 0} = \int_{-\infty}^{t} ds R(t-s) F(s) \tag{9.7}$$

with $R(s)$ the so-called "response". Equation (9.7) is a direct consequence of the linearity of the Langevin equation. In general, for non-linear equations, one may still use (9.7) to define the response function, assuming to have neglected terms of higher order in $F(t)$, which makes sense if $F(t)$ is small enough. Obviously, in the impulsive case $F(t) = F_0 \delta(t)$ one immediately has

$$R(t) = \frac{\langle \delta V(t) \rangle}{F_0}. \tag{9.8}$$

It is straigthforward to realize that, in our case:

$$R(t) = \frac{C(t)}{T_{tr}}, \tag{9.9}$$

which integrated on time gives

$$\mu \equiv \int_0^\infty R(t) = \frac{1}{T_{tr}} D \tag{9.10}$$

which is known as Einstein relation. The integral on the left hand side, μ, is the so-called mobility: it corresponds to the ratio $\mu = V_\infty / F_0$, when V_∞ is the asymptotic velocity reached by the intruder if a constant force F_0 is applied from time 0 (i.e. $F(t) = F_0 \theta(t)$).

The Einstein relation is a particular case of a more general theorem which is valid for small perturbations of a system at equilibrium, i.e. a system with stationary probability in phase space given by $\sim \exp(-\beta H(\mathbf{r}, \mathbf{v}))$. In such a system, when the perturbation appears as an additive contribution $-h(t)A(\mathbf{r}, \mathbf{v})$ to the Hamiltonian, it is found for the linear response [93, 120]

$$R_{Oh} = \frac{\langle O(t) \rangle_{h(t)} - \langle O(t) \rangle_{h \equiv 0}}{\delta h} = -\langle O(t) \dot{A}(0) \rangle_{h \equiv 0}. \tag{9.11}$$

This is a fundamental result expressing a deep relation between linear response to a perturbation and correlations measured in the absence of the perturbation. In the last decade a large amount of scientific literature has been devoted to the study of generalization of this relation to non-equilibrium situations [120].

9.2   Time reversibility

The condition of thermodynamic equilibrium, which is at the base of Eq. (9.11), can be stated in a very general way, from the point of view of dynamics. Let us assume that we have a generic evolution

equation for our system which generates trajectories

$$\Omega_0^t \equiv \{\mathbf{r}(s), \mathbf{v}(s)\}_{s=0}^t \tag{9.12}$$

starting from an initial condition $\mathbf{r}(0), \mathbf{v}(0)$. The evolution can be stochastic (as in Eq. (8.15)) or deterministic with random initial conditions. In both cases we have an ensemble of possible trajectories. Let us assume that we are somehow able to determine the probability "weight" of each Ω_0^t: $P(\Omega_0^t)$. Finally, let us assume to have defined a time inversion operator $\mathcal{T}$

$$\mathcal{T}\Omega_0^t = \{\mathbf{r}(t - s), -\mathbf{v}(t - s)\}_{s=0}^t. \tag{9.13}$$

Obviously $\mathcal{T}^2 = \mathcal{I}$ (the identity operator). The condition of time reversibility simply states that

$$P(\Omega_0^t) = P(\mathcal{T}\Omega_0^t). \tag{9.14}$$

9.2.1 The case of Markov processes

For a continuous time Markov process $\sigma(t)$, a trajectory is described by the sequence of visited states $(\sigma_0, \sigma_1, \sigma_2, ..., \sigma_n)$ and the time of permanence in each state $(t_0, t_1, t_2, ..., t_n$ with $\sum t_i = t)$ and its probability is

$$P(\Omega_0^T) = p(\sigma_0, 0)p_{perm}(\sigma_0, t_0)W(\sigma_0 \to \sigma_1)p_{perm}(\sigma_1, t_1)...W(\sigma_{n-1} \to \sigma_n)p_{perm}(\sigma_n, t - t_{n-1}), \tag{9.15}$$

where $p(\sigma, t)$ is the probability of finding the process in state σ at time t, $p_{perm}(\sigma, t)$ is the probability of staying for a time t in state σ, and $W(\sigma \to \sigma')$ is the conditional probability of changing state from σ to σ'. In this case, condition (9.14) is satisfied if and only if

1. the system is in the stationary state, i.e. the time is very large and any memory of the initial condition is lost; at large times one has $p(\sigma, t) \to \mu(\sigma)$ the so-called invariant probability;

2. for any couple of states σ and σ', the transition rates and the invariant measure must satisfy the following condition

$$\mu(\sigma)W(\sigma \to \sigma') = \mu(\sigma')W(\sigma' \to \sigma). \tag{9.16}$$

called "detailed balance condition".

9.2.2 Detailed balance for the granular intruder

As seen in Lecture 7, when $N \gg 1$ the gas evolution is not perturbed by the intruder, which implies that the granular intruder performs a Markov process. An analysis of the transition rates related to the collision with the gas [145] shows that these rates satisfy detailed balance with respect to a Gaussian invariant probability, if $p(\mathbf{v})$ is Gaussian, otherwise they do not satisfy detailed balance. Anyway one has to consider the combined effect of the two baths, i.e. the collisions with the gas together with the stochastic force of the external bath. It is not difficult to realize that this total rate cannot satisfy detailed balance with respect to any invariant probability. The conclusion is that, in general, the granular intruder - as a Markov process - *does not* satisfy detailed balance, i.e. does not satisfy time reversibility, i.e. it is not an equilibrium process. Given in different words, one has always the possibility - measuring suitable observable (thes worst case is that one has to measure exactly the probability of all trajectores) - to discriminate between the correct time direction and its inverse. This should not be possible at equilibrium.

9.3 Entropy production

Whenever condition (9.14) is not satisfied, one may distinguish between the forward and the backward time direction, measuring some current. Spatially extended systems reveal their non-equilibrium properties through the appearance of spatially directed currents. For instance, a substance coupled to two

thermostats at different temperatures $T_1 > T_2$, is crossed by a heat current flowing from temperature T_1 to T_2. Anyway, the definition of equilibrium based on the probability of trajectories, allows to construct a more general and abstract "current" which is able to reveal the presence of a time-arrow:

$$J_t = \lim_{t \to \infty} \frac{1}{t} \langle \mathcal{W}_t \rangle \tag{9.17}$$

with

$$\mathcal{W}_t = \log \frac{P(\Omega_0^t)}{P(\mathcal{T}\Omega_0^t)}. \tag{9.18}$$

The current defined in (9.17) is called "entropy production rate" and the *stochastic variable* in (9.18) is said "fluctuating entropy production". This latter quantity has been extensively analyzed in [102].

It is immediate to see that - in the stationary state, one has

$$\log \frac{\mathrm{prob}(\mathcal{W}_t = x)}{\mathrm{prob}(\mathcal{W}_t = -x)} = e^x \tag{9.19}$$

which is called "fluctuation relation" (or sometimes "transient fluctuation relation"). This is a simpler version of a very general relation which is valid (with appropriate definitions of its object) also for chaotic deterministic systems [57, 58, 66].

For Markov processes one easily finds

$$\mathcal{W}_t = \log \frac{p(\sigma_0, 0)}{p(\sigma_n, t)} + \sum_{i=0}^{n-1} \log \frac{W(\sigma_i \to \sigma_{i+1})}{W(\sigma_{i+1} \to \sigma_i)} \approx \sum_{i=0}^{n-1} \log \frac{W(\sigma_i \to \sigma_{i+1})}{W(\sigma_{i+1} \to \sigma_i)} \tag{9.20}$$

where the last approximation is true for large times (and even for large times, when the system is not bounded, it may be not true, see for instance the discussion in [142]).

9.3.1   Observables related to entropy production

It is clear that the entropy production defined in (9.18) is very difficult to be measured as it is: even in simulations, one needs an expression for $P(\Omega_0^t)$ which is not easy to be calculated for a generic process. This is simplified for Markov processes, but the problem of "experimentally" accessing (9.18) remains open, when a model (e.g. transition rates) is not available. In many situations, however, it can be seen that entropy production is strictly related to the power injected by non-conservative forces acting on the system divided by some kind of temperature, e.g.

$$J_t \approx \beta \dot{w}_{nc} \tag{9.21}$$

where w_{nc} is the work of non-conservative forces: this work often is given as product of a generalized force and an interal current generated by the force (for instance a difference of potential generating a charge current). Unfortunately this relation is not as general as hoped: it is sufficient to realize that there are many non-equilibrium situations where a temperature is not well defined (for instance if two thermostats are coupled to the system). Relation (9.21) is considered to be valid in all situations *near equilibrium*, where - for instance - the so-called "non-equilibrium thermodynamics" fairly describes the system [49] and entropy production has a definition in terms of thermodynamic currents and generalized thermodynamic forces.

An instructive example of calculation of the entropy production can be given for a simple process which is a slight generalization of Eq. (9.1):

$$\dot{v} = -\Gamma v + F(t) + \mathcal{E} \tag{9.22}$$

with Gaussian noise $\langle \mathcal{E} \rangle = 0$, $\langle \mathcal{E}(t)\mathcal{E}(t') \rangle = 2T\Gamma\delta(t - t')$, and where $F(t) = F_c + F_{nc}$ is a sum of a conservative force $F_c = -U'(x)$ and a non-conservative force $F_{nc}(t)$. This is also the equation that governs the process of pulling a terminal of a macromolecule anchored to a surface and surrounded by water; this system has been studied in recent experiments [103, 149].

To compute the probability of a trajectory, it is sufficient to consider discrete times $t_0 + k\tau$ with τ arbitrarily small and $k \in [0, n]$ with n being the integer part of $(t - t_0)/\tau$. Since the noise is Gaussian and delta-correlated, the sequence of variables $\eta_k = \eta(t_0 + k\tau)$ has the probability density

$$P[(\eta_n, t|...|\eta_0, 0)] \propto \exp\left(-\frac{1}{2}\sum_{k=0}^{n}\eta_k^2\tau\right) \tag{9.23}$$

which, in the limit $\tau \to 0$, becomes

$$P[(\eta_n, t|...|\eta_0, 0)] \propto \exp\left(-\frac{1}{2}\int_0^t ds\eta^2(s)\right). \tag{9.24}$$

Equation (9.22) tells us that $\eta(t) = (\dot{v} + \Gamma v - F)/\sqrt{2\Gamma T}$, which finally gives us

$$P[\{\eta(t)\}] \propto \exp(-L), \tag{9.25}$$

where

$$L = \frac{1}{4\Gamma T}\int_0^t ds\,(\dot{v} + \Gamma v - F)^2 =$$
$$\int_0^t \frac{\dot{v}^2 + \Gamma v^2 + F^2 - 2F\dot{v}}{4\Gamma T}ds + \frac{v^2(t) - v^2(0) + 2\{U[x(t)] - U[x(0)]\}}{4T} - \frac{\int_0^t F_{nc}(s)v(s)ds}{2T} \tag{9.26}$$

is called the thermodynamic action, To find the most probable path from $(x_0, 0)$ to (x_t, t), it is sufficient to minimize the action (9.26) while keeping fixed the endpoints.

The entropy production reads:

$$\mathcal{W}_t = \log\frac{P(\Omega_0^t)}{P(\mathcal{T}\Omega_0^t)} = \frac{\Delta H}{T} + \frac{\int_0^t F_{nc}(s)v(s)ds}{T} \tag{9.27}$$

where $\Delta H = \frac{v^2(t) - v^2(0)}{2} + U[x(t)] - U[x(0)]$. Eq. (9.27), for large times, allows one to identify the work done by non-conservative forces $w_{nc}(t) = F_{nc}(t)v(t)$ done by the external non-conservative force (divided by T) as the entropy produced during the time t. This is an example of the result by Kurchan [99] and by Lebowitz and Spohn [102] about the Fluctuation Relation for stochastic systems.

9.3.2 The paradox of large mass granular intruder

Equation (9.27) shows that, if non-conservative forces are absent, the entropy production is non-extensive in time, i.e. its production rate is zero, which is equivalent to say that the system is in equilibrium, as expected. This result holds, for example, for the granular intruder with very large mass, described by Eq. (8.15). Could we expect this result? The intruder is coupled to *two* different baths, one is the original (external) thermostat, the second is the "gas" surrounding the intruder, which acts as a bath in the large mass limit. What about energy fluxes in this system?

The energy injection rates of the two termostats [167] are

$$Q_b = \langle \mathbf{V}(t) \cdot (\boldsymbol{\xi}_b - \gamma_b\mathbf{V})\rangle = 2\frac{\gamma_b}{M}(T_b - T_{tr}) \tag{9.28}$$
$$Q_g = \langle \mathbf{V}(t) \cdot (\boldsymbol{\xi}_g - \gamma_g\mathbf{V})\rangle = 2\frac{\gamma_g}{M}(T_g' - T_{tr}) \tag{9.29}$$

It is easy to see that the balance of fluxes $Q_b = -Q_g$ is equivalent to formula (8.18) for T_{tr}. This balance implies that, if $T_{tr} < T_b$, then $T_{tr} > T_g'$. When $\alpha < 1$, the two fluxes are different from zero, i.e. energy is flowing from the external driving, through the tracer, into the granular bath.

Apparently, this contradicts the "equilibrium" nature of the Langevin equation (8.15): the tracer dynamics is Markovian and stationary, and the equation satisfies detailed balance with respect to the Gaussian invariant distribution. As already discussed in [145], this is not a paradox but only a consequence of Molecular Chaos and the separation of time-scales which allows us to write Equation (8.1)

without memory terms. The absence of memory terms implies that both ξ_b and ξ_g are white noises and makes them undistinguishable: an observer which can only measure $\mathbf{V}(t)$ cannot obtain separate measures of Q_b and Q_g, but only a measure of the total energy flow $Q = M\langle \mathbf{V} \cdot \dot{\mathbf{V}} \rangle = 0$ which hides out the presence of energy currents. A more detailed analysis, e.g. by relaxing the Molecular Chaos approximation, should put in evidence the different time-correlations of the two baths: eventually, the observer, by means of some "filter", should be able to sort out their different contributions Q_b and Q_g. This is an example where memory plays a crucial role in the non-equilibrium characterization of a system [143].

We expect that time reversibility (detailed balance) is a symmetry, for the intruder, which is broken in the following cases: 1) at small values of M; 2) when the non-Gaussian behavior of the gas velocities is taken into account; 3) when Molecular Chaos is violated [138]; 4) when the tracer has asymmetric properties with respect to some spatial axis (ratchet case) [43]. In the next subsection we discuss this last case.

9.3.3 Non-equilibrium properties of the granular ratchet

As discussed in Lecture 8, when the intruder is not isotropic and its anisotropy breaks symmetry with respect to a fixed direction (for instance in the triangle example of Fig. 8.1), a spontaneous constant force F appears, see for instance Eq. (8.26). This leads to an asymptotic average velocity $\overline{V} = F/M\gamma$.

The time extensive contribution to the entropy production for this system reads

$$\mathcal{W}_t = \log \frac{P(\Omega_0^t)}{P(\mathcal{T}\Omega_0^t)} \approx \frac{T_r - T_g}{4T_r T_g} \sqrt{2\pi T_g} \gamma [x(t) - x(0)] \tag{9.30}$$

Note that on average $\mathcal{W}_t > 0$ since $T_r < T_g$ and $x(t) < x(0)$. It is always $\langle |x(t) - x(0)| \rangle \sim t$ since the ratchet has an average constant velocity $\overline{V}$.

In conclusion the asymmetry unveils the non-equilibrium property of the granular intruder even in the large mass limit. It is interesting at this point, in order to close the circle of this chapter, to verify that the breakdown of time reversal also breaks the Fluctuation Dissipation relation.

It is immediate to see that, for this system, the linear response reads

$$R = \frac{\langle V(t)V(0) \rangle - \overline{V}^2}{T_r}, \tag{9.31}$$

which is a *violation* of the Einstein relation $R = C(t)/C(0)$ (e.g. Eq. (9.9)). As expected, in the absence of detailed balance, the Fluctuation-Dissipation relation breaks down. This example is quite simple: indeed the equation for the massive ratchet can be recast in an equation for the variable $z(t) = V(t) - \overline{V}$ which is an equilibrium Langevin equation, for this variable response and correlation are proportional as in the Einstein relation. Anyway, such a re-casting hides out the lack of time-reversal symmetry expressed by relation (9.30): the reason is that the new variable $z(t)$ has not a well defined symmetry with respect to time-reversal ($V(t) - \overline{V}$ goes into $-V(t) - \overline{V}$ when time is inverted). Our analysis in terms of $V(t)$ (and not $z(t)$) is therefore the only one consistent and the breakdown of the Fluctuation-Dissipation relation is real, even if very simple.

More general out-of-equilibrium Fluctuation-Dissipation relations can be found in the very recent literature, see for instance [47, 104, 157, 120, 7].

Lecture 10

Numerical methods

10.1 General problem

Two protocols of simulation of granular fluids are discussed in this lesson. They may of course be used also for (elastic) molecular fluids. The first one, the Direct Simulation Monte Carlo (DSMC), in its "ideal" limit (small enough cells, and many particles per cell), is a numerical procedure to solve the Boltzmann Equation, in both spatial homogeneour or non-homogeneous situations. The second method, the Event Driven Molecular Dynamics (EDMD), has the aim of reproducing the exact dynamics of hard bodies. The two methods differ in the fact that the first *assumes* (i.e. imposes) the Molecular Chaos, the second doesn't, but of course may - in dilute limits - be compatible with it: in conclusion, the EDMD is more general. The two methods are similar in the fact that both separate the dynamics in two contributions: the "streaming" (free flight, balistic or under the action of external fields) and "collisions" (particle-particle and particle-boundaries).

As an example, we consider here a system of N identical hard particles of diameter σ in d dimensions, in a volume V (say $V = L^d$), with periodic boundary conditions and under the action of external forces (deterministic and/or stochastic) such that the dynamics of particle i when it is *not* in contact with other particles, obeys the equations

$$\dot{\mathbf{r}}_{\mathbf{i}} = \mathbf{v}_{\mathbf{i}} \tag{10.1}$$
$$\dot{\mathbf{v}}_{\mathbf{i}} = \mathbf{f}(\mathbf{r}_{\mathbf{i}}, \mathbf{v}_{\mathbf{i}}),$$

where $\mathbf{f}$ is the external force (it may contain stochastic variables, which are identically and independently distributed for all particles). Collisions are described by the usual collision rule (2.14). Initial conditions are "equilibrium-like", i.e. particles are randomly distributed in the whole volume and velocities are extracted from a Maxwell-Boltzmann distribution with zero average and temperature T_0 [1]. In the EDMD it is important to exclude initial conditions with overlapping particles.

10.2 The Direct Simulation Monte Carlo (DSMC also called "BIRD" method)

The volume is divided into m_c equal non-overlapping cells of volume $V_c = V/m_c$. A number $\tilde{N} = hN$ with $h \geq 1$ of particles is simulated: the number $\tilde{N}$ is called the *fictive number* of particles, while N is the *real* number of particles: the reason for introducing this fictive number will be clear in the following. Time is discretized in finite time-steps of length δt. At each time step two updates are performed

---

[1] note that homogeneous random distribution is not the correct "equilibrium" spatial distribution for interacting particles, i.e. at finite density, but pair correlations should be taken into accounts; if one really needs an exact "equilibrium" starting point, then an equilibration transient - with elastic collisions - may be performed before starting the real - granular - dynamics.

1. *streaming update*: in this part the Eqs. (10.1) are solved to evolve the dynamical variables $\{\mathbf{r}_i(t), \mathbf{v}_i(t)\}$ (with $i \in (1, \tilde{N})$) to $\{\mathbf{r}_i(t + \delta t), \mathbf{v}'_i(t + dt)\}$; the solution is usually approximate (i.e. valid for $\delta t \rightarrow 0$);

2. *collision update*: in this part the velocities $\{\mathbf{v}'_i(t + dt)\}$ are evolved to $\{\mathbf{v}_i(t + dt)\}$ computing possible collisions through a stochastic ("Monte Carlo" like) recipe repeated in each cell k ($k \in (1, m_c)$):

   (a) denote by N_c the number of fictive particles in the cell, and by $n_c = N_c/(hV_c)$ the *real* density in the cell; finally, denote by $\hat{\mathbf{u}}_c = \frac{\sum_{i=1}^{N_c} \mathbf{v}_i}{N_c}$ the average velocity in the cell and by $T_c = \frac{\sum_{i=1}^{N_c} |\mathbf{v}_i - \hat{\mathbf{u}}|^2}{dN_c}$ the "temperature" in the cell

   (b) compute the average number of collisions $\omega(n_c, T_c)\delta t$ for a particle in a homogeneous gas at density n_c and temperature T_c, assuming that the distribution is close to a Maxwellian (use formula (4.26))

   (c) compute the total number of collisions expected in the cell $nc = N_c \omega(n_c, T_c)\delta t/2$ (the factor 2 is due to fact that each collision involves two particles);

   (d) consider that nc is a non-integer number, in general, so it must be approximated to an integer nc'; a reasonable choice is to take $nc' = [nc]$ (integer part) with probability $nc - [nc]$ and otherwise $nc' = [nc] + 1$; this is equivalent to say that $\langle nc' \rangle = nc$;

   (e) perform nc' collisions in the following way

      - denote by v_{max} a good estimate of $max_{ij}|\mathbf{v}_i - \mathbf{v}_j|$ (maximum over all possible pairs of particles in the cell); finding the real maximum is not efficient; a good compromise is finding a global maximum (valid for all cells) during an initial transient, and then keep it fixed and equal for all cells, during the rest of the simulation;
      - choose a random pair i, j of particles in the cell;
      - choose a random unit vector $\hat{n}$ (isotropically in space);
      - compute $vr = (\mathbf{v}_i - \mathbf{v}_j)\dot{\hat{n}}$
      - discard the pair if $vr > 0$ (and repeat the cycle with a new pair);
      - choose a random number x, uniform in $[0, 1)$;
      - discard the pair if $vr/v_{max} < x$;
      - the last three passages are equivalent to accept the pair with probability proportional to $vr\Theta(vr)$
      - perform the collision, updating $\mathbf{v}_i$ and $\mathbf{v}_j$; update the collision counter.
      - repeat until the collision counter reaches nc'

   (f) repeat for all m_c cells

3. repeat until t reaches the end of the simulation.

The above method solves the inhomogeneous Boltzmann equation when the radius of cells is smaller than the "expected inhomogeneities" (in principle it should be smaller than the mean free path, but in hydrodynamic situations it is sufficient for it to be smaller than typical length of gradients) and the number of fictive particles is large enough to guarantee Molecular Chaos (if particles in a cell are too few, they may instantly "recollide" in a manner which is not physical in dilute situations). If expected inhomogeneities are small, cells will be large enough to accomodate enough particles and make recollisions very unlikely: in these cases it is common to use $N = \tilde{N}$, i.e. $h = 1$. When $h > 1$, one must - of course - rescale the value of the density field by h.

10.2.1 Variants

- **homogeneous variant**: indeed, this is not a variant, but just the case $m_c = 1$; in this case spatial coordinates are not necessary; this method is useful to study the evolution (or stationarity) of the velocity distribution function $P(\mathbf{v}, t)$

- **time clock**: in this method, usually preferred in homogeneous ($m_c = 1$) situations, one does not compute the number of collisions mc of a cell, but simply evolves an internal clock τ of the cell - starting from $\tau = t$ - and stops doing collisions when $\tau = t + \delta t$; the clock advances by fixed amounts $\delta\tau = 1/v_{max}$ at all tentatives of collisions, even those that are discarded; since collisions are performed with probability $\propto vr\theta(vr)P(\mathbf{v}_i)P(\mathbf{v}_j)$, it is easily checked that the average number of collisions per particle is $\omega\delta t$; this methods has the advantage of reproducing also the *fluctuations* of the number of collisions.

10.3 Event Driven Molecular Dynamics

In principle, time is not discretized (it will be clear that this is true only in idealized situations), for this reason the algorithm is called "event-driven": the simulation time jumps from an event occurred at time t and the successive events occurred at time t', provided that no events occur between t and t'. This algorithm is useful when the interacting potential is piecewise constant, with discontinuities at given relative positions r^*: for instance, the hardcore potential has such a property (it is $V(r) = 0$ for $r > r^* = \sigma$ and $V(r) = \infty$ for $r \leq r^*$). Events are all configurations such that a couple of particles comes at relative position r^*.

10.3.1 Main trick

- after initialization of positions and velocities, the list of future events (collisions) is built; this requires to solve the streaming dynamics of each pair of particles (ignoring all other particles) and find the first time t^* at which they collide; this event is put into the list if t^* is finite and larger than t (the actual time);

- since the algorithm requires the streaming dynamics to be solved to determine, with the larger possible accuracy, the time of occurrence of an event, it may become necessary to introduce a maximum delay δt: events will be put in the list only if they occur before $t + \delta t$; this similar to introducing a time-discretization in steps of length dt; this is not necessary if the streaming dynamics only involves free fligths or ballistic fligths with gravity;

- the first event, occurring - say - at time t^* in the list is the only one to be *sure*; all particles are updated with streaming dynamics up to the time of this event; the velocities of the two particles involved in the event are also updated with the collision rule; time is updated to t^*;

- the list of events is re-built to keep into account the new velocities of the two collided particles (we will see how to optimize this step);

- the cycle is repeated, finding the new first event, until the list of events is empty (e.g. no more collision may happen) or the maximum simulation time is reached.

Sometimes, "measurement events" are also introduced at given times, in order to have all particles updated when some observable must be computed, written on disk, analyzed, etc. The stochastic dynamics involved in the thermostat described in Eqs. (4.37), is usually simulated adding "bath events" occurring at times $t_i = i\delta t$, with $\delta t < 1/\omega$ (with ω the average collision frequency of a particle): at each of these events, velocities of particles are updated using a discretized version of equations (4.37). This of course requires to re-build the list of future events.

10.3.2   Optimizations

Let us analyze the order of magnitude of timescales in the simulation. A simulation - to be meaningful - must be performed for a given number of collision per particle. Assuming that density and average energy per particle are stationary, the average collision frequency is stationary too, so the total simulation time will scale as $N t_c(N)$ where t_c is the compuation time to perform a collision. A collision in general requires: bulding the list, finding the first event and performing the collision. The last task does not depend on N. Building the list requires $\sim N^2$. The list includes $\sim N^2$ events. Finding the first event by browsing the whole list requires a cycle of length $\sim N^2$. The total simulation time will scale as $\sim N^3$.

Two main optimization tricks are used.

- *quick sort*: to reduce the time needed to find the first even in the list, standard search tricks are used; they usually involve a smart way of building the list ("tree-sort" or "heap-sort"); the search task is heavily reduced and its computation time becomes $\sim N \log N$

- *table trick*: the volume is divided into $m_c \propto N$ non-overlapping cells; only events occurring between particles in the same cell are put into the list; this reduces the time to build the list, from $\sim N^2$ to $\sim N \times N/m_c \sim N$; events representing a particle crossing the boundary of a box must also be included, they are $\sim m_c \sim N$; for finite diameter σ, it must be taken into account the fact that a particle may belong to more (up to 2^d) cells

The use of these two trickes reduced the time of a simulation to $\sim N^2 \log N$.

Bibliography

[1] B. J. Alder. Triplet correlations in hard spheres. *Phys. Rev. Lett.*, 12(12):317–319, 1964.

[2] B. J. Alder and T. E. Wainwright. Studies in molecular dynamics. I. General method. *J. Chem. Phys.*, 31(2):459–466, 1959.

[3] B. J. Alder and T. E. Wainwright. Phase transition in elastic disks. *Phys. Rev.*, 127(2):359–361, 1962.

[4] B.-J. Alder and T. E. Wainwright. Velocity autocorrelations for hard spheres. *Phys. Rev. Lett.*, 18(23):988–990, 1967.

[5] B. J. Alder and T. E. Wainwright. Decay of the velocity autocorrelation function. *Phys. Rev. A*, 1(1):18–21, 1970.

[6] R. A. Bagnold. Experiments on a gravity-free dispersion of large solid spheres in a Newtonian fluid under shear. *Proc. Royal Soc. London*, 225:49–63, 1954.

[7] M. Baiesi, C. Maes, and B. Wynants. Fluctuations and response of nonequilibrium states. *Phys. Rev. Lett.*, 103:010602, 2009.

[8] P. Bak, C. Tang, and K. Wiesenfeld. Self-organized criticality: An explanation of $1/f$ noise. *Phys. Rev. Lett.*, 59(4):381–384, 1987.

[9] P. Bak, C. Tang, and K. Wiesenfeld. Self-organized criticality. *Phys. Rev. A*, 38(1):364–375, 1988.

[10] A. Baldassarri, U. M. B. Marconi, and A. Puglisi. Influence of correlations on the velocity statistics of scalar granular gases. *Europhys. Lett.*, 58:14, 2002.

[11] G. C. Barker and A. Metha. Transient phenomena, self-diffusion, orientational effects in vibrated powders. *Phys. Rev. E*, 47(1):184, 1993.

[12] G. W. Baxter, R. P. Behringer, T. Fagert, and G. A. Johnson. Pattern formation in flowing sand. *Phys. Rev. Lett.*, 62(24):2825, 1989.

[13] M. Becker and W. Hauger. Granular material - an experimental realization of a plastic Cosserat continuum. In O. Mahrenholtz and A. Sawczuk, editors, *Poznan*, pages 23–39, Poland, 1982. Warszawa.

[14] M. Becker and H. Lippmann. Plane plastic flow of granular model material. experimental setup and results. *Archiv of Mechanics*, 29(6):829–846, 1977.

[15] E. Ben-Naim, J. B. Knight, and E. R. Nowak. Slow relaxation in granular compaction. *J. Chem. Phys.*, 100:6778, 1996.

[16] B. Bernu and R. Mazighi. One-dimensional bounce of inelastically colliding marbles on a wall. *J. Phys. A: Math. Gen.*, 23:5745, 1990.

[17] D. L. Blair and A. Kudrolli. Velocity correlations in dense granular gases. *Phys. Rev. E*, 64(5):050301, 2001.

[18] V. Bobylev. Exact solutions of the nonlinear boltzmann equation and the theory of relaxation of a maxwellian gas. Teoret. Mat. Fiz., 60:280–310, 1984.

[19] N. Bogdanova-Bontcheva and H. Lippmann. Rotationssymmetrisches ebenes Fließen eines granularen Modellmaterials. *Acta Mechanica*, 21:93–113, 1975.

[20] J.-P. Bouchaud, M. E. Cates, and P. Claudin. Stress distribution in granular media and nonlinear wave equation. *J. Phys. I*, 5:639–656, 1995.

[21] J. P. Bouchaud, L. F. Cugliandolo, J. Kurchan, and M. Mezard. *Spin Glasses and Random Fields*. World Scientific, 1998.

[22] A. Brahic. Dynamical evolution of viscous discs. astrophysical applications to the formation of planetary systems and to the confinement of planetary rings and arcs. In T. Pöschel and S. Luding, editors, *Granular Gases, volume 564 of* Lectures Notes in Physics. Springer-Verlag, 2001.

[23] J. J. Brey, J. W. Dufty, C. S. Kim, and A. Santos. Hydrodynamics for granular flow at low density. *Phys. Rev. E*, 58(4):4638, 1998.

[24] J. J. Brey, J. W. Dufty, and A. Santos. Kinetic models for granular flow. *J. Stat. Phys.*, 97:281, 1999.

[25] J. J. Brey, F. Moreno, and J. W. Dufty. Model kinetic equation for low-density granuar flow. *Phys. Rev. E*, 54:445–456, 1996.

[26] J. J. Brey and A. Prados. Linear response of vibrated granular systems to sudden changes in the vibration intensity. 2001.

[27] J. J. Brey, M. J. Ruiz-Montero, and D. Cubero. Homogeneous cooling state of a low-density granular flow. *Phys. Rev. E*, 54:3664–3671, 1996.

[28] J. J. Brey, M. J. Ruiz-Montero, R. Garcia-Rojo, and J. W. Dufty. Brownian motion in a granular gas. *Phys. Rev. E*, 60:7174, 1999.

[29] N. V. Brilliantov, F. Spahn, J. M. Hertzsch, and T. Pöschel. Model for collisions in granular gases. *Phys. Rev. E*, 53(5):5382, 1996.

[30] R. Brockbank, J. M. Huntley, and R. Ball. Contact force distribution beneath a three-dimensional granular pile. *J. Phys. II France*, 7:1521–1532, 1997.

[31] R. L. Brown and J. C. Richards. *Principles of Powder Mechanics*. Pergamon Press, Oxford, 1970.

[32] G. Bunin, Y. Shokef, and D. Levine. Frequency-dependent fluctuation-dissipation relations in granular gases. *Phys. Rev. E*, 77:051301, 2008.

[33] E. Caglioti, V. Loreto, H. J. Herrmann, and M. Nicodemi. A "Tetris-like" model for the compaction of dry granular media. *Phys. Rev. Lett.*, 79(8):1575–1578, 1997.

[34] C. S. Campbell. Rapid granular flows. *Ann. Rev. Fluid Mech.*, 22:57, 1990.

[35] C. S. Campbell. Rapid granular flows. *Ann. Rev. Fluid Mech.*, 22:57, 1990.

[36] C. S. Campbell and C. E. Brennen. Computer simulation of granular shear flows. *J. Fluid. Mech.*, 151:167, 1985.

[37] C. S. Campbell and A. Gong. The stress tensor in a two-dimensional granular shear flow. *J. Fluid Mech.*, 164:107, 1986.

[38] H. Caram and D. C. Hong. Random-walk approach to granular flows. *Phys. Rev. Lett.*, 67(7):828, 1991.

[39] W. F. Carnahan and K. E. Starling. Equation of state for nonattracting rigid spheres. *J. Chem. Phys.*, 51(2):635–636, 1969.

[40] S. Chapman and T. G. Cowling. *The mathematical theory of nonuniform gases*. Cambridge University Press, London, 1960.

[41] R. Clausius. *Ann. Phys.*, 105, 1858.

[42] S. N. Coppersmith, C. Liu, S. Majumdar, O. Narayan, and T. A. Witten. Model for force fluctuations in bead packs. *Phys. Rev. E*, 53(5):4673–4685, 1996.

[43] G. Costantini, A. Puglisi, and U. M. B. Marconi. A granular brownian ratchet model. *Phys. Rev. E*, 75:061124, 2007.

[44] C. A. Coulomb. *Acad. R. Sci. Mem. Math. Phys. par Divers Savants*, 7:343, 1773.

[45] M. Coulomb. Theorie des Machines Simples. *Academie des Sciences*, 10:166, 1781.

[46] K. Craig, R. Buckholz, and G. Domoto. An experimental study of the rapid flow of dry cohesionless metal powders. *J. Appl. Mech.*, 53:935, 1986.

[47] A. Crisanti and F. Ritort. Violation of the fluctuation-dissipation theorem in glassy systems: basic notions and the numerical evidence. *J. Phys. A*, 36:R181, 2003.

[48] P. G. de Gennes. Introduction a la physique des poudres, cours au collège de france. 1995.

[49] S. R. de Groot and P. Mazur. *Non-equilibrium thermodynamics*. Dover Publications, New York, 1984.

[50] P. Deltour and J.-L. Barrat. Quantitative study of a freely cooling granular medium. *J. Phys. I France*, 7:137–151, 1997.

[51] T. G. Drake. Structural features in granular flows. *J. of Geophysical Research*, 95(B6):8681–8696, 1990.

[52] Y. Du, H. Li, and L. P. Kadanoff. Breakdown of hydrodynamics in a one-dimensional system of inelastic particles. *Phys. Rev. Lett.*, 74(8):1268–1271, 1995.

[53] F. C. E Azanza and P. Moucheront. Experimental study of collisional granular flows down an inclined plane. *J. Fluid Mech.*, 400:199, 1998.

[54] E. E. Ehrichs, H. M. Jaeger, G. S. Karczmar, J. B. Knight, V. Kuperman, and S. R. Nagel. Granular convection observed by magnetic resonance imaging. *Science*, 267:1632–1634, 1995.

[55] H. Ernst. Nonlinear model-Boltzmann equations and exact solutions. *Phys. Rep.*, 78:1–171, 1981.

[56] M. H. Ernst, J. R. Dorfman, W. R. Hoegy, and J. van Leeuwen. Hard-sphere dynamics and binary-collision operators. *Physica*, 45:127, 1969.

[57] D. J. Evans, E. G. D. Cohen, and G. P. Morriss. Probability of second law violations in shearing steady flows. *Phys. Rev. Lett.*, 71:2401, 1993.

[58] D. J. Evans and D. J. Searles. Equilibrium microstates which generate second law violating steady states. *Phys. Rev. E*, 50:1645, 1994.

[59] E. Falcon, S. Fauve, and C. Laroche. Cluster formation, pressure and density measurements in a granular medium fluidized by vibrations. *Eur. Phys. J. B*, 9:183–186, 1999.

[60] E. Falcon, S. Fauve, and C. Laroche. An experimental study of a granular gas fluidized by vibrations. In T. Pöschel and S. Luding, editors, *Granular Gases*, volume 564 of *Lectures Notes in Physics*, Berlin Heidelberg, 2001. Springer-Verlag.

[61] E. Falcon, R. Wunenburger, P. Evesque, S. Fauve, C. Chabot, Y. Garrabos, and D. Beysens. Cluster formation in a granular medium fluidized by vibrations in low gravity. *Phys. Rev. Lett.*, 83:440–443, 1999.

[62] L. T. Fan, Y.-M. Chen, and F. S. Lai. Recent developments in solids mixing. *Powder Technol.*, 61:255, 1990.

[63] M. Faraday. On a peculiar class of acoustical figures; and on certain forms assumed by groups of particles upon vibrating elastic surfaces. *Philos. Trans. R. Soc. London*, 52:299, 1831.

[64] K. Feitosa and N. Menon. Breakdown of energy equipartition in a 2d binary vibrated granular gas. *Phys. Rev. Lett.*, 88:198301, 2002.

[65] K. Feitosa and N. Menon. Fluidized granular medium as an instance of the fluctuation theorem. *Phys. Rev. Lett.*, 92:164301, 2004.

[66] G. Gallavotti and E. G. D. Cohen. Dynamical ensembles in stationary states. *J. Stat. Phys.*, 80:931, 1995.

[67] I. Goldhirsch. Kinetics and dynamics of rapid granular flows. In H. J. Herrmann, J.-P. Hovi, and S. Luding, editors, *Physics of dry granular media - NATO ASI Series E 350*, pages 371–400, Dordrecht, 1998. Kluwer Academic Publishers.

[68] I. Goldhirsch. Note on the definition of stress for discrete systems. preprint, 1999.

[69] I. Goldhirsch and M.-L. Tan. The single-particle distribution function for rapid granular shear flows of smooth inelastic disks. *Phys. Fluids*, 8(7):1752–1763, 1996.

[70] I. Goldhirsch, M.-L. Tan, and G. Zanetti. A molecular dynamical study of granular fluids I: The unforced granular gas in two dimensions. *Journal of Scientific Computing*, 8:1–40, 1993.

[71] I. Goldhirsch and G. Zanetti. Clustering instability in dissipative gases. *Phys. Rev. Lett.*, 70(11):1619–1622, 1993.

[72] A. Goldshtein and M. Shapiro. Mechanics of collisional motion of granular materials. Part 1. General hydrodynamic equations. *J. Fluid Mech.*, 282:75–114, 1995.

[73] P. K. Haff. Grain flow as a fluid-mechanical phenomenon. *J. Fluid Mech.*, 134:401–430, 1983.

[74] Hagen. Über den Druck und die Bewegung des trockenen Sandes. *Monatsberichte der königlich, preußischen Akademie der Wissenschaften zu Berlin*, page 35, 19. Jan. 1852.

[75] D. M. Hanes and D. L. Inman. Observations of rapidly flowing granular-fluid materials. *J. Fluid Mech.*, 150:357, 1985.

[76] J. Hemmingsson. A sandpile model with dip. *Physica A*, 230:329–335, 1995.

[77] H. J. Herrmann. Simulation of granular media. *Physica A*, 191:263, 1992.

[78] J.-M. Hertzsch, F. Spahn, and N. V. Brilliantov. On low-velocity collisions of viscoelastic particles. *J. Phys. II*, 5:1725–1738, 1995.

[79] M. A. Hopkins and M. Y. Louge. Inelastic microstructure in rapid granular flows of smooth disks. *Phys. Fluids A*, 3(1):47, 1991.

[80] D. Howell, R. P. Behringer, and C. Veje. Stress fluctuations in a 2d granular Couette experiment: A continuous transition. *Phys. Rev. Lett.*, 82(26):5241–5244, 1999.

[81] M. Huthmann and A. Zippelius. Dynamics of inelastically colliding rough spheres: Relaxation of translational and rotational energy. *Phys. Rev. E*, 56(6):6275–6278, 1997.

[82] H. M. Jaeger, J. B. Knight, C. Liu, and S. R. Nagel. What is shaking in the sandbox? *MRS Bulletin May 1994*, XX(5):25–31, 1994.

[83] H. A. Janssen. Versuche über Getreidedruck in Silozellen. *Zeitschr. d. Vereines deutscher Ingenieure*, 39(35):1045–1049, 1895.

[84] J. T. Jenkins and M. W. Richman. Kinetic theory for plane shear flows of a dense gas of identical, rough, inelastic, circular disks. *Phys. of Fluids*, 28:3485–3494, 1985.

[85] J. T. Jenkins and S. B. Savage. A theory for the rapid flow of identical, smooth, nearly elastic, spherical particles. *J. Fluid Mech.*, 130:187–202, 1983.

[86] L. P. Kadanoff. Built upon sand: Theoretical ideas inspired by granular flows. *Rev. Mod. Phys.*, 71(1):435–444, 1999.

[87] R. Khosropour, J. Zirinsky, H. K. Pak, and R. P. Behringer. Convection and size segregation in a couette flow of granular material. *Phys. Rev. E*, 56(4):4467–4473, 1997.

[88] J. B. Knight. External boundaries and internal shear bands in granular conveciton. *Phys. Rev. E*, 55(5):6016–6023, 1997.

[89] J. B. Knight, E. E. Ehrichs, V. Kuperman, J. K. Flint, H. M. Jaeger, and S. R. Nagel. Experimental study of granular convection. *Phys. Rev. E*, 54(5):5726–5738, 1996.

[90] J. B. Knight, C. G. Fandrich, C. N. Lau, H. M. Jaeger, and S. R. Nagel. Density relaxation in a vibrated granular material. *Phys. Rev. E*, 51(5):3957–3962, 1995.

[91] J. B. Knight, H. M. Jaeger, and S. R. Nagel. Vibration-induced size separation in granular media: The convection connection. *Phys. Rev. Lett.*, 70(24):3728–3731, 1993.

[92] Krook and T. T. Wu. Formation of maxwellian tails. *Phys. Rev. Lett.*, 36:1107–1109, 1976.

[93] R. Kubo, M. Toda, and N. Hashitsume. *Statistical physics II: Nonequilibrium stastical mechanics*. Springer, 1991.

[94] A. Kudrolli and J. P. Gollub. Studies of cluster formation due to collisions in granular material. In *Powders & Grains 97*, page 535, Rotterdam, 1997. Balkema.

[95] A. Kudrolli and J. Henry. Non-gaussian velocity distributions in excited granular matter in the absence of clustering. *Phys. Rev. E*, 62(2):R1489–92, 2000. e-print cond-mat/0001233.

[96] A. Kudrolli, M. Wolpert, and J. P. Gollub. Cluster formation due to collisions in granular material. *Phys. Rev. Lett.*, 78(7):1383–1386, 1997.

[97] V. Kumaran. Temperature of a granular material "fluidized" by external vibrations. *Phys. Rev. E*, 57(5):5660–5664, 1998.

[98] V. Kuperman, E. E. Ehrichs, H. M. Jaeger, and G. S. Karczmar. A new technique for differentiating between diffusion and flow in granular media using magnetic resonance imaging. *Rev. Sci. Instrum.*, 66(8):4350–4355, 1995.

[99] J. Kurchan. Fluctuation theorem for stochastic dynamics. *J. Phys. A*, 31:3719, 1998.

[100] L. Landau and E. Lifschitz. *Theory of elasticity*. MIR, Moscow, 1967.

[101] L. D. Landau and E. M. Lifchitz. *Mécanique des fluides*. Éditions MIR, 1971.

[102] J. L. Lebowitz and H. Spohn. A Gallavotti-Cohen-type symmetry in the large deviation functional for stochastic dynamics. *J. Stat. Phys.*, 95:333, 1999.

[103] J. Liphardt, S. Dumont, S. B. Smith, I. Tinoco, and C. Bustamante. Equilibrium information from nonequilibrium measurements in an experimental test of Jarzynski's equality. *Science*, 296:1832, 2002.

[104] E. Lippiello, F. Corberi, and M. Zannetti. Off-equilibrium generalization of the fluctuation dissipation theorem for ising spins and measurement of the linear response function. *Phys. Rev. E*, 71:036104, 2005.

[105] C. Liu. Spatial patterns of sound propagation in sand. *Phys. Rev. B*, 50, 1994.

[106] C. Liu and S. R. Nagel. Sound in sand. *Phys. Rev. Lett.*, 68(15):2301–2304, 1992.

[107] C. Liu and S. R. Nagel. Sound in a granular material: Disorder and nonlinearity. *Phys. Rev. B*, 48:15646, 1993.

[108] C. Liu, S. R. Nagel, D. A. Schecter, S. N. Coppersmith, S. Majumdar, O. Narayan, and T. A. Witten. Force fluctuations in bead packs. *Science*, 269:513, 1995.

[109] D. Lohse and R. Rauhè. Creating a dry variety of quicksand. *Nature*, 432:689, 2004.

[110] W. Losert, L. Bocquet, T. C. Lubensky, and J. P. Gollub. Particle dynamics in sheared granular matter. *Phys. Rev. Lett.*, 85(7):1428–1431, 2000. e-print cond-mat/0004401.

[111] W. Losert, D. G. W. Cooper, J. Delour, A. Kudrolli, and J. P. Gollub. Velocity statistics in excited granular media. *Chaos*, 9:682, 1999.

[112] W. Losert, D. G. W. Cooper, J. Delour, A. Kudrolli, and J. P. Gollub. Velocity statistics in vibrated granular media. *Chaos*, 9(3):682–690, 1999. e-print cond-mat/9901203.

[113] S. Luding, E. Clément, A. Blumen, J. Rajchenbach, and J. Duran. Anomalous energy dissipation in molecular dynamics simulations of grains: The "detachment effect". *Phys. Rev. E*, 50:4113, 1994.

[114] S. Luding, E. Clément, A. Blumen, J. Rajchenbach, and J. Duran. Studies of columns of beads under external vibrations. *Phys. Rev. E*, 49(2):1634, 1994.

[115] S. Luding, M. Huthmann, S. McNamara, and A. Zippelius. Homogeneous cooling of rough dissipative particles: Theory and simulations. *Phys. Rev. E*, 58:3416–3425, 1998.

[116] C. K. K. Lun. Kinetic theory for granular flow of dense, slightly inelastic, slightly rough spheres. *J. Fluid Mech.*, 233:539–559, 1991.

[117] C. K. K. Lun and S. B. Savage. A simple kinetic theory for granular flow of rough, inelastic, spherical particles. *J. Appl. Mech.*, 54:47, 1987.

[118] C. K. K. Lun, S. B. Savage, D. J. Jeffrey, and N. Chepurniy. Kinetic theories for granular flow: inelastic particles in couette flow and slightly inelastic particles in a general flowfield. *J. Fluid. Mech.*, 140:223–256, 1984.

[119] U. M. B. Marconi, A. Petri, and A. Vulpiani. Janssen's law and stress fluctuations in confined dry granular materials. *Physica A*, 280:270, 2000.

[120] U. M. B. Marconi, A. Puglisi, L. Rondoni, and A. Vulpiani. Fluctuation-dissipation: Response theory in statistical physics. *Phys. Rep.*, 461:111, 2008.

[121] P. A. Martin and J. Piasecki. Thermalization of a particle by dissipative collisions. *Europhys. Lett.*, 46:613, 1999.

[122] S. McNamara and S. Luding. Energy nonequipartition in systems of inelastic, rough spheres. *Phys. Rev. E*, 58:2247–2250, 1998.

[123] S. McNamara and W. R. Young. Inelastic collapse and clumping in a one-dimensional granular medium. *Phys. Fluids A*, 4(3):496–594, 1992.

[124] S. McNamara and W. R. Young. Inelastic collapse in two dimensions. *Phys. Rev. E*, 50(1):R28–R31, 1994.

[125] A. Mehta and S. F. Edwards. Statistical mechanics of powder mixtures. *Physica A*, 157:1091, 1989.

[126] F. Melo, P. B. Umbanhowar, and H. L. Swinney. Transition to parametric wave patterns in a vertically oscillated granular layer. *Phys. Rev. Lett.*, 72(1):172–175, 1994.

[127] F. Melo, P. B. Umbanhowar, and H. L. Swinney. Hexagons, kinks, and disorder in oscillated granular layers. *Phys. Rev. Lett.*, 75(21):3838–3841, 1995.

[128] T. H. Metcalf, J. B. Knight, and H. M. Jaeger. Standing wave patterns in shallow beds of vibrated granular material. *Physica A*, 236:202–210, 1997.

[129] D. M. Mueth, G. F. Debregeas, G. S. Karczmar, P. J. Eng, S. R. Nagel, and H. M. Jaeger. Signatures of granular microstructure in dense shear flows. *Nature*, 406:385–389, 2000. e-print cond-mat/0003433.

[130] D. M. Mueth, H. M. Jaeger, and S. R. Nagel. Force distribution in a granular medium. *Phys. Rev. E.*, 57(3):3164–3169, 1998.

[131] S. R. Nagel. Instabilities in a sandpile. *Rev. of Mod. Phys.*, 64(1):321, 1992.

[132] M. Nicodemi, A. Coniglio, and H. J. Herrmann. Compaction and force propagation in granular packings. *Physica A*, 240:405, 1997.

[133] S. Ogawa. Multitemperature theory of granular materials. In S. C. Cowin and M. Satake, editors, *Proc. of US-Japan Symp. on Continuum Mechanics and Statistical Approaches to the Mechanics of Granular Media*, page 208, Fukyu-kai, 1978. Gakujutsu Bunken.

[134] J. S. Olafsen and J. S. Urbach. Clustering, order and collapse in a driven granular monolayer. *Phys. Rev. Lett.*, 81:4369, 1998. e-print cond-mat/9807148.

[135] J. S. Olafsen and J. S. Urbach. Velocity distributions and density fluctuations in a 2d granular gas. *Phys. Rev. E*, 60:R2468, 1999.

[136] J. A. G. Orza, R. Brito, T. P. C. van Noije, and M. H. Ernst. Patterns and long range correlations in idealized granular flows. *Int. J. of Mod. Phys. C*, 8:953, 1997.

[137] J. M. Ottino and D. V. Khakhar. Mixing and segregation of granular materials. *Ann. Rev. Fluid Mech.*, 32:55, 2000.

[138] A. Puglisi, A. Baldassarri, and A. Vulpiani. Violations of the Einstein relation in granular fluids: the role of correlations. *J. Stat. Mech.*, page P08016, 2007.

[139] A. Puglisi, V. Loreto, U. M. B. Marconi, A. Petri, and A. Vulpiani. Clustering and non-gaussian behavior in granular matter. *Phys. Rev. Lett.*, 81:3848, 1998.

[140] A. Puglisi, V. Loreto, U. M. B. Marconi, and A. Vulpiani. Clustering and non-gaussian behavior in granular matter. *Phys. Rev. Lett.*, 81:3848, 1998.

[141] A. Puglisi, V. Loreto, U. M. B. Marconi, and A. Vulpiani. Kinetic approach to granular gases. *Phys. Rev. E*, 59:5582–5595, 1999.

[142] A. Puglisi, L. Rondoni, and A. Vulpiani. Relevance of initial and final conditions for the fluctuation relation in markov processes. *J. Stat. Mech.*, page P08010, 2006.

[143] A. Puglisi and D. Villamaina. Irreversible effects of memory. *Europhys. Lett.*, 88:30004, 2009.

[144] A. Puglisi, P. Visco, A. Barrat, E. Trizac, and F. van Wijland. Fluctuations of internal energy flow in a vibrated granular gas. *Phys. Rev. Lett.*, 95:110202, 2005.

[145] A. Puglisi, P. Visco, E. Trizac, and F. van Wijland. Dynamics of a tracer granular particle as a nonequilibrium markov process. *Phys. Rev. E*, 73:021301, 2006.

[146] O. Reynolds. On the dilatancy of media composed of rigid particles in contact. *Philos. Mag. Ser. 5*, 50-20:469, 1885.

[147] K. Ridgway and R. Rupp. Flow of granular material down chutes. *Chem. Proc. Eng.*, 51:82, 1970.

[148] H. Risken. *The Fokker-Planck equation: Methods of solution and applications*. Springer- Verlag, Berlin, 1989.

[149] F. Ritort. Nonequilibrium fluctuations in small systems: From physics to biology. *invited contribution to "Advances in Chemical Physics" (to appear)*, 137:xx, 2007.

[150] F. Rouyer and N. Menon. Velocity fluctuations in a homogeneous 2d granular gas in steady state. *Phys. Rev. Lett.*, 85(17):3676, 2000.

[151] A. Samadani and A. Kudrolli. Segregation transitions in wet granular matter. *Phys Rev. Lett.*, 85(24):5102–5105, 2000.

[152] A. Samadani, A. Pradhan, and A. Kudrolli. Size segregation of granular matter in silo discharges. *Phys. Rev. E*, 60(6):7203–7209, 1999.

[153] S. B. Savage. Gravity flow of cohesionless granular materials in chutes and channels. *J. Fluid Mech.*, 92:53, 1979.

[154] S. B. Savage. The mechanics of rapid granular flows. *Adv. Appl. Mech.*, 24:289, 1984.

[155] S. B. Savage and D. J. Jeffrey. The stress tensor in a granular flow at high shear rates. *J. Fluid. Mech.*, 110:255, 1981.

[156] S. B. Savage and M. Sayed. Stresses developed by dry cohesionless granular materials sheared in an annular shear cell. *J. Fluid Mech.*, 142:391–430, 1984.

[157] T. Speck and U. Seifert. Restoring a fluctuation-dissipation theorem in a nonequilibrium steady state. *Europhys. Lett.*, 74:391, 2006.

[158] P. Sunthar and V. Kumaran. Temperature scaling in a dense vibrofluidized granular material. *Phys. Rev. E*, 60(5):1951–1956, 1999.

[159] C. Tang and P. Bak. Critical exponents and scaling relations for self-organized critical phenomena. *Phys. Rev. Lett.*, 60(23):2347–2350, 1988.

[160] S. T. Thoroddsen and A. Q. Shen. *Phys. Fluids*, 13, 2001.

[161] P. B. Umbanhowar, F. Melo, and H. L. Swinney. Localized excitations in a vertically vibrated granular layer. *Nature*, 382:793–796, 1996.

[162] T. P. C. van Noije and M. H. Ernst. Velocity distributions in homogeneous granular fluids: the free and the heated case. *Granular Matter*, 1(2):57–64, 1998. e-print cond-mat/9803042.

[163] T. P. C. van Noije and M. H. Ernst. Cahn-hilliard theory for unstable granular flows. *Phys. Rev. E*, 61:1765–1782, 2000.

[164] T. P. C. van Noije, M. H. Ernst, and R. Brito. Ring kinetic theory for an idealized granular gas. *Physica A*, 251:266–283, 1998.

[165] T. P. C. van Noije, M. H. Ernst, R. Brito, and J. A. G. Orza. Mesoscopic theory of granular fluids. *Phys. Rev. Lett.*, 79:411, 1997.

[166] A. Vespignani and S. Zapperi. *Phys. Rev. Lett.*, 78.

[167] P. Visco. Work fluctuations for a Brownian particle between two thermostats. *J. Stat. Mech.*, page P06006, 2006.

[168] J. Šmid and J. Novosad. Pressure distribution under heaped bulk solids. *I. Chem. E. Symposium Series*, 63:D3/V/1–12, 1981.

[169] T. C. L. W. Losert, L. Bocquet and J. P. Gollub. Particle dynamics in sheared granular matter. *Phys. Rev. Lett.*, 85:1428, 2000.

[170] O. R. Walton and R. L. Braun. Stress calculations for assemblies of inelastic spheres in uniform shear. *Acta Mechanica*, 63:73, 1986.

[171] O. R. Walton and R. L. Braun. Viscosity, granular-temperature, and stress calculations for shearing assemblies of inelastic, frictional disks. *J. Rheol.*, 30(5):949–980, 1986.

[172] S. Warr and J. M. Huntley. Energy input and scaling laws for a single particle vibrating in one dimension. *Phys. Rev. E*, 52(5):5596–5601, 1995.

[173] S. Warr, J. M. Huntley, and G. T. H. Jacques. Fluidization of a two-dimensional granular system: Experimental study and scaling behavior. *Phys. Rev. E*, 52(5):5583–5595, 1995.

[174] S. Warr, G. T. H. Jacques, and J. M. Huntley. Tracking the translational and rotational motion of granular particles: use of high-speed photography and image processing. *Powder Technol.*, 81:41–56, 1994.

[175] R. D. Wildman, J. M. Huntley, and D. J. Parkar. Convection in highly fluidized three-dimensional granular beds. *Phys. Rev. Lett.*, 86(15):3304–3307, 2001.

[176] T. Zhou and L. P. Kadanoff. Inelastic collapse of three particles. *Phys. Rev. E*, 54:623, 1996.